



**AUSTRALIAN ATOMIC ENERGY COMMISSION**  
**RESEARCH ESTABLISHMENT**  
**LUCAS HEIGHTS**

**METEOROLOGICAL RESEARCH STUDIES**  
**AT JERVIS BAY, AUSTRALIA**

by

**G. H. CLARK**  
**E. O. K. BENDUN**

July 1974

ISBN 0 642 99642 3



AUSTRALIAN ATOMIC ENERGY COMMISSION  
RESEARCH ESTABLISHMENT  
LUCAS HEIGHTS

METEOROLOGICAL RESEARCH STUDIES  
AT JERVIS BAY, AUSTRALIA

by

G. H. CLARK  
E. O. K. BENDUN

ABSTRACT

A climatological study of the winds and temperatures from the Jervis Bay region which commenced in October 1970 has shown the presence of a coastal sea breeze and secondary bay breeze circulation system. In an attempt to define the influence of the Murray's Beach site on the local atmospheric dispersion, special smoke plume photography studies were conducted in the lower atmosphere.

In June 1972 a meteorological acoustic sounding research programme was initiated at the Jervis Bay settlement. The aims of the research are to calibrate the sounder in terms of surface wind, turbulence and temperature measurements pertinent to a description of the lower atmospheric dispersion potential. Preliminary results on six months' data have shown encouraging correlations between the acoustic sounder patterns and particularly the wind direction turbulence traces.

National Library of Australia card number and ISBN 0 642 99642 3

The following descriptors have been selected from the INIS Thesaurus to describe the subject content of this report for information retrieval purposes. For further details please refer to IAEA-INIS-12 (INIS: Manual for Indexing) and IAEA-INIS-13 (INIS: Thesaurus) published in Vienna by the International Atomic Energy Agency.

CLIMATES; DAILY VARIATIONS; EARTH ATMOSPHERE; JERVIS BAY REACTOR; METEOROLOGY; RAIN; REACTOR SITES; SEAWATER; TEMPERATURE MEASUREMENT; TURBULENCE; WEATHER; WIND

## CONTENTS

	Page
1. INTRODUCTION	1
2. THE AAEC ACOUSTIC SOUNDING RESEARCH PROGRAMME	1
2.1 An Introduction to Acoustic Sounding	1
2.2 The AAEC Acoustic Sounder System at Jervis Bay	2
2.3 Supporting Meteorological Instrumentation at Jervis Bay	2
2.4 Data Analysis Methods	4
2.5 Preliminary Remarks on a Statistical Analysis of the Acoustic Sounder Records from 23rd June 1972 to 4th January 1973	6
3. WIND OBSERVATIONS IN THE JERVIS BAY REGION	7
3.1 Introduction	7
3.2 The Wind Rose Study	8
3.3 A Study of Wind Direction Turbulence	11
3.4 Wind Persistence in the Jervis Bay Area	15
4. SMOKE PLUME PHOTOGRAPHY	16
4.1 Background	16
4.2 A Method for Determining the Smoke Plume Geometry	17
4.3 Experimental Procedures	19
4.4 Results	20
5. ATMOSPHERIC STABILITY, TEMPERATURES AND RAINFALL IN THE JERVIS BAY REGION	22
5.1 Atmospheric Stability Analysis	22
5.2 A Climatology of Temperatures from Jervis Bay	23
5.3 Surface Sea Water Temperature Measurements	23
5.4 Rainfall Studies at Jervis Bay	24
5.5 A Comment on the Bushfire Potential in Jervis Bay Against 1972 Rainfall Figures	25
6. ACKNOWLEDGEMENTS	26
7. REFERENCES	26

Table 1 Acoustic sounder pattern classification

Table 2 Mean half-hour wind direction codes

Table 3 A comparison of the vane response characteristics of the Bendix-Friez  
aerovane and the Dines pressure tube anemograph

Table 4 A description of the wind direction turbulence trace types

Table 5 A classification system for the net all wave radiometer traces

Table 6 A frequency (%) table of sounder pattern categories versus temperature  
difference data

(continued)

## CONTENTS (continued)

- Table 7 The diurnal variation of the sounder patterns
- Table 8 A description of the wind recording station network, Jervis Bay
- Table 9 Frequency of occurrence (%) of various temperature differences or atmospheric stability classes
- Table 10 The relationship of the wind direction turbulence trace types to temperature difference or atmospheric stability
- Table 11 The frequency (%) occurrence of the wind direction turbulence traces versus wind speed (a) Night (b) Day
- Table 12 Pasquill's atmospheric turbulence categories
- Table 13 A table relating the wind speed, direction turbulence trace types, and the Pasquill-type turbulence categories
- Table 14 Frequency (%) distribution of Pasquill-type turbulence categories (a) Jervis Bay settlement (b) Murray's Beach
- Table 15 A frequency (%) table of wind direction versus turbulence trace types
- Table 16 Persistence of all wind directions combined
- Table 17 The diurnal variation of atmospheric stability measurements at Jervis Bay settlement 23. 6.72 to 4. 1.73
- Table 18 Murray's Beach and Bowen Island temperatures
- Table 19 Tabulation of rainfall and wind data from Murray's Beach, Bowen Island and Jervis Bay settlement for the months of heavy rainfall
- Table 20 A comparison of the 1972 and 11-year average rainfall for Bowen Island
- 
- Figure 1 Location, area of Jervis Bay
- Figure 2 Topographical features of the Jervis Bay area
- Figure 3 Schematic diagram of an acoustic sounder
- Figure 4 Sounder record pattern types
- Figure 5 Sounder records
- Figure 6 Wind direction turbulence trace types
- Figure 7 (a) 0300 EST wind direction roses all seasons combined  
(b) 0900 EST wind direction roses all seasons combined  
(c) 1500 EST wind direction roses all seasons combined  
(d) 2100 EST wind direction roses all seasons combined

(continued)

## CONTENTS (continued)

- Figure 8 (a) 0900 EST wind direction roses summer season  
(b) 0900 EST wind direction roses autumn season  
(c) 0900 EST wind direction roses winter season  
(d) 0900 EST wind direction roses spring season
- Figure 9 (a) 1500 EST wind direction roses summer season  
(b) 1500 EST wind direction roses autumn season  
(c) 1500 EST wind direction roses winter season  
(d) 1500 EST wind direction roses spring season
- Figure 10 (a) 0900 EST wind speed and direction roses all seasons combined  
(b) 1500 EST wind speed and direction roses all seasons combined
- Figure 11 (a) The diurnal variations in the occurrence of the wind direction turbulence categories from the Dines anemograph at the Jarvis Bay settlement 23. 6.72 to 4. 1.73  
(b) The diurnal variations in the occurrence of the wind direction turbulence categories from the Dines anemograph at Murray's Beach 24. 2.71 to 18. 2.72
- Figure 12 The diurnal variations of the direction turbulence categories 5 to 10 from the Dines anemograph
- Figure 13 The diurnal variation of 'stable' turbulence categories with restricted turbulence (6, 7, 8 and 9) and smooth flow (5, 10)
- Figure 14 (a) Lateral diffusion ( $\sigma_y$ ) as a function of downwind distance from source  
(b) Vertical diffusion ( $\sigma_z$ ) as a function of downwind distance from source
- Figure 15 (a) Wind direction persistence Jarvis Bay 23. 6.72 to 5. 1.73  
(b) Wind direction persistence Murray's Beach 18. 2.71 to 24. 2.72
- Figure 16 Wind direction persistence all directions combined
- Figure 17 (a) Wind direction turbulence trace persistence at Jarvis Bay 23. 6.72 to 5. 1.73  
(b) Wind direction turbulence trace persistence at Murray's Beach
- Figure 18 Location of camera positions and smoke generator at Murray's Beach
- Figure 19 Comparison of the time exposure and time series of instantaneous photographic techniques at 1224 EST on 7. 6.71
- Figure 20 The Dines anemograph wind record on the 7. 6.71 during the smoke plume experiment at Murray's Beach
- Figure 21 A plot of the vertical standard deviation of the smoke plume envelope ( $\sigma_z(x)$ ) versus distance downwind from the source
- Figure 22 Aerial photographs of the land and sea smoke plumes on 10. 6.71
- Figure 23 (a) A plot of the horizontal standard deviation of the smoke plume envelope ( $\sigma_y(x)$ ) versus distance downwind from the source 7. 6.71  
(b) A plot of the horizontal standard deviation of the smoke plume envelope ( $\sigma_y(x)$ ) versus distance downwind from the source 8. 6.71  
(c) A plot of the horizontal standard deviation of the smoke plume envelope ( $\sigma_y(x)$ ) versus distance downwind from the source 10. 6.71

(continued)

## CONTENTS (continued)

- Figure 24 Atmospheric stability wind roses
- Figure 25 Minimum temperatures at Murray's Beach (Stevenson screen level) and Bowen Island
- Figure 26 Maximum temperatures at Murray's Beach (Stevenson screen level) and Bowen Island
- Figure 27 Ground level and Stevenson screen minimum temperatures at Murray's Beach
- Figure 28 The annual cycle of air and sea water temperatures measured at Murray's Beach, Jervis Bay
- Figure 29 Monthly averaged air temperatures from Murray's Beach and Bowen Island at Jervis Bay
- Figure 30 A graph relating the seasonal variations in the sea water temperature difference between 1500 and 0900 EST
- Figure 31 Rainfall for Jervis Bay area
- Figure 32 Wind roses for days of rain 0900 EST data
- Figure 33 Wind roses for days of rain 0900 and 1500 EST data

## APPENDIX A Sand Drift Pole Data

- Figure A1 Murray's Beach sand drift measuring points



## 1. INTRODUCTION

In 1970, tenders were called for the proposed construction of a nuclear power station at a site near Murray's Beach on the shores of Jervis Bay, Australian Capital Territory (ACT) (Figure 1). Plans were formulated immediately to conduct detailed environmental studies of the surrounding areas. The biology, oceanography and geology were investigated extensively in the following eighteen months, but the meteorological studies were not initiated until August 1970.

The site chosen for the proposed nuclear power station is located in a complex topographical and meteorological environment (Figure 2). The site is surrounded by water on three sides with the Tasman Sea in the east and Jervis Bay in the north and west sectors. In addition, near the site the local topography has many small undulations and disturbances which are likely to exert a significant influence on the mesometeorology of the area.

Initially, the main purpose of the meteorological studies was to attempt to define the influence of the mesometeorology on the atmospheric dispersion potential of the region. Under normal circumstances such studies would continue for a duration of three to five years. During this time, climatological information on the pertinent meteorological variables could be collected and processed prior to a meteorological environmental impact statement.

In the case of Murray's Beach, the original meteorological studies were interrupted by the announcement of a deferment of the Jervis Bay nuclear power station for twelve months from June 1971, and a subsequent indefinite deferment from June 1972. This caused a withdrawal of manpower and services, with the result that the initial study was discontinued in January 1972.

Thereafter, there has been a complete change in emphasis of the meteorological studies in the Jervis Bay region. The meteorological station was relocated in the Jervis Bay settlement, 4.83 km west of the Murray's Beach site. By necessity, it was converted to a semi-automatic operation with only brief daily inspection by the local Forestry Department rangers. Atmospheric acoustic sounding, a novel technique for remotely probing the dynamic behaviour of the lower atmosphere, was subsequently introduced as the major research programme. Currently, all effort is being concentrated on calibrating the acoustic sounding technique in terms of parameters relevant to the atmospheric dispersion potential measurements.

In Section 2 the associated meteorological instrumentation, data analysis techniques and preliminary results are presented for the acoustic sounding research programme in the Jervis Bay settlement. Then follows a discussion on the climatological wind and turbulence statistics for both Murray's Beach and the Jervis Bay settlement. The techniques of smoke plume photography were used to give quantitative estimates of the atmospheric dispersion near Murray's Beach and these are reported in Section 4. There is a brief discussion on the temperature, atmospheric stability and rainfall climatologies followed by an appendix presenting the sand drift pole data to conclude the report on the Jervis Bay meteorology studies.

## 2. THE AAEC ACOUSTIC SOUNDING RESEARCH PROGRAMME

### 2.1 An Introduction to Acoustic Sounding

In 1968 the novel technique of acoustic sounding was introduced as a remote meteorological probe capable of monitoring the dynamic behaviour of the lower atmosphere (McAllister *et al.* 1968). Acoustic sounding involves the transmission of sound waves, a scattering of these from irregularities of the atmospheric acoustic refractive index, and reception of the echoes at a ground based station. Theory has shown that when the transmitter and receiver are coincident (monostatic system), the back scattered energy is dominantly a function of the spatial variations of temperature. If the transmitter and receiver are separated and the sound follows an oblique path (bistatic system), the acoustic scattering is also a function of the spatial variability of the wind fluctuations.

The design of an acoustic sounder is determined by its subsequent research or operational application and is a function of many variables. In practice, a short pulse of acoustic energy is directed into the atmosphere with echoes from the scatterers being received almost immediately following transmission. The strength of the received signal is not only a function of the intensity of the scatterers, but also of the atmospheric attenuation along the ray path. It has been shown (Harris 1966) that when a high frequency carrier wave (e.g. 2,000 Hz at 10°C, 50% relative humidity) is used, the atmospheric attenuation is approximately 1.2 dB per 100 m, whereas a lower frequency (e.g. 125 Hz) under similar atmospheric conditions has the attenuation reduced to approximately 0.034 dB per 100 m. Thus the effective range of an acoustic sounder might only be 200 m (Beran 1970) when operating at 2,000 Hz. However at low frequencies, even though there is a reduced atmospheric attenuation and consequent greater range available, wind produced noise causes a rapid decrease in the signal to noise ratio. Therefore, these two opposing factors need to be balanced with the experimental requirements when designing an acoustic sounding system.

## 2.2 The AAEC Acoustic Sounder System at Jervis Bay

The system which was supplied to the AAEC by the RAAF Physics Department at the University of Melbourne is fully described in Shaw (1971) and Shaw, Bourne and Moncur (1972); a schematic diagram is shown in Figure 3. The power amplifier (100 watts output) is driven by a pulsed tone of 1,300 Hz with a pulse length of 0.2 sec (giving a height resolution of 30.48 m). The pulse repetition frequency is variable but was set at 0.1 pulses per second, or one pulse every 10 seconds, which gives a maximum unambiguous height range of 1,372 m.

To maintain a satisfactory signal to noise ratio, it is necessary to surround the acoustic sounder transceiver with an anechoic acoustic shield which prevents spurious or permanent echoes from being detected by the transceiver. Among the other research groups there have been various methods used for the acoustic absorbing medium; these have included, hay bales, brick or concrete walls, plastic sponge covered plywood etc. (Gething 1972).

At Jervis Bay it was decided to follow an approach similar to that of the RAAF Physics Department (Shaw 1971). The recommendation was that the horn transceiver and parabolic dish be sunk into a three metre deep hole in the ground. However, because of a hard subsurface layer of sandstone it was impractical to excavate the hole; instead an above ground crater-like earthen barrier was constructed using compacted black loam.

This acoustic sounder 'hole' has not proved as effective as those below ground level because of the stronger winds and 'noise' levels away from the earth-atmosphere boundary. Other supplementary measures are currently being investigated; these include the placement of a two metre high barrier of 76.2 mm thick fibre glass wool batts mounted in frames in an octagonal configuration about the dish in the hole. There has been a marginal improvement in the quality of the records since this was implemented.

## 2.3 Supporting Meteorological Instrumentation at Jervis Bay

**Temperature Sensors.** Before an intelligent interpretation of the acoustic sounder records can be made for a station like Jervis Bay, it is essential to have a reliable supporting meteorological instrument system in close proximity to the experimental site. The ideal station should have measured values of atmospheric stability, relative humidity and wind data continuously recorded at varying levels to the altitudes of interest (of the order of 1,000 m). Clearly this approach is impractical. Instead, it is a general practice to locate the instrumentation on convenient platforms in the lower 100 metres of the atmosphere.

The only suitable tower available in the Jervis Bay settlement was initially instrumented with thermistor temperature sensors at the 3 and 33 m levels to give a measure of the atmospheric stability. Later a wet bulb sensor was placed in a Stevenson screen so that the advent of the sea breeze and other related atmospheric marine boundary layer phenomena could be studied. The YSI

No. 44030 type of precision thermistor enables the ambient temperature to be measured between 0 and 40°C and temperature difference to have a range between -10 and +10°C.

*Net All Wave Radiometer.* The net all wave radiation has been estimated using a CSIRO designed Funk net all wave radiometer. This was placed 3 m above an uneven grass surface which has a temperature similar to that of the ambient air. At this altitude there is an integrating effect of the underlying surface without significant errors from long wave radiation originating in the intervening air layer (Idso and Cooley 1971). Although it is not a perfect location for the radiometer, already some interesting features have been observed under conditions of high atmospheric stability when complex wave patterns are detected on the acoustic sounder records. Both temperature and radiometer data are recorded on a Honeywell multichannel chart recorder.

*Data Collection From 'Above' 30 Metres.* To gather meteorological data from higher in the atmosphere, instruments can be flown aloft using either a model aeroplane or a balloon mounted system. Already there has been a field trip to Jervis Bay along with personnel from the School of Earth Sciences at Macquarie University. The weather proved unsuitable for studying conditions of high atmospheric stability and further experiments are required. At present a small instrument package suitable for tethering below a balloon platform is being constructed by the Instrumentation and Control Division at the AAEC Research Establishment. This will measure the altitude using a linear displacement transducer attached to the bellows of an aneroid barometer. The wet and dry bulb temperatures will also be monitored simultaneously. A small pressure sensitive transistor is also under investigation as the altitude sensor. Reports of this experimentation will be made at a later date.

*Wind Measurement.* The ground level wind measurements in the Jervis Bay settlement are recorded by a Dines pressure tube anemograph Mk. II. This is mounted on a 4 m tower above a caravan which houses the 24 h recording drum and ink pen system. Both the turbulent wind speed and direction fluctuations are recorded on separate traces of the chart.

*Rainfall Recording.* Daily rainfall measurements are taken by the officer in charge of the Forestry Department's Section at Jervis Bay. For 12 months a Lambrecht pluviograph was principally used for comparison with the occurrence of noise on the acoustic sounder.

*Vertical Wind Measurement.* In initial analysis of the acoustic sounder traces it was felt that measurements of the vertical wind speed were necessary when interpreting the vertical movements of the observed scattering layers. A CSIRO 'Fluxatron' (Hicks, Dyer and King 1967) will soon be installed. This instrument correlates the vertical wind speed and temperature fluctuations to give a measure of the turbulent heat flux being generated in the lower atmosphere. Not only will this allow study of the wave pattern phenomena under high atmospheric stability conditions, but also investigation of the thermal plume breakdown of the nocturnal surface radiation inversion after sunrise.

*Automatic Data Acquisition Systems.* Recently, several automatic weather stations have been acquired for use in the climatological surveys. Epsilon Industries Ltd. (UK) has supplied a 12-channel Weather Watcher station which records data on a 12.7 mm magnetic tape cassette at frequencies ranging from one channel scan per 5 min. to one channel scan per hour. Each cassette tape will hold approximately 120 days' data when recording at one channel scan per 5 min. This cassette tape is then translated onto 8-level computer compatible paper tape. Using a computer code developed to analyse the paper tape, the data is converted to hourly averages, standard deviations and wind frequency tables which are then stored on computer disk. All computer disk data sets are updated with subsequent paper tape input.

The other climatological station is the CSIRO designed RIMCO digital event recorder. This instrument records data directly onto 5-level computer compatible paper tape. Instead of the absolute values of the meteorological variable being recorded, only changes in the quantities are detected. The present station has six input channels available. These are filled by two bidirectional sensors which show both positive and negative variations in the sensor (e.g. humidity - one

count for  $\pm 1\%$  change; wind direction – one count for a  $6^\circ$  clockwise or anticlockwise rotation of the vane) and two unidirectional sensors (wind run – one count for 1 km of air flow; rainfall – one count for 1 point [0.25 mm] of rain). The bidirectional sensors have a different code for either sense of change and therefore require two input channels. The paper tape data is then subject to similar computer analysis to that mentioned for the Epsilon station.

After initial field testing at Lucas Heights, these stations will be deployed to areas similar to Jervis Bay for any future meteorological site evaluations.

## 2.4 Data Analysis Methods

The techniques of data analysis have been specifically chosen so that the acoustic sounder records can be interpreted in terms of ground level measurements of the meteorological variables. When sufficient data has been collected, these meteorological variables and thus the acoustic sounder patterns will be related to estimates of the atmospheric dispersion potential in the lower atmosphere.

With all data from the Jervis Bay settlement being recorded on strip and drum charts, there was a considerable task in physically extracting and tabulating the eight data variables. A preliminary examination of the acoustic sounder records showed frequent temporal variations in the pattern types. It was therefore decided to extract all the chart data at half hour intervals for twenty four hours per day during the observation period.

*The Acoustic Sounder Records.* After the preliminary examination of the acoustic sounder records, fourteen pattern types were chosen according to the description in Table 1 and the examples in Figure 4.

A range in quality of the traces in Figure 4 was deliberately chosen and is usually a function of the recorder performance. The presence of atmospheric scattering layers is shown by shades of grey in the trace, ranging from white for a zero intensity to black for a maximum strength scattering. The recorder chart paper is pressure and heat sensitive, the pressure being controlled by the intensity of the echo signal received by the transceiver.

Although each acoustic sounder pattern type is coded at half hour intervals, it is important to make the coding in the context of the preceding and succeeding several hours of record. This can be better emphasised by reference to Figure 5 where five day records are shown together with the pattern type coding. When considering the descending and ascending patterns (types 9, 10, 11 and 12), at least two hours of record covering the half hour of interest must be viewed. As an example of the interpretation of the cascading echo patterns (types 11 and 12) see the record on the 10th September 1972 between 2000 and 2400 EST. In cases where there is a transition between trace types within the two hour example period, the numbers are coded onto the charts. The frequent occurrence of trace type 0 superimposed on, and sometimes completely blanking out, other pattern types is directly related to the occurrence of wind or rain noise due to the acoustic shielding defects in the system.

At present it is not known whether the choice of pattern types is unique to the Jervis Bay site or if it could be applied universally in future studies with entirely different topographical and meteorological conditions. To date only six months' accumulation of data has been analysed and during this time the acoustic sounder has been out of action for 20% of the observation periods.

In an attempt to test the uniqueness and universality of the classification system, it is proposed to take similar records from several other stations currently operating in Australia. To eliminate the influence of the marine boundary layer an inland site similar to Mt. Isa in Queensland or Canberra in the ACT would be suitable. However, if a different topographical location still under a marine influence was to be studied, Point Cook in Victoria would be a likely choice. At present acoustic sounders supplied by the RAAF Physics Department are operating at all these locations and approaches have been made to the various authorities for access to the records.

*The Dines Pressure Tube Anemograph Charts.* When considering analysis methods for any anemograph records an important point to be considered is the response characteristics of the instrument and whether these are sufficiently sensitive for the required study. The following trace coding methods have taken into account the response behaviour of the Dines pressure tube anemograph (Air Ministry Meteorological Office 1956) under varying meteorological situations and also the final application of the data.

Four pieces of data were extracted from the wind records for each half hour interval. The mean half hour wind speed and amplitude of the speed fluctuations were coded in knots or miles per hour and later converted to  $\text{m sec}^{-1}$  in the computer program. The separate mean wind direction trace was coded to eight sectors of the compass as shown in Table 2.

Coding of the wind direction turbulence traces has been based on two previous research studies. Working on a meteorological control program for the nuclear reactor at Brookhaven National Laboratory, Singer and Smith (1953) classified the wind direction traces from a Bendix-Friez aerovane into five gustiness categories. In 1964, while investigating low turbulence flow, Slade (1969) further extended the Brookhaven Type D trace into five additional categories. Both of these earlier studies used data from altitudes ranging between 30 and 450 m.

Before basing the Jervis Bay coding system on the results of these two studies, a comparison was made of the response characteristics of the Bendix-Friez aerovane and the Dines pressure tube anemograph.

Mazzarella (1972) has comprehensively reviewed the specifications of a wide range of wind measuring instruments. Even though the Bendix-Friez propeller type anemometer operates on an entirely different principle to the Dines anemograph, he shows that both instruments are suitable for urban pollution studies and have very similar characteristics (Table 3).

The following ten wind direction turbulence trace types are therefore based on the response characteristics of the Dines anemograph or a similar instrument and consist of an amalgamation of the Singer and Smith (1953) and Slade (1969) approaches. In his classification system Slade mentions that his trace types 3 and 4 could have a meandering (long period oscillation) component superimposed. In the Jervis Bay trace classification this feature has been explicitly included as trace types 8 and 9 (Figure 6). The examples show a broad range and quality of trace for a two hour segment. The interpretation of the traces is similar to those of the acoustic sounder in that coding for each half hour interval should also be in the context of the overall trend in the trace behaviour. The physical mechanism behind each trace type should also be considered (Table 4).

*Temperature Charts.* Data on the ambient dry bulb and wet bulb temperatures and temperature difference have been extracted to  $0.1^{\circ}\text{C}$  accuracy. Calibration of the installation has shown that these temperatures are reliable to  $\pm 0.5^{\circ}\text{C}$ .

*Net All Wave Radiation Traces.* To date there has only been limited data extraction and no computer analysis of the net all wave radiation records. In future, a planimeter will be used to give the hourly integrated radiation values. A coding system is also being developed for the trace type (Table 5). Preliminary inspection of the nocturnal records has shown some relationship between 'disturbed' radiometer traces and complex patterns on the acoustic sounder. These trends may be more fully explored on a climatological time scale.

*Summary.* All data from the meteorological station at Jervis Bay will be extracted and placed on computer cards prior to storage in disk data sets on the IBM360/50 digital computer at Lucas Heights. Computer codes have been written and will be updated to use the data for multivariate correlation analyses.

## 2.5 Preliminary Remarks on a Statistical Analysis of the Acoustic Sounder Records from 23rd June 1972 to 4th January 1973

*The Wind Records and Acoustic Sounder Patterns.* In general, with some noteworthy exceptions, the echo patterns occur in association with the wind turbulence categories as expected on theoretical grounds. The intensity and vertical extent of particular echo patterns are generally related to the intensity of mechanical turbulence (high frequency turbulence); however, most echoes occur in situations of light winds and low intensity turbulence.

Thin scattering layers near the surface not exceeding 304.8 m in depth (type 1 pattern), occur predominantly with very light winds ( $< 1 \text{ m sec}^{-1}$ ), very low intensity turbulence and no mechanical turbulence. By contrast, the thick scattering layers near the surface, 609.6 m or more in extent (type 2), occur relatively frequently in association with light intermittent mechanical turbulence and wind speeds between 1 and 2  $\text{m sec}^{-1}$ .

Uniform scattering layers, particularly the thin ones (types 1 and 2), near the surface are associated predominantly with easterly winds. Complex and wavy scattering (types 3 and 4) near the surface occur more frequently with westerly rather than easterly winds.

Double scattering layers (types 5 and 6) occur predominantly with very light winds ( $< 1 \text{ m sec}^{-1}$ ) and low intensity turbulence mainly from an easterly direction. The intensity or vertical extent of this type of echo pattern does not appear to be related to the amount or intensity of mechanical turbulence.

Multiple or complex scattering layers of strong intensity (type 8 pattern) occur most frequently in light winds with light to moderate turbulence which is mostly of a mechanical nature. Multiple or complex layers (type 7) which are not well developed occur in a variety of turbulence conditions. No particular wind direction is preferred with either strong or weak multiple or complex scattering layers.

Ascending echoes (type 9) in the incipient stage (i.e. while emerging near the surface) are associated mainly with light winds, frequently from a northerly direction, and with light mechanical turbulence. When these echoes are aloft (type 10), the wind direction is mostly from the north with a more intense convective type of turbulence.

Descending echoes occur with very light winds from a north easterly direction particularly when near the surface (type 12). There is very little or no turbulence whilst the echo is aloft, and this is slightly enhanced when near the surface and merging with the bottom scattering layer.

The thermal plume pattern (type 13) occurs together with convective turbulence and easterly winds of about 2  $\text{m sec}^{-1}$ .

*Temperature Difference Records and the Acoustic Sounder Patterns.* The temperature difference data taken over 30 m on the Forestry Department radio mast in the Jervis Bay settlement was compared with the simultaneous sounder pattern categories (Table 6). With unstable atmospheric stability conditions (temperature gradient  $< -1^\circ\text{C}$  per 30 m) the ascending echoes (types 9 and 10) are prominent together with the convective thermal plumes (type 13). This relationship between unstable temperature gradients and the ascending echoes suggests that these patterns are linked to the nocturnal inversion break-up following sunrise.

The double echo patterns (types 5 and 6) show only slight dependence on atmospheric stability with isothermal ( $0^\circ\text{C}$  per 30 m) conditions being more favourable. Likewise, the complex echo patterns (types 7 and 8) are independent of the prevailing atmospheric stability on the basis of the available data. However, with the onset of the surface temperature inversion conditions, the surface echo patterns (types 1 to 4) become prominent. In this case the complex surface echo (type 3) pattern predominates with inversion strength of intensity  $> 1^\circ\text{C}$  per 30 m.

*The Diurnal Variation in the Acoustic Sounder Patterns.* With such a subjective record analysis technique and considering the short period of data collection, no definite statements can be made on the mechanisms behind the various acoustic sounder patterns. Instead, the following comments are only an interpretation of trends requiring more detailed analysis in the future (Table 7).

As expected, the no data trace 0 has a peak of occurrence in the daylight hours when the low level wind and turbulence noise are strongest. The uniform, shallow scattering layer (type 1) forms after 1700 EST and develops into a deeper layer (type 2) around 2200 EST. The more complex or wavy patterns (types 3 and 4) appear soon after 2200 EST and persist until 0600 EST. Although this appears to be a logical progression for sounder patterns 1 to 4, more data is required to establish if this proposal has any physical basis.

There are several maxima in the diurnal frequency distribution of the double layered pattern type 5. The first occurs between 1300 and 1500 EST and is related to the discussion on pattern types 9 and 10 below. The second peak is found just after sunset and the last occurs at midnight. At present, there is no physical explanation for these observations. The elevated double layered echo (type 6) has been related to the presence of subsidence inversions in other studies (Shaw 1971). Again the peak observation time is after 1800 EST, an observation which may tie in with Ball's theory (1960) on the diurnal height variation of the subsidence inversion. With a dissipation in solar radiational heating of the lower atmosphere near sunset, the appearance of the double echo may be associated with the slow sinking of the subsidence inversion layer.

The weak multiple echo pattern type 7 is independent of the diurnal cycle but type 8 has a definite frequency maximum approaching sunset (around 1600 EST). Although not exclusive, there is generally a progression from the emerging (type 9) to the ascending (type 10) echo pattern. At Jervis Bay, this progression starts as pattern 9 about 0700 EST and changes to pattern 10 after 0900 EST. One interpretation of this behaviour in the echo patterns is that the transition represents the break-up and rise of the surface radiation inversion following sunrise.

A further interesting postulate is made for a similar sequence of events later in the morning. Again pattern type 9 is initially observed at near 1100 EST and this changes to type 10 by 1400 EST. It is suggested that this dynamic transition may be due to the sea or bay breeze which moves inland and undercuts the terrestrial air mass. The occurrence of the double echo pattern type 4 in the early afternoon may also be another feature of the marine boundary layer. Further correlations of the acoustic sounder patterns with the wet and dry bulb temperature data are required to substantiate this aspect.

In a similar manner to patterns 9 and 10, there is frequently a progression from the descending (type 11) to the merging (type 12) pattern. From the data, it appears there may be two periods in which this pattern behaviour occurs. The first commences in the late afternoon (1600 EST) and is finally complete later in the evening (2100 EST); the second is also a nocturnal phenomenon commencing near 0400 EST and finishing around 0700 EST. To further investigate these patterns, data has been collected from the meteorological station at HMAS Albatross in order to establish the temporal and spatial extent of this phenomenon.

### 3. WIND OBSERVATIONS IN THE JERVIS BAY REGION

#### 3.1 Introduction

Nuclear facilities are frequently sited in a coastal area to take advantage of the availability of abundant cooling water. When confronted with the task of describing the mechanisms behind atmospheric dispersion in a marine environment, the mesometeorologist is faced with a perplexing and many-sided problem. The usual combination of complex topography and land-sea-air mass configurations requires considerable effort in even attempting to understand the basic features of the prevailing meteorological environment.

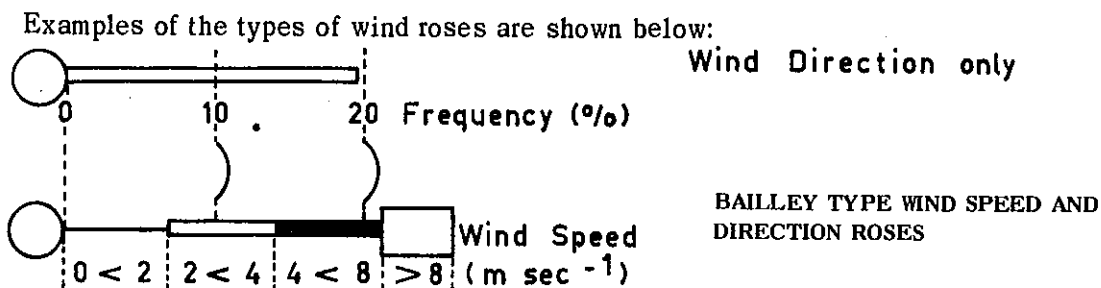
Such a confused situation exists in the Jervis Bay region where the proposed nuclear power station site at Murray's Beach is surrounded on three sides by water (Figure 2). Wind data in the area are available from six sources for differing periods of time and of varying quality. Table 8 explains the details of these data sources. It should be emphasised that the data available are not strictly of a climatological time scale (usually taken as 5 years); however, they will help in describing the various mechanisms.

The wind analyses fall into three categories. The first looks at the semi-climatological wind roses as a function of the seasonal and diurnal patterns. Then follows a comparison of the turbulence features at Murray's Beach and Jervis Bay settlement as detected by the Dines anemograph, with some preliminary comments on the atmospheric dispersion potential of each site. Finally there is a short discussion on the wind direction and turbulence persistence analyses on data from the Dines anemograph.

### 3.2 The Wind Rose Study

**Wind Roses.** A study of the long term wind roses from the Jervis Bay region has been completed using the IBM360/50 digital computer at Lucas Heights (except those wind roses supplied by the Bureau of Meteorology for HMAS Albatross). At both HMAS Albatross and the Jindivik airstrip in calm conditions (zero wind speed) no wind direction was taken; however, at other stations in the network this data was included because of the greater sensitivity in the vane than the wind speed sensor.

These analyses are divided into three sections. The first two present only wind direction roses independent of wind speed measurements and the last shows the Bailey type wind direction and speed roses. In this last case the frequency of occurrence of 'no data available' increases at several stations because of frequent faults in the wind speed sensors during the survey period (e.g. Bowen Island - 32% of all observations are faulty for the 0900 EST wind rose).



**The Diurnal Wind Patterns.** Combining all the seasonal data, wind direction roses are plotted in Figure 7 for 0300, 0900, 1500 and 2100 EST. Manual observations from Bowen Island and the Murray's Beach meteorological compound were only taken at 0900 and 1500 EST.

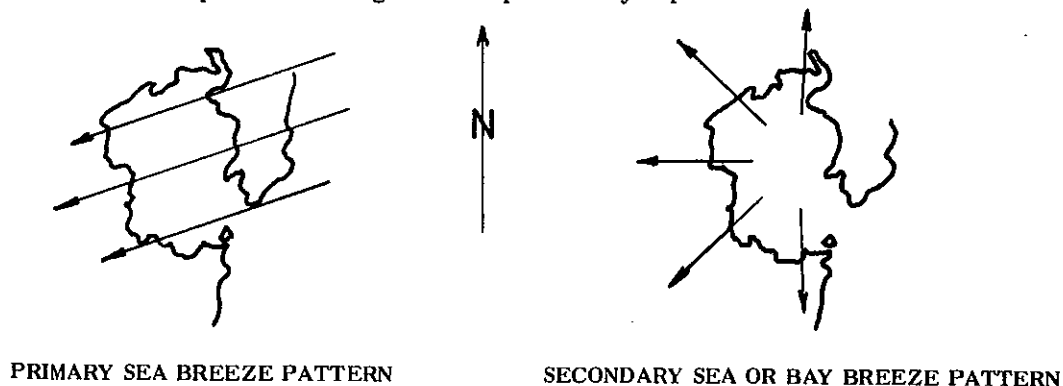
At 0300 EST (Figure 7a), there is a predominance of winds with west and south-westerly components. At the inland HMAS Albatross station this situation is accentuated by a high frequency of calm conditions (31%) and a nocturnal drainage of air down from the foot-hills of the Great Dividing Range. The short six month period of data collection at the Jervis Bay settlement may account for an increase in north-west winds by comparison with the westerly and northerly components measured on Jindivik airstrip. In general, there is an indication of an off-shore movement in the 0300 EST wind roses.

By 0900 EST (Figure 7b), there is still a strong nocturnal influence present with a predominance of winds from the south-west to north-west sector detected by all stations in the region. Again there is a definite emphasis on westerly winds at HMAS Albatross (35% frequency). There are also interesting differences indicated between the Murray's Beach manual and Dines anemograph data. The strong presence of westerly winds in the anemograph records is diminished in



the manual observations with the north-east winds becoming more dominant. The increased importance of the on-shore north-east breeze is also reflected in the manual observations taken from Bowen Island. Therefore the shorter period of anemograph data may not be quite as representative as the longer manual data collection period.

The diurnal nature of the sea breeze circulation emerges in the 1500 EST wind direction roses (Figure 7c). North-easterly winds predominate at all stations except the Jervis Bay settlement. In Jervis Bay settlement there is an increased northerly influence which may be due to a secondary sea breeze circulation pattern (hereafter referred to as a bay breeze) forming across the shores of Jervis Bay itself, in addition to the primary circulation across the main coastline. The increased contribution of south-easterly winds at HMAS Albatross also aids the bay breeze theory. The mechanisms postulated might be simplistically represented below:



More detailed correlations between the wind, solar radiation and temperature records are necessary to verify this hypothesis.

In the 2100 EST wind records there is still evidence of remnants of the daytime sea breeze. Both the Murray's Beach and Jindivik airstrip Dines anemographs still detect the north-east breeze although the nocturnal north-west to south-westerly breezes are beginning to assume an increasing importance. The true wind rose at HMAS Albatross is obscured by the 41% frequency of calm conditions, however the westerly drainage winds once again predominate.

*Summary.* There is a clear diurnal cycle in the wind circulation patterns observed in the Jervis Bay region. During the daytime, the north-easterly sea breeze predominates with a suggestion of a bay breeze forming across the land-sea mass boundary of Jervis Bay itself under certain meteorological conditions (as yet undefined).

After persisting until 2100 EST or later, the sea breeze decays under increasing atmospheric stability when the nocturnal winds prevail from the north-west to south-west quarter. These off-shore winds suggest a land breeze or topographically-induced light wind feature.

*Seasonal Wind Patterns.* Seasonal wind direction roses are presented for 0900 and 1500 EST from five of the six data sources in the instrument network. The six month period of data from Jervis Bay settlement was not considered. Various trends which emerged in the study of the diurnal wind patterns have been emphasised and confirmed by the following analyses.

The seasonal 0900 EST wind direction roses are initially presented as Figure 8. In Summer (Figure 8a) with just four hours of solar radiation heating following sunrise, the sea breeze circulation (north-easterly winds) is clearly present. The bay breeze pattern is also observed at both HMAS Albatross and Jindivik airstrip. It is a little surprising that the south-easterly bay breeze winds are detected at the inland HMAS Albatross station in the 0900 EST wind roses; however, it may indicate that the bay breeze precedes the stronger north-easterly sea breeze in some circumstances. The strong contribution of southerly winds detected by the Murray's Beach Dines anemograph again can only be attributed to the duration of the sampling period.

By Autumn the 0900 EST wind direction roses (Figure 8b) have lost nearly all signs of an early generation of the sea and bay breezes which are now replaced by winds from the north-west to south-west quadrant. The presence of winds from this sector is emphasised most dramatically by the wind roses from the Winter season (Figure 8c). In both Autumn and Winter the nocturnal wind regime appears to persist beyond 0900 EST before being disturbed by the weak solar radiation heating or convective turbulence influences.

In part, comments on the disruptive influence of convective turbulence still apply to the Spring wind roses (Figure 8d). However, the reappearance of north-easterly winds suggests a regeneration of the sea breeze, probably late in October and November.

A hint of the development of the sea breeze in the 0900 EST seasonal wind rose is more fully supported by studying the 1500 EST Summer data (Figure 9a). The north-east winds predominate at all stations with the bay breeze again evident in the Jindivik airfield and HMAS Albatross data. All four stations on the southern reaches of Jervis Bay indicate an increased probability of southerly winds.

The southerly influence remains in Autumn (Figure 9b) as westerly winds exert a greater influence. With the exception of the Jindivik airstrip, there is virtually no contribution from northerly winds.

In Winter (Figure 9c) there is still a weak presence of the sea breeze; however, this diminishes directly with the intensity of the solar radiation heating of the land mass. Instead the off-shore winds from the south-west and north-west assume a greater importance. The Spring wind roses, similar to those observed at 0900 EST, show a swing to the easterly on-shore winds in the afternoon (Figure 9d).

*Summary.* As was to be expected, there is a seasonal variation in the wind patterns over the Jervis Bay region. Even at 0900 EST there is evidence of the sea breeze in the Summer wind roses; however, this influence diminishes in effect through the Autumn and Winter seasons when the north-west to south-west winds dominate. The sea breeze observed at 1500 EST is still observed in Winter to a much lesser degree. In general the analyses of the seasonal wind roses show that when the daytime easterly influence wanes, winds from the westerly sector increase in importance.

*Wind Direction and Speed Roses.* Combined wind direction and speed (Bailey type) roses are presented for all seasons combined at 0900 and 1500 EST. As mentioned previously, the frequency of occurrence of days of no observations increased markedly at several stations owing to continual instrumentation faults.

At 0900 EST (Figure 10a) winds in the south to west sector have slightly stronger speeds by comparison with those in other directions. Most wind speeds fall below  $8 \text{ m sec}^{-1}$  at both 0900 and 1500 EST (Figure 10b). The lack of standardisation of instrumentation through the network could have led to the occasional inconsistency between data sources.

*Conclusions.* The following features have emerged from the analyses of wind records from the Jervis Bay region:

- ♦ The diurnal variation of winds is from a daytime on-shore wind (mainly with a north-east component) to a night time off-shore breeze (from the south-west to north-west sector). This cycle is likely to be associated with the diurnal sea-land breeze circulation regime.
- ♦ The advent of the sea breeze and its importance diminishes with seasonal change from Summer to Winter, although it is still present, to a much lesser degree, during the months of weak solar radiation heating.

- ♦ A bay breeze circulation within the Jervis Bay region is postulated to explain the appearance of a secondary maximum in the wind direction roses at the Jervis Bay settlement and HMAS Albatross.
- ♦ In general, most wind speeds are below  $8 \text{ m sec}^{-1}$  and average  $\sim 4 \text{ m sec}^{-1}$ .

### 3.3 A Study of Wind Direction Turbulence

Measurement of wind direction turbulence is an essential aspect of the evaluation of the relative effects of the local topography and roughness features (mechanical turbulence generation) and convective heating (thermal turbulence generation) on the atmospheric dispersion potential of a particular site. The ten wind direction turbulence trace types have been fully described in Section 2.

Data presented in the following section are taken from the Dines anemograph which operated at both Murray's Beach (18th February 1971 to 24th February 1972) and the Jervis Bay settlement (23rd June 1972 to 4th January 1973). Similar statistics have been extracted for both sites to make a direct comparison of the differing meteorological influences. The data from Murray's Beach was available for only 57% of the observation period, whereas the performance of the anemograph in the Jervis Bay settlement was more consistent with 85% data recovery.

In the original studies, Singer and Smith (1953) and Slade (1969) positioned their anemometers high into the atmosphere (some experiments at 100 m altitude). By contrast, the Dines anemograph at both Jervis Bay sites were located at only 10 m above ground level. At these altitudes the smooth wind traces (types 5 and 10) are expected more frequently than higher in the atmosphere (Slade 1969).

The following analyses will attempt to show the various mechanisms behind the different trace types by comparing them with other meteorological measurements. A description of the turbulence traces in terms of the atmospheric dispersion potential will be used to relate them to the Pasquill dispersion categories. A final comparison of the turbulence trace to wind direction will assist in defining the local topographical influences at both sites.

*The Diurnal Variations in the Turbulence Trace Types.* In Figures 11a and 11b there is a clear diurnal cycle in the turbulence trace types. At both Murray's Beach and the Jervis Bay settlement there is only a small amplitude wave for trace 1 with a daytime maximum and a small but finite nocturnal contribution. This contrasts with the findings of Singer and Smith (1953) who showed that gustiness class 1 had purely convective origins.

Turbulence trace 2 occurs more frequently at Murray's Beach than Jervis Bay settlement. The diurnal wave is irregular at both sites with a peak frequency occurring at 1300 EST in Murray's Beach and 1600 EST in Jervis Bay. A difference between the sites is seen in the diurnal frequency distribution of turbulence trace type 3. Overall it is observed only half as often at Murray's Beach relative to the Jervis Bay settlement. The more turbulent trace 4 occurs with similar cyclic pattern and frequencies at both sites.

On combining all the 'stable' atmospheric wind traces (5 to 10) it is apparent that the distribution at Murray's Beach is slightly tilted towards a latter hour of the day. Another interesting feature is the relatively high daytime frequency of occurrence with the minimum never falling below 10% at Murray's Beach but dwindling to 1% at the Jervis Bay settlement 3 miles to the west. This is a direct reflection of the topographical influences at both sites.

To further investigate this feature trace types 5 to 10 were plotted individually as Figures 12a and 12b. The high daytime frequency of occurrence of these traces in Murray's Beach is accentuated by turbulence traces 7, 8 and 9. Nevertheless the meandering trace type 10 is still present later in the day, even at 1200 EST.

By separating the Slade (1969) stable traces into those with restricted turbulence (6, 7, 8, 9) and those with smooth flow (5 and 10), it is clear that Murray's Beach is the site where mechanical turbulence exerts a more profound influence, whereas under nocturnal conditions mechanical turbulence as exemplified by traces 6, 7, 8 and 9 is more important in the Jervis Bay settlement (Figure 13).

Smooth flow traces have a similar probability of occurrence at both sites; however, the peak frequency is lagged by three hours at Murray's Beach (0600 EST) in relation to the Jervis Bay settlement. One explanation for this behaviour may be the onset of nocturnal off-shore winds which move slowly across the bay, first intercepting the Jervis Bay settlement and later bringing more stable conditions to the Murray's Beach site.

*The Relationship of the Turbulence Trace Types to Atmospheric Stability.* Temperature difference data measured over 30 m on the radio mast in the Jervis Bay settlement were compared with the turbulence trace types. In Table 9 the frequency of occurrence of the temperature difference intervals for the period 23rd June 1972 to 4th January 1973 shows that 93% of all stability measurements fall within the range  $-3$  to  $+3^{\circ}\text{C}$  per 30 m.

The frequency distribution of turbulence traces versus temperature intervals or atmospheric stability (Table 10) has been normalised with respect to the frequency of occurrence of the individual trace types. Traces 1 and 3 predominate with unstable temperature gradients ( $< -1^{\circ}\text{C}$  per 30 m). With increasing atmospheric stability ( $-1$  to  $0^{\circ}\text{C}$  per 30 m), the daytime wind traces (types 1, 2, 3 and 4) assume equal importance together with the meandering, weak turbulence traces 8 and 9. All the so-called 'smooth flow' traces (Slade 1969) are prominent under inversion conditions with the non-turbulent trace 5 most outstanding.

It is apparent from the comparison of the turbulence trace types with atmospheric stability that traces 1 and 3 are associated with atmospheric instability and therefore have a strong relationship to the presence of convective turbulence (Singer and Smith 1953). Traces 2 and 4 show only a slight dependence on unstable temperature gradients, but rapidly diminish in importance with increasing stability. Only traces 8 and 9 assume a new importance near isothermal conditions; however, all traces 5 to 10 are present under inversion conditions.

*The Relationship Between Wind Direction Turbulence and Wind Speeds.* In Table 11, there has been no normalisation with respect to the frequency of occurrence of the turbulence traces when making a comparison of these variables with the wind speed intervals. Both Murray's Beach and the Jervis Bay settlement show similar trends in the data, however, generally the winds are stronger at the inland site.

During both night and day the strongest winds are associated with traces 2 and 4, the mean being in the range  $4$  to  $8\text{ m sec}^{-1}$ . During the night, trace 3 occurs less frequently without the solar radiation generating forces, but when detected it has an average speed in the range  $2$  to  $4\text{ m sec}^{-1}$ . The turbulence traces 6 to 9 again indicate improved atmospheric dispersion conditions over the smooth traces 5 and 10 (average wind speed  $0 < 1\text{ m sec}^{-1}$ ).

*The Relationship of the Wind Direction Turbulence Traces to Atmospheric Dispersion Potential.* In an attempt to gain further insight into the mechanisms behind the various wind direction turbulence traces, the traces have been related to other meteorological variables measured near the ground. The data presented is limited in its application because of the short observation periods involved - one year at Murray's Beach and six months at the Jervis Bay settlement. Thus the following summary of the atmospheric dispersion potential of the trace types must be considered in this context.

The turbulence trace types will be discussed individually:

- Trace type 1: typical of the presence of convective turbulence, being associated with atmospheric instability and having a daytime peak occurrence. Trace 1 significantly aids atmospheric dispersion on days of light wind and strong radiation heating. At night the occurrence of turbulence traces similar to type 1 may be associated with other generating mechanisms (e.g. conditional instability in the atmosphere).
- Trace type 2: most frequently observed during both night and day, there is an irregular diurnal cycle in trace 2 with only a slight stability dependence under unstable conditions. An increase in stability diminishes the importance of trace 2. With stronger winds, this turbulence trace is purely mechanical in origins with strong powers of atmospheric dispersion.
- Trace type 3: has a clear diurnal cycle with a strong dependence on atmospheric instability. By contrast with trace 1, trace 3 is associated with stronger winds ( $2-4 \text{ m sec}^{-1}$ ) and therefore may have origins in both mechanical and convective turbulence.
- Trace type 4: shows a similar diurnal variation and atmospheric stability dependence to trace 2, but is usually associated with higher wind speeds. With an overall average frequency of occurrence of 25%, this trace is indicative of the most favourable atmospheric dispersion conditions.
- Trace type 5: is usually a nocturnal phenomenon associated with atmospheric stability and light winds. There is minimal atmospheric dispersion and consequently a potential for high ground level pollution concentrations with these conditions.
- Trace type 6: essentially a nocturnal turbulence trace, it is associated with inversion conditions and is thus an important nocturnal dispersion mechanism.
- Trace type 7: comments for trace type 6 apply also to type 7. Stronger nocturnal winds lead to improved dispersion conditions.
- Trace types 8 and 9: essentially a nocturnal phenomenon, traces 8 and 9 occur in near isothermal conditions and persist later in the day. The meandering component of the trace may be indicative of weaker thermal turbulence with limited mechanical turbulence (high frequency component) superimposed.
- Trace type 10: associated with light winds and under strong inversion conditions, the meandering (stepping) of the trace will lead to slightly improved dispersion conditions over trace 5.

#### *The Relationship of the Turbulence Trace Types to the Pasquill Dispersion Categories.*

From the previous descriptive sections, an understanding was gained of the physical mechanisms behind the wind direction turbulence traces recorded by the Dines anemograph. To obtain quantitative estimates of the atmospheric dispersion, it is planned to formulate a relationship between these turbulence traces and the Pasquill-type turbulence categories (Pasquill 1961). This involves Pasquill's original table which related the wind speeds and radiation conditions to the six turbulence categories (Table 12), and the turbulence traces with the wind speed intervals from data collected at various sites. A seventh turbulence category type F1 was postulated by E. Charash (AAEC unpublished report) to represent atmospheric dispersion under strong inversion (high atmospheric stability) conditions. Table 13 shows the resulting relationship between the wind direction turbulence traces, wind speed and the Pasquill-type turbulence categories.

It should be noted that although distributions of the Pasquill-type categories are included for all wind speeds and turbulence traces, in practice many of the turbulence traces will have no

observations above a certain wind speed, (e.g. turbulence trace 1 has zero observations with wind speeds  $> 4 \text{ m sec}^{-1}$  (Table 11a)).

The distributions from Table 13 can now be applied to the turbulence trace versus wind speed table (Table 11) for a comparison of the Pasquill turbulence category climatology from Murray's Beach and the Jervis Bay settlement (Table 14). During the day (0700 to 1900 EST) Pasquill category A is observed more often in the Jervis Bay settlement than at Murray's Beach with wind speeds  $< 4 \text{ m sec}^{-1}$ . A peak daytime frequency of occurrence of slight atmospheric instability (type C) is translated to a lesser degree to the nocturnal distribution. At night the neutral stability category type D predominates with a greater contribution from the stronger inversion categories. The persistence of the inversion categories (types E and F) into the daytime period only reflects the fact that the surface inversions are not destroyed until after 0700 EST.

Pasquill (1961) has drawn curves to relate the turbulence categories to the variation of the horizontal and vertical standard deviations with distance downwind (Figure 14). The additional strong inversion turbulence category type F1 is plotted from data presented in an unpublished AAEC report. It should be mentioned that the atmospheric dispersion estimates derived from these curves are suitable only for an ideal flat plain terrain and as such may be incorrect by up to an order of magnitude when applied to a site with more complex terrain features. Estimates of the ground level pollution concentrations may then be calculated by using the simplified Gaussian or similar standard dispersion formulae.

*The Relationship Between Wind Direction and Turbulence Trace Types.* When an air mass traverses a variety of sea and land mass features, there is a change in the nature of the wind turbulence. For instance, over a sea or flat-plain type of terrain the degree of mechanical turbulence is much less than over a series of hills, topographical or vegetal disturbances. The wind direction dependence of the turbulence traces is therefore an important feature of the local atmospheric dispersion influences of a particular site.

In Table 15 the frequencies of the turbulence trace types total 100% for each wind direction. The following discussion will be concerned with the direction turbulence wind roses for each site. It is important that reference be made to earlier wind climatology studies when interpreting the turbulent nature of the winds.

*Jervis Bay Settlement.* Analysis of the wind direction records from the Jervis Bay settlement has shown in general that nocturnal winds prevail from the south-west to north-west sector with the major daytime wind being a north-easterly sea breeze and a bay breeze from the north direction.

From Table 15, the bay breeze from the north is seen to be more turbulent (traces 2 and 4 = 69%) than the north-easterly sea breeze which is more convective in nature (trace 3 = 20%). An interesting feature is the relatively high frequency of occurrence of the meandering stable trace type 10 with north-east and easterly winds. It is suggested that these atmospheric conditions prevail soon after sunset lasting until after 2100 EST (see Figure 7d) when the off-shore winds begin to develop.

The nocturnal north-west wind also shows a peak with turbulence trace 10, but in general the more turbulent traces (2 and 4) prevail from this direction. A peak in the restricted turbulence trace type 7 is indicated in all winds from the south to east quadrant.

In summary, it can be said that with daytime on-shore winds, especially at light wind speeds, convective turbulence is important at the Jervis Bay settlement. However, in general the dispersive mechanical turbulence is most important at this site.

*Murray's Beach Meteorological Compound.* At Murray's Beach, the nighttime winds prevail from the north-west to south-west sector, turning to the on-shore north-easterly winds during the day. The wind direction turbulence trace statistics are different in this environment to those at the Jervis

Bay settlement. At Murray's Beach there is virtually no contribution from the thermal turbulence traces to the dispersion character of the north-east sea breeze. Instead, over 70% of winds from this direction exhibit strong mechanical mixing (traces 2 and 4). Likewise winds from the east to south-east sector also show a predominance of the turbulent traces 2, 4 and 7. The degree of influence of the hills and cliffs as the air mass moves inland across the coast may be reflected in these observations.

By contrast the winds from the west or off-shore sector now show a tendency to the more stable traces although still indicating a strong presence of mechanical turbulence (traces 2 and 4 ~ 50%). Traces 8, 9 and 10 all indicate a peak frequency for this wind direction sector.

In summary, it can be said that convective turbulence is negligible when compared to the effects of mechanical turbulence at Murray's Beach. The local generation of mechanical turbulence with all wind directions can be attributed to the coastal hills with a north to south axis and to a lesser degree, the local vegetation.

### 3.4 Wind Persistence in the Jervis Bay Area

To correctly describe the atmospheric dispersion climatology and evaluate pollution dosages, it is essential to introduce the concept of wind persistence into the dosage calculations (Shirvaikar *et al.* 1969). The following analyses are based on other research by Shirvaikar (1972) who made an intersite comparison of wind direction persistence conditions. These analyses have been extended to include a study of persistence of the wind direction turbulence trace types. This is effectively a study of the persistence of various atmospheric dispersion conditions.

Data were analysed from the Dines anemograph at Murray's Beach (24th February 1971 to 18th February 1972) and the Jervis Bay settlement (23rd June 1972 to 4th January 1973). When the instrument was faulty and/or no data were available, these periods were considered as breaks in the persistence. An averaging time of one hour at Murray's Beach and half an hour at the Jervis Bay settlement with 45° sector widths for the wind direction were used in the analyses. By increasing the sector width and/or the averaging times, there will be an effective increase in the persistence values (Van der Hoven 1969). In the Jervis Bay analyses, if the wind direction or turbulence traces were bordering between two sectors or trace types respectively, alternate values were extracted, thus limiting the persistence to the period of averaging.

*Wind Direction Persistence.* The cumulative probability (%) versus persistence (hours) are plotted on Figure 15a for the Jervis Bay settlement results and Figure 15b for the Murray's Beach data. The persistence was similar for all wind directions at the Jervis Bay settlement, except for winds from the south-east and south which have a slightly higher probability of a longer persistence. However winds from these directions occur infrequently at the Jervis Bay settlement and are not associated with any peculiar marine boundary influence.

The wind direction persistence curves from Murray's Beach (Figure 15b) all have a similar slope with northerly and southerly winds being the most persistent. Combining all the wind directions and comparing the curves with the 1969 results from Tarapur, India (Shirvaikar 1972), the Murray's Beach winds have a greater persistence than both the Jervis Bay settlement and Tarapur which are very similar (Figure 16) at longer persistences. These differences are emphasised in Table 16.

The dissimilarity between Murray's Beach and the other two sites is probably due to the differing sector widths and averaging times. Without more extensive analyses into the implications behind the variation of these two parameters on the persistence and dosage calculations, a direct comparison cannot be made of the sites.

*Persistence of the Wind Direction Turbulence Traces.* Comparison of the results of persistence calculations between sites is again restricted by the different analyses procedures. Comments will therefore be restricted to the individual results followed by a general summary of the persistence of atmospheric dispersion conditions (Figure 17).

The anemograph data from the Jervis Bay settlement indicates that traces 2 and 4 are those most likely to have a long persistence. The persistence trend of trace 2 is matched by trace 7 which represents only slightly worse atmospheric dispersion conditions. Because trace 2 is often observed at this site (29% frequency of occurrence), apparently there is a frequent return of short persistence periods for this trace.

At Murray's Beach the more turbulent traces (types 2 and 4) also have a greater probability of longer persistence periods (Figure 17b). For example, 50% of occasions with traces 2 and 4 have a persistence of  $\leq 4.6$  hours and  $\leq 6.0$  hours respectively. Trace 7, with continuous mechanical type turbulence of restricted amplitude, has a similar probability curve to the convective turbulence trace type 3. All the smooth flow traces show similar trends which indicate a frequent change from one trace type to another, but not necessarily a dramatic change in the atmospheric dispersion conditions.

In summary, it has been shown that difficulties arise from the different analysis techniques used for the Jervis Bay settlement and Murray's Beach data. However, it appears that the more turbulent traces (types 2 and 4) have a higher probability of longer persistence and there is, therefore, a greater probability of thoroughly dispersing any accumulated atmospheric pollutants. The other traces show, in general, varying degrees of persistence with the cumulative frequency decreasing as the direction turbulence traces become smoother.

The wind persistence analyses offer the possibility of future intersite comparisons of wind turbulence statistics which could eventually be incorporated as a basic part of the AAEC meteorological site survey procedure. In future, one interesting extension of the analyses could be the inclusion of similar trace types (e.g. 2 and 4; 6, 7, 8 and 9; 5 and 10; 1 and 3) as one group. This would enable a study of the persistence of atmospheric dispersion conditions leading to pollution doses of the same level.

#### 4. SMOKE PLUME PHOTOGRAPHY

##### 4.1 Background

Atmospheric dispersion of contaminants is influenced by the intensity of atmospheric turbulence. Atmospheric turbulence has mainly mechanical or thermal origins. The intensity of mechanical turbulence would be much higher over a site with many topographic disturbances (hills, valleys, escarpments etc.) and diverse vegetation features, than over a terrain with flat plain features. Stronger winds generate higher mechanical turbulence whereas, under conditions of light winds and strong radiation heating of the lower atmosphere, convective or thermal turbulence is a most important mechanism for atmospheric dispersion.

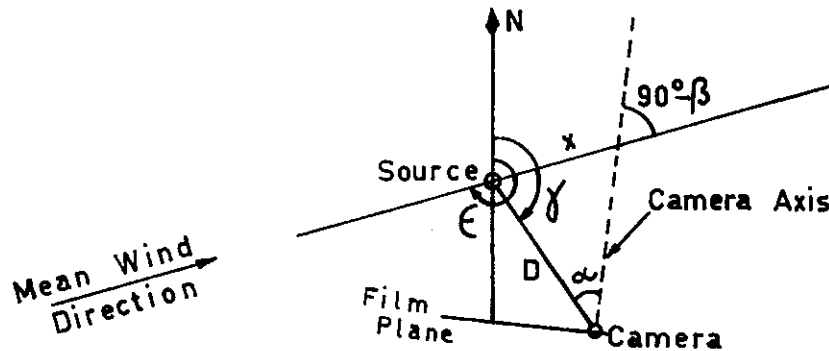
To gain further knowledge on the effect of the site on atmospheric dispersion, a study of visible smoke plumes was conducted using photographic techniques. At Jervis Bay a smoke plume was continuously emitted from a ground level source located in complex terrain near Murray's Beach. To derive meaningful measurements of the smoke plume dispersion parameters, instantaneous fluctuations needed to be integrated using time exposure photographs. However, before it could be confirmed that the plume envelope from the time exposure photograph was truly representative of the integrated smoke plume, several comparative experiments were made with simultaneous time lapse photographs.

A method for single camera photography developed by Halitsky (1961) was modified and used to determine the smoke plume geometry. Atmospheric dispersion parameters were then computed using a method developed by Gifford (1959). Results of the horizontal dispersion estimates of smoke plumes over land and sea were obtained from instantaneous aerial photographs.



#### 4.2 A Method for Determining the Smoke Plume Geometry

In the time exposure photograph of a three dimensional smoke plume, a two dimensional image is projected onto the focal plane of the camera. With a knowledge of the average wind direction at the source of emission during the exposure period and the orientation of the camera focal plane, the horizontal dimensions of the smoke plume envelope can be computed (Halitsky 1961):



where  $\alpha$  is the horizontal angle between the camera axis and camera to source line

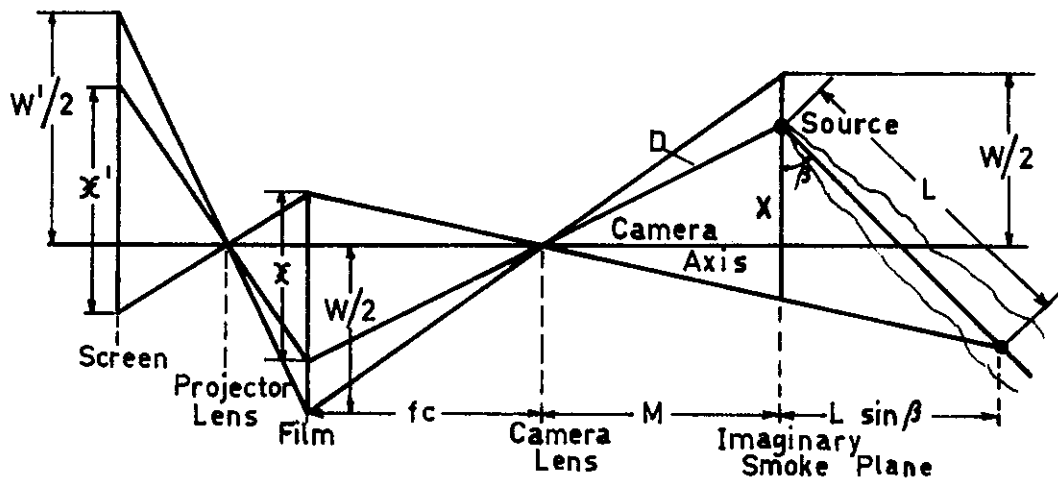
$\gamma$  horizontal angle from north to the camera to source line

$\beta$  horizontal angle between film plane and the mean wind direction

$\epsilon$  horizontal angle from north to the mean wind

D camera to source distance

A plan view of the plume geometry and camera, projector screen orientation is shown below:



GEOMETRY OF THE SMOKE PLUME, FILM AND PROJECTED IMAGE

(Halitsky 1961)

The screen magnification is  $XMAG = \frac{W'/2}{W/2} = \frac{W'}{W}$  where W is the frame width.

Considering the plan view of the plume geometry

$$\frac{x'}{x} = XMAG \quad (1)$$

The film and imaginary smoke plume image also give

$$\frac{X}{x} = \frac{M}{fc} = \frac{D \cos \alpha}{fc} \quad (2)$$

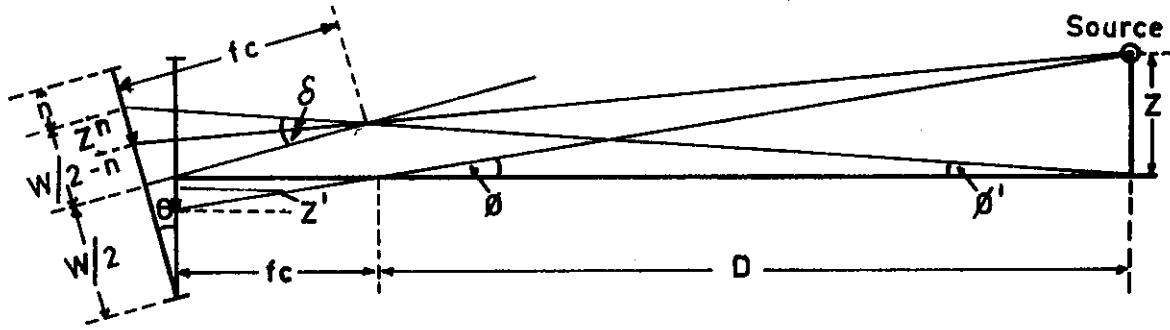
Combining Equations (1) and (2)

$$X = \frac{D \cos \alpha}{fc} \cdot \frac{x'}{XMAG} \quad (3)$$

From Halitsky's method (1961), the actual horizontal plume dimension  $L$  is now given by

$$L = \frac{\frac{D \cos \alpha \cdot x'}{fc \cdot XMAG}}{\cos \beta + \sin \beta \tan \alpha - \frac{x' \sin \beta}{fc \cdot XMAG}} \quad (4)$$

The vertical plume rise above the source could not be calculated directly from Halitsky (1961) owing to the camera tilt during the experiment. The camera tilt  $\theta$  can be estimated from the known relative heights of the camera and source and position of the source on the tilted film plane:



GEOMETRY OF THE TILTED CAMERA AND SMOKE SOURCE

The angle  $\phi$  subtended by the source which is height  $Z$  above the camera position, is given by

$$\phi = \tan^{-1}(Z/D)$$

From the geometry  $\delta = \phi + \phi' \simeq \theta + \phi$

$$\tan \delta = \frac{W/2 - n}{fc}$$

$$\therefore \theta = \tan^{-1} \left( \frac{W/2 - n}{fc} \right) - \tan^{-1} (Z/D) \quad (5)$$

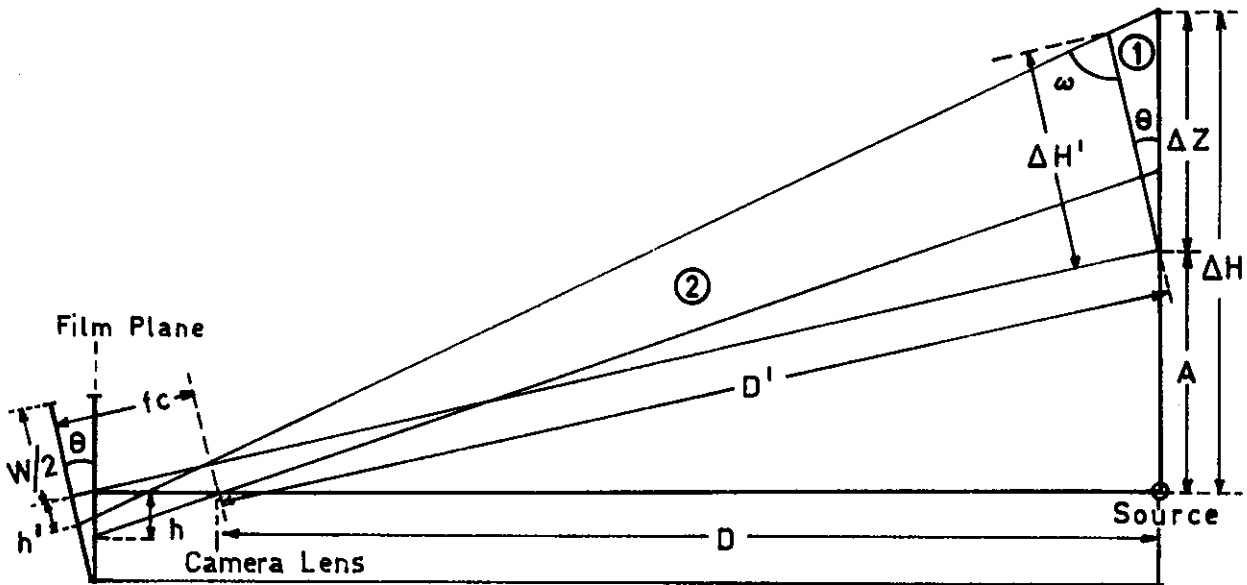
The vertical geometry of the camera and smoke plume is shown below:

$$A = D \tan \theta + \frac{W}{2} \left( \frac{1}{\cos \theta} - 1 \right) \quad (6)$$

Applying the sine rule in Triangle (1)

$$\frac{\Delta H'}{\sin(\omega - \theta)} = \frac{\Delta Z}{\sin(180 - \omega)}$$

$$\therefore \Delta Z = \frac{\Delta H' \sin \omega}{\sin(\omega - \theta)} \quad (7)$$



GEOMETRY OF THE TILTED CAMERA USED IN CALCULATING THE VERTICAL PLUME RISE

From the geometry of Triangle (2)

$$\frac{h'}{fc} = \frac{\Delta H'}{D'} \text{ and } D' = \frac{D}{\cos \theta} + \frac{W}{2} \tan \theta \quad (8)$$

Combining Equations (6), (7) and (8) gives the plume rise:

$$\Delta H = D \tan \theta + \frac{W}{2} \left( \frac{1}{\cos \theta} - 1 \right) + \frac{D' h'}{fc} \frac{\sin \omega}{\sin(\omega - \theta)} \quad (9)$$

A method developed by Gifford (1959) relates the vertical ( $\sigma_z^2(x)$ ) and horizontal ( $\sigma_y^2(x)$ ) variances to the plume height and width measurements in the transcendental equation

$$\begin{aligned} \sigma_y^2(x) &= Y^2 \left[ \ln \frac{e Y_m^2}{\sigma_y^2(x)} \right]^{-1} \\ \sigma_z^2(x) &= Z^2 \left[ \ln \frac{e Z_m^2}{\sigma_z^2(x)} \right]^{-1} \end{aligned} \quad (10)$$

where  $\begin{cases} Y_m \\ Z_m \end{cases}$  = maximum half  $\begin{cases} \text{width} \\ \text{height} \end{cases}$  of the plume.

$\begin{cases} Y \\ Z \end{cases}$  = half  $\begin{cases} \text{width} \\ \text{height} \end{cases}$  of the smoke plume.

With an initial estimate from the graph of the roots of this equation, a Newton iterative method yielded values of  $\sigma_z(x)$  and  $\sigma_y(x)$  for the different experiments.

### 4.3 Experimental Procedures

The terrain around the proposed nuclear power station site at Murray's Beach rises to 91.4 m above mean sea level and has a dense coverage of low ti-tree and other native flora. Closer to the bay there is a stand of native gum trees with heights ranging to 30 m. Under normal operating conditions at a nuclear power station, any atmospheric emissions of radioactive aerosols

are likely to be at building level or from a low chimney stack. With this in mind, a hill south-east of the site was chosen for locating the smoke generator. From there the white oil fog smoke plume was clearly visible to the two camera stations (Figure 18). However it was best positioned for winds with an east-west component.

To the west, towards the Jervis Bay settlement, the land is more undulating with a flat area surrounding the Jindivik airfield. In future, it is proposed to locate a second smoke generator here so that a comparison can be made of the flat plain versus complex terrain atmospheric dispersion under similar thermal turbulence conditions.

When attempting to study dispersion under changing atmospheric stability regimes, it is essential to have a good colour contrast between the plume and the background sky. With a white oil fog plume this means that a dull grey overcast sky is photographically inferior to a clear blue background. In some ways this restricts the daytime observations to fine, sunny days and therefore limits the range of atmospheric stability regimes which can be investigated. Enquiries have so far failed to find a manufacturer of a non-white neutral buoyancy smoke which would have universal application.

For nocturnal photography there needs to be either artificial illumination (Clark 1970) or natural moonlight (Shirvaikar *et al.* 1970) for good definition of the plume envelope. However, time exposure photography is far easier under nocturnal conditions. To date no night studies have been conducted at Jervis Bay, although some are planned during future field trips to the area.

Long time exposure photographs taken in the daytime requiring semi-opaque neutral density filters (filter factor  $10^3$  or  $10^4$ ) can sometimes lead to reciprocity failure in the film. Reciprocity failure (Culkowski 1961) results from a changing film sensitivity with diminishing light intensity. This factor could lead to a spurious smoke plume envelope being detected on the time exposure photograph. To prove that our photographic techniques were not the subject of reciprocity failure, simultaneous time lapse photographs were taken during three experiments. As an example, this involved taking 12 instantaneous photographs at 5 second intervals on a Canon Dial 35/2, half frame, self winding camera during a one minute time exposure using a camera with an aperture setting of f11 and neutral density filter factor of 3000.

The instantaneous photographs then needed to be superimposed for a direct comparison with the time exposure photograph. Various methods were tried including tracing the envelope of the individual plumes, superimposing these, and then defining the integrated plume envelope by the density of lines. Without a sophisticated line densitometer this method proved too subjective.

A photochemical superimposition method proved successful. The series of instantaneous images were exposed for a short interval of time onto a slow reacting photographic paper. With careful alignment of each image an integrated plume eventually emerged. Typical examples of the results can be seen in Figure 19 together with the plume envelopes traced from the prints. In all three experiments there was good agreement between time lapse and time exposure methods. In future all experiments will use a single camera, dense lens filter time exposure techniques, and a knowledge of the geometry of the test site to study the vertical atmospheric dispersion of the smoke plume.

#### 4.4 Results

In conjunction with a detailed study of the water current movements in the ocean and Jervis Bay environs, a series of smoke plume experiments was performed in early June 1971. A Cessna 170 aeroplane equipped with mounted cameras photographed developments in the dispersion of an ocean dye plume as well as the land-based smoke plume. On several occasions a pyrotechnic smoke generator was ignited on a sea raft platform to compare the horizontal atmospheric dispersion and wind direction over a rough (land) and relatively smooth (sea) surface. Simultaneously, the

land-based smoke plume was photographed using time exposure techniques to give estimates of the vertical dispersion.

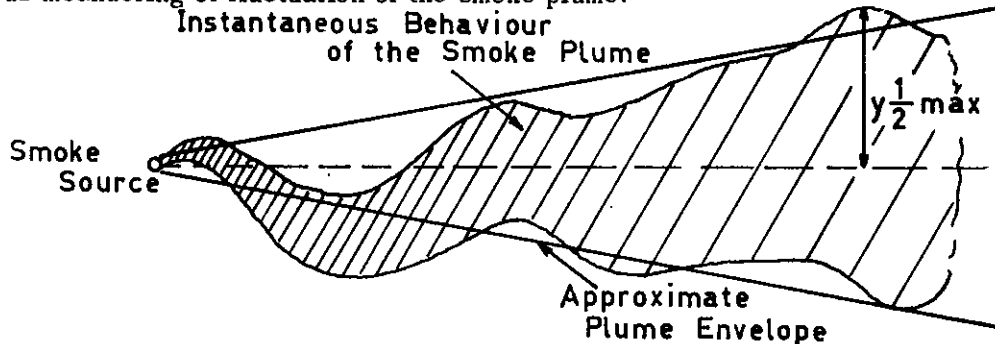
**Vertical Atmospheric Dispersion Estimates.** During the morning of June 7th 1971 when all the reported vertical plume dispersion experiments were conducted, the winds were light and variable in direction (Figure 20). Initially there was a light breeze from the west to north-west which veered to the south-east with the advent of an on-shore breeze at 1200 EST.

The mean wind direction was also observed at the source of the smoke plume, independent of the Dines anemograph operating in the Murray's Beach meteorological compound. Both the recorded traces and observations compared favourably. These data, together with the photographic measurements were substituted in Equations (9) and (4) to calculate, respectively, the height above source of the plume envelope and distance down the mean wind direction. Using a knowledge of the terrain contours, the vertical plume height above ground level was calculated and the maximum plume height estimated. In Figure 21 the vertical standard deviation  $\sigma_z$  is plotted on a log-log scale versus the distance downwind.  $\sigma_z$  was computed using the Gifford (1959) transcendental Equation 10.

When compared with the Pasquill type A dispersion curve, the experimental plots show, in general, greater vertical dispersion. There appears to be little dependence on wind direction and thus topography variations under the prevailing conditions. Instead, the vertical atmospheric dispersion is almost totally convective in origin. This was confirmed by on-site observations of frequent puffs of smoke being transported vertically by the buoyant thermals. The occurrence of the turbulence trace type 1 on the Dines anemograph charts also suggested very unstable atmospheric conditions were prevailing during this morning.

**Horizontal Dispersion Estimates.** In the aerial studies to investigate the horizontal dispersion of the land and sea smoke plumes, only instantaneous photographs could be taken owing to the motion of the aeroplane (Figure 22). Also a time series of the instantaneous photographs could not be taken, so new analysis techniques were devised.

In all cases a plume envelope was drawn to account for both the dispersion within, and instantaneous meandering or fluctuation of the smoke plume:



ANALYSIS OF THE INSTANTANEOUS AERIAL PHOTOGRAPH

After estimating the maximum half width ( $Y_{1/2} \max$ ) and taking representative points on the plume envelope downwind of the source, Equation (10) was used in an analysis similar to that for the vertical dispersion, to give estimates of the horizontal standard deviation  $\sigma_y$  (Figure 23a).

There is evidence of quite rapid variations in the behaviour of the horizontal dispersion on the 7th June 1971 (Figure 23a). Instead of following the trend of  $\sigma_z$  (Figure 21), the horizontal standard deviations are not typical of unstable atmospheric conditions (Pasquill type A) but suggest a more stable atmosphere (Pasquill type E). The horizontal winds were so light and variable during the day, that this offers the only explanation for the reduced horizontal dispersion.

On the 8th June 1971 (Figure 23b) there was a 5/8 cirro- to alto-stratus cloud cover with an average wind speed of  $2.5 \text{ m sec}^{-1}$  gusting to  $5 \text{ m sec}^{-1}$  prior to 1200 EST. At midday, this subsided to a calm and turned from the north-west to a north-easterly direction. The curves are similar to the Pasquill type D neutral stability turbulence category, but again there is an under-estimation of  $\sigma_y$ . There is an interesting comparison of the sea and land smoke plumes. To a distance of 40 metres from the source, both sea and land dispersion are similar; however, with greater distances downwind the sea plumes remain narrower than those with the more turbulent overland trajectory.

The sea-land atmospheric dispersion difference was again evident on the 10th June 1971 (Figure 23c). The experimental curves continued to have a steeper slope than the Pasquill curves being similar to the neutral atmospheric stability case (type D). This observation compares fairly well with the type 3 direction turbulence trace from the north-west with near calm conditions.

In summary, it can be said that the aerial technique to study the horizontal dispersion of smoke plumes probably underestimates the true values. This arises from the method of roughly delineating the smoke plume envelope from the instantaneous photograph.

**Conclusions.** A photographic technique and analysis methods have been devised to study the horizontal and vertical dispersion of a visible smoke plume. To date only a limited range of atmospheric conditions have been investigated, but in future there are likely to be wider applications for photogrammetry in the AAEC meteorological site surveys.

## 5. ATMOSPHERIC STABILITY, TEMPERATURES AND RAINFALL IN THE JERVIS BAY REGION

Data on a semi-climatological time scale were collected during the meteorological studies near Murray's Beach as well as the subsequent acoustic sounding research programme at the Jervis Bay settlement. Initially, a 30 m tower at a location south-west of Murray's Beach (the Jindivik control tower) was instrumented with temperature sensors for atmospheric stability measurements. Inaccessibility to the site for instrument servicing purposes resulted in insurmountable data extraction problems which precluded presentation of the results in this report. Instead, the diurnal variations of atmospheric stability categories from records collected at the Jervis Bay settlement are indicated for a shorter period of time.

Brief mention is made of the dry bulb, ground and Stevenson screen minimum temperatures and the sea water temperatures measured at Murray's Beach. These results are compared with similar statistics from the small Bowen Island meteorological station which is still in operation. With such a complex land-sea mass configuration which has affected the behaviour of air masses traversing the area, it is likely there will be similar complicated horizontal rainfall patterns. Both the rainfall climatology and days of heavy rainfall were studied from data collected at three observation stations.

### 5.1 Atmospheric Stability Analyses

**Analysis for the Jervis Bay Settlement.** Similar to the preliminary results presented for the acoustic sounding research at the Jervis Bay settlement, the atmospheric stability measurements span a period of only six months, from 23rd June 1972 to 4th January 1973. In Table 17 the diurnal variation of the atmospheric stability (temperature gradient) categories shows a predictable trend. The surface temperature inversions begin to form after 1700 EST and develop to their strongest intensity by 0200 EST. The inversion break-up processes commence about 0700 EST and are complete by 1000 EST when approximately dry adiabatic conditions ( $-1$  to  $0^\circ\text{C}$  per 30 metres) are established. With further solar radiation heating the atmosphere becomes progressively more unstable until 1200 EST. Thereafter most temperature gradients are observed in the range  $-2$  to  $0^\circ\text{C}$  per 30 metres until about sunset.

*Atmospheric Stability Wind Roses.* The presentation of wind direction roses for the different atmospheric stability categories in a sense only confirms the findings of the diurnal wind analyses in Section 3. In Figure 24 there is a trimodal distribution of winds from the north, south-east and south-west directions with atmospheric instability. The north-east sea breeze and northerly bay breeze become prominent in near isothermal conditions. Off-shore winds from the west to north-west sector exert a stronger influence with increasing intensity of the surface inversions.

## 5.2 A Climatology of Temperatures from Jervis Bay

*Temperatures from Murray's Beach and Bowen Island.* Monthly mean temperature data from Murray's Beach and Bowen Island are presented for the sixteen months from October 1970 to January 1972 (Table 18). Using these data, there is a brief discussion on the relationship between the Murray's Beach and Bowen Island minima and maxima temperatures, followed by the annual variation of the ground level (0.05 m above the surface) and Stevenson screen minima temperatures. The section on temperatures is concluded by a comparison of the sea water and dry bulb temperatures measured near Murray's Beach.

*Temperature Minima and Maxima at Bowen Island and Murray's Beach.* The temperature minima measured on the island station are about 3°C warmer than on the mainland Murray's Beach site (Figure 25). A comparison of the temperature maxima shows that this difference is reduced to about 1.5°C with improved horizontal and vertical mixing of the atmosphere (Figure 26). This indicates that at least the trends are correct. Under stable inversion conditions, the air mass over water is warmer, but this should revert to a hotter land air mass with increased solar radiation heating. The fact that the temperature maxima do not reverse suggests that an instrument exposure problem exists for the Bowen Island station.

The annual cycle of temperature minima from Murray's Beach (Figure 27) has a peak in February, thereafter decreasing until the July to September period. The positive temperature difference (inversion) between the ground and Stevenson screen levels steadily increases to 2°C by the winter months. In October, there was an abrupt change to greater than 5°C in both 1970 and 1971. This suggests an increase in intensity of the low level inversions during this month; however, further investigations are needed to establish the relationship between the microscale inversions (0.05 to 1 metre) and those detected higher in the atmosphere (of the order of 100 to 500 m altitude).

## 5.3 Surface Sea Water Temperature Measurements

Before discussing the biological effects of a thermal discharge of waste water from a nuclear power station, it is essential to investigate the natural, and sometimes substantial, temperature fluctuations in the sea water. In these endeavours, the surface sea water temperature was sampled twice daily at 0900 EST and 1500 EST as part of the routine meteorological observations in the Murray's Beach area.

Initially, a thermometer was floated from a rock ledge at one end of Murray's Beach; however this method had possible radiation and exposure errors. Then the sea water was sampled by filling a thermos flask, inserting a thermometer through a cork seal and taking a reading after equilibrium had been reached.

The monthly mean 0900 EST and 1500 EST sea water and air temperatures from Murray's Beach were plotted for the survey period December 1970 to January 1972, (Figure 28). It is seen that the maxima of both the air and sea water temperatures occur simultaneously in February, but that the minimum air temperature in July precedes that of the sea water temperature by about 15 days. The amplitudes of the annual sea water temperature cycles (8.4°C at 0900 EST and 8.7°C

at 1500 EST) are reduced with respect to those of the air temperature (11.7 °C at 0900 EST and 8.7 °C at 1500 EST).

To check the disturbances in the smooth annual cycle which occurred after October 1971, the air temperatures at 0900 EST and 1500 EST were plotted from the Murray's Beach and Bowen Island observations (Figure 29). The difference in magnitude of the monthly averages from the two stations can probably be attributed to the variation in the exposures of the thermometers. On Bowen Island there is no radiation shielding of the sensor, whereas the Murray's Beach thermometer is naturally ventilated in a Stevenson screen. Nevertheless, similar trends are evident in the two air temperature curves, with a decrease in the rise of the temperature from October 1971 to January 1972. The unusually low January 1971 averages from Bowen Island are due to only five observations being made during this month. As a result it can be stated that the sea water temperature curves plotted after October 1971 reflect geophysical variations rather than systematic errors in the measurement technique.

To further investigate the diurnal cycle of the sea water temperature, monthly averages were extracted for the differences between the 1500 EST and 0900 EST readings. By contrast to the curves presented as Figures 28 and 29 there is no annual cycle discernible (Figure 30). The average diurnal variation until October 1971 is about +0.6 °C, but thereafter this rises to +1.2 °C. Changes of this magnitude are not thought to have any significant biological effects on marine organisms, however, on individual occasions variations greater than 2 °C were observed. These data were extracted for a fourteen month period but only represented 59% of all days, as personnel were unavailable for weekend work on most occasions. Out of 246 days, 35 were in the category of greater than 2 °C.

$\Delta T_s$  = (Sea Water Temperature)

1500 EST		0900 EST
$+2 \leq \Delta T_s < +3$	$\Delta T_s \geq +3$	$-3 < \Delta T_s \leq -2$
28	6	1

Annually, 2.64% of all days will have diurnal changes in the sea water temperature of greater than 3 °C in magnitude.

**Conclusions.** The sea water temperatures at Murray's Beach analysed over fourteen months from December 1970 to January 1972 showed an annual cycle with an amplitude of 8.5 °C. The diurnal temperature variations were greater than 3 °C on 2.64% of all days per year, with the average variation between 0900 and 1500 EST being +0.8 °C.

#### 5.4 Rainfall Studies at Jervis Bay

**Comparison of Murray's Beach, Bowen Island and Jervis Bay Settlement Data.** One important symptom of a diverse and complex mesometeorology of a region is the horizontal variability of the rainfall measurements. At Jervis Bay, three stations were located in close proximity to the Murray's Beach power station site. These were in the Forestry Department's area at the Jervis Bay settlement, in the meteorological compound at Murray's Beach and on Bowen Island. All stations had the small Professional type rain gauge with an inverted conical head ducting the water into a graduated cylinder below. Data were available from October 1970 to December 1972 at both Bowen Island and the Jervis Bay settlement; however these were terminated at the end of January 1972 for the Murray's Beach meteorological station.

Simultaneous histograms of the monthly rainfall totals are plotted for the survey period (Figure 31). Several features of the histograms are outstanding and require a more detailed study. With a monthly rainfall total of less than 76.2 mm, all stations measure to within 12.7 mm of each other, with Murray's Beach, in general, having the highest and Bowen Island the lowest recordings.



However, in the three months of very heavy rainfall (December 1970, February 1971 and January 1972) this trend changes, with the Jervis Bay settlement now measuring significantly more rain than the other two stations ( $> 25.4$  mm).

On closer inspection of these three months' data, some interesting features were revealed (Table 19). In general, winds having an easterly component lead to marked differences in the horizontal distribution of rainfall, whereas those from the south do not lead to such disparity in the station recordings.

One explanation of this observation may lie in the diversity of the land-sea mass trajectories with changing wind directions as the air moves inland. For instance with prevailing east to north-east wind, the air mass on reaching Bowen Island is only starting to rise as it passes over the land. At Murray's Beach the land trajectory of the air mass is a little longer; however, on traversing the four miles across Jervis Bay to the Jervis Bay settlement, the local topography will have exerted a more significant influence and consequently a heavier rainfall could result. By contrast, with a prevailing southerly wind the land trajectory at Murray's Beach and Jervis Bay settlement would be similar, whereas Bowen Island still would be forcing the air mass to rise on its initial interception with a land mass. As a result, a lower rainfall reading might be predicted on Bowen Island under a southerly wind regime.

To further investigate these trends on a climatological basis, all days were classified into 12.7 mm rainfall categories up to 63.5 mm per day. Because there were so few observations above 25.4 mm per day, all occurrences were regrouped into a  $> 25.4$  mm category. Two approaches were used for the wind analysis; one set of results is shown for the simultaneous measurement of wind direction and rainfall at 0900 EST (Figure 32) and in a second analysis the 1500 EST wind direction (Figure 33) was compared with the 0900 EST rainfall reading on the following day. In this way a knowledge of the actual time and period of rainfall is not necessary.

In Figure 32 a comparison of the no rain and rainfall wind roses shows a diminished contribution in the west to north-west sector and a significant increase in the south and south-west wind contributions for days of rain. It is difficult to reflect upon changes in the wind rose patterns with increasing rainfall as the number of observations rapidly decreases. However, it might be observed that the south-east to north-east sector seems to contribute increasingly more with intensity of rainfall at the expense of the south-west influence.

This trend is also reflected in the 1500 EST wind roses from both Bowen Island and Murray's Beach (Figure 33). In all cases the north-east sea breeze is predominant, however the south-west and southerly winds are favoured on days of rain, with the easterly influence increasing with increasing rainfall total.

**Summary.** It is local knowledge that the rainfall patterns through the NSW south coast regions covering the Jervis Bay region can vary rapidly with distance inland and parallel to the coast. In this brief section the relationship of the wind directions to the occurrence of rainfall has been investigated. The following features have emerged:

1. On days of heavy rainfall ( $> 76.2$  mm) the horizontal variations in rainfall recordings are greatest.
2. A prevailing wind with an easterly component seems to bring the heavy rainfall, however there is also an increased contribution from the south to south-west winds when comparing days of positive to no rainfall.

#### 5.5 A Comment on the Bushfire Potential in Jervis Bay Against 1972 Rainfall Figures

In late 1972 and early 1973, bushfires devastated large areas of the Jervis Bay nature territory with resulting widespread destruction of heath, pine plantations, gum trees and other natural species of flora and fauna. One of the primary reasons for such a critical bushfire poten-

tial was the abnormally low rainfall during the last half of 1972. In Table 20, the 1972 rainfall figures are compared with an 11-year average for the Bowen Island station. In all months the 1972 recorded rainfall was below average with July, September and December having below 7.62 mm.

Similarly a comparison of three seasons maximum temperature data for December showed 1972 to be 3 °C above average. In combination with the low rainfall observations, these high temperatures led to a drying of the vegetation with disastrous consequences when the flashpoint was reached.

## 6. ACKNOWLEDGEMENTS

The authors wish to acknowledge the continuing advice and guidance given to the project by Mr. E. Charash and Mr. D. R. Davy, Head of the Health Physics Research Section. Personnel from the following departments and sections have also made considerable contributions: Mr. Jim Alexander and the rangers of the Department of Conservation and Agriculture, Jervis Bay; Dr. Ian Bourne of the RAAF Physics Department, University of Melbourne; Mr. John Carrington, Bowen Island, ACT; members of the Instrumentation and Control Division, the Applied Mathematics and Computing Section and Environment and Public Health Division of the AAEC Research Establishment, and the Earth Sciences Department, Macquarie University. All this help is gratefully recorded.

## 7. REFERENCES

- Air Ministry Meteorological Office (1956) – Handbook of Meteorological Instruments. Part I Instruments for Surface Observations. HMSO, London.
- Ball, F.K. (1960) – Control of inversion height by surface heating. *Quart. J. Roy. Met. Soc.* 86 (370) 483–494.
- Beran, D.W. (1970) – Application of acoustics to meteorology. Report II, Project EAR, Meteorology Dept., University of Melbourne.
- Charash, E. (1971) – Turbulent diffusion in the ocean and bay in the Jervis Bay area. *Proc. Conf. Australian Marine Sciences Assoc.*, Brisbane.
- Clark, G.H. (1970) – Studies in air pollution meteorology. M.Sc. Thesis, University of Melbourne.
- Culkowski, W.M. (1961) – Time exposure photography of smoke plumes, US Atomic Energy Commission Report ORO-359.
- Gething, J.T. (1972) – Current achievements and aspirations in acoustic remote sensing (A report on the NOAA Workshop in Atmospheric Acoustics, Boulder, Colorado, 6–7 July 1972). *Met. Dept. University of Melbourne*.
- Gifford, F.J. (1959) – Smoke plumes as quantitative air pollution indices. *Int. J. Air Pollut.* 2: 42–50.
- Halitsky, J. (1961) – Single camera measurement of smoke plumes. *Int. J. of Air and Water Pollut.* 4 (3/4) 185–189.
- Harris, C.M. (1966) – Absorption of sound in air versus humidity and temperature. *J. Acoust. Soc. Amer.* 18 (2) 274–283.
- Hicks, B.B., Dyer, A.J. and King, K.M. (1967) – The fluxatron – a revised approach to the measurement of eddy fluxes in the lower atmosphere. *J. Appl. Meteorol.*, 6 (2) 408–413.

- Idso, S.B. and Cooley, K.R. (1971) – The vertical location of net radiometers . 1 – The effects of the underlying air layer. J. Meteorol. Soc. of Jap. 49 (5) 343–349.
- McAllister, L.G., Pollard, J.R., Mahoney, A.R. and Shaw, P.J.R. (1968) – Acoustic sounding – a new approach to the study of atmospheric structure. WRE Tech. Note CPD (T) 160, Salisbury, South Australia.
- Mazzarella, D.A. (1972) – An inventory of specifications for wind measuring instruments. Bull. Amer. Meteorol. Soc. 53 (9) 860–871.
- Pasquill, F. (1961) – Estimation of the dispersion of windborne materials. The Meteorological Magazine, 90 (1063) 33–49.
- Shaw, N. (1971) – Acoustic sounding of the atmosphere. PhD. Thesis, Department of Physics, RAAF Academy, University of Melbourne.
- Shaw, N., Bourne, I. and Moncur, R. (1972) – Acoustic and high resolution radiosonde soundings of the lower atmosphere. Bureau of Met., Working paper 153, 25/4058.
- Shirvaikar, V.V., Kapoor, R.K. and Sharma, L.N. (1969) – A finite plume model based on wind persistence for use in environmental dose evaluation. Atmos. Environ. 3: 135–144.
- Shirvaikar, V.V., Sitaraman, V., Kapoor, R.K., Sundarajan, A., Sharma, L.N. and Sastry, P.L.K. (1970) – Micrometeorological and atmospheric diffusion studies at nuclear power station sites in India . Part II – Atmospheric diffusion studies. Indian J. Meteorol. Geophys. 21 (4) 529–538 .
- Shirvaikar, V.V. (1972) – Persistence of wind direction. Atmos. Environ. 6: 889–898.
- Singer, I.A. and Smith, M.E. (1953) – Relation of gustiness to other meteorological variables. J. Meteorol. 10. (2) 121-126.
- Slade, D.H. (1969) – Low turbulence flow in the planetary boundary layer and its relation to certain air pollution problems. J. Appl. Meteorol. 8 (4) 514–522.
- Van der Hoven J. (1969) – Wind persistence probability. ESSA Tech. Memo. EARLTM – ARL 10, 31.



**TABLE 1**  
**ACOUSTIC SOUNDER PATTERN CLASSIFICATION**

Code	Characteristics
0	Missing, indefinable or random noise – these records usually occur under strong wind or rain type conditions when the ambient noise levels saturate the incoming acoustic signals. They are characterised by a uniform grey, a white ( = saturation of the pre-amplifier) or a homogeneous grey mottled type of record.
1	Bottom layer only, homogeneous and/or 'spiky', thin ~ 150 m thick – a uniform intensity pattern with vertical spikes not exceeding 150 – 300 m, but sometimes varying in height with time. Usually associated with only a slight mottling of the chart above the surface layer.
2	Bottom layer only, homogeneous and/or 'spiky', thick > 300 m – similar comments apply as for pattern type 1. The uniform vertical 'spikes' or 'grass' type of records show no horizontal layering and are usually associated with low ambient noise and wind turbulence levels.
3	Bottom layer only, wavy and/or complex, thin ~ 300 m – the patterns can form horizontal layers (wavy) or intensity variations (complex) which vary both in height with time and also echo intensity.
4	Bottom layer only, wavy and/or complex, thick ~ 450 m – usually more intense near the ground, these patterns show temporal height variability in the horizontal layers. The complex layers may also have higher frequency waves or spikes with intermittent echo free zones.
5	Double layer, separation indistinct or small – when viewed over several hours of record there is generally a clear zone less than 150 m thick separating two distinct layers of stronger echoes. This zone is not always echo free but can have a mottled effect or noise superimposed. The continuity of the clear zone contrasts with the intermittent appearance of similar zones in pattern types 3 and 4. The layers are usually horizontal, neither ascending nor descending with time.
6	Double layer, separation distinct or large – these records are observed under a variety of conditions; during either day or night; with high or low ambient noise levels. The upper layer is usually thinner ( ~ 150 m thick) than the lower layer and clearly separated by 300 to 600 m generally echo free zones. Again the layers are horizontal and neither descend nor ascend with time.
7	Multiple or complex layers, weak intensity – these echo patterns may appear at any altitude and usually have more than two horizontal wave type layers with indistinct separations. Frequently intermittent or fragmented layers or patches are observed in the case of the complex patterns. In general there is no overall ascent or descent with time, but individual layers may show considerable height variability on a shorter time scale. The mottled grey record synonymous with the higher ambient noise levels is usually superimposed on these patterns.

(continued)

TABLE 1 (continued)

Code	Characteristics
8	Multiple or complex layers, strong intensity – the intense multiple layers are typified by distinct echo free zones usually varying in thickness with time. In the case of the complex echo patterns higher ambient noise levels are usually observed with high frequency waves (period of 5 to 10 minutes) and large amplitudes ( $\sim 300$ m). Again there may be intermittent or fragmented layers or patches of echoes in this pattern group.
9	Ascending echo, emerging or incipient – this echo pattern has its origins in a layer close to the ground and emerges to give an ascending echo with clear separation from the surface layer. Several hours of record need to be viewed in order to extrapolate back in time to the incipient echoes which usually only last for a period of about one hour.
10	Ascending echo, advanced – this echo pattern may not only have its origin in the type 9 pattern but it may also be present as a separate entity higher in the atmosphere. The rate of rise of these layers is about $225 \text{ m h}^{-1}$ . In general the mottled effect or higher ambient noise levels are superimposed.
11	<p>Descending echo, clear or large separation – again this pattern must be interpreted over several hours. The layer thickness may vary in time with an intermittent intensity. There is usually a stronger surface echo of type 1 or 2 associated with the descending layer under nocturnal conditions. During the daytime, type 13 echoes are typically observed being generated from the surface layer below the elevated echo.</p> <p><u>Note:</u> In classifying the cascading or multiple descending layers, the individual layers should be traced until merging with the surface layer (becomes type 12) and then reclassified as type 11 for the succeeding pattern (see example in Figure 5).</p>
12	Descending echo, merging with the bottom layer – the merging of the descending echo with the surface layer may take several hours, but occasionally it has been observed to occur much more quickly. A thickening of the surface echo pattern usually results. The transition from pattern type 11 to 12 occurs when the separation between the descending and surface layers becomes indistinct and/or $< 150$ m.
13	Thermal plume type structure with well defined 'spikes' or 'grass' in the echo patterns – these patterns are typified by broad based intense echoes usually tapering with height to leave echo free zones reaching nearly to the ground. Having thermal origins, these patterns usually occur during the daytime, however, this is not an exclusive condition. If observed at nighttime, the wind and consequently the ambient noise levels are much lower than during the day.

**TABLE 2**  
**MEAN HALF-HOUR WIND DIRECTION CODES**

Direction		Code
N	337.5 to 22.5 Degrees	1
NE	22.5 to 67.5 "	2
E	67.5 to 112.5 "	3
SE	112.5 to 157.5 "	4
S	157.5 to 202.5 "	5
SW	202.5 to 247.5 "	6
W	247.5 to 292.5 "	7
NW	292.5 to 337.5 "	8
	No Data	9

**TABLE 3**  
**A COMPARISON OF THE VANE RESPONSE CHARACTERISTICS OF THE**  
**BENDIX-FRIEZ AEROVANE AND THE DINES PRESSURE TUBE ANEMOGRAPH**

(Mazzarella 1972)

Sensor	Specifications				
	Damping Ratio	Distance Constant (63% recovery) (m)	Damped Natural Wavelength (m)	Starting Threshold (km h <sup>-1</sup> )	Range (km h <sup>-1</sup> /deg.)
Bendix-Friez Aerovane 3 bladed Propeller	0.28	4.6		4.5	161/200°
Vane		10.4	12.5		579/540°
Dines Pressure Tube Anemograph Pressure Tube	0.31			> 5.6	161/200°
Vane		13.8	16.2	1.9	

TABLE 4

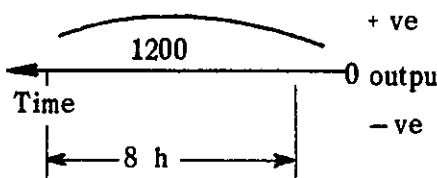
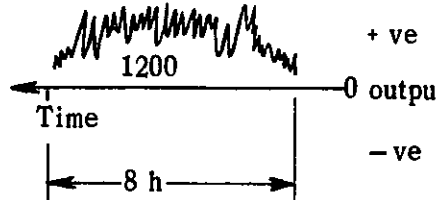
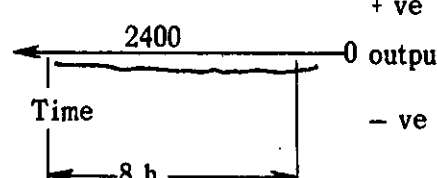
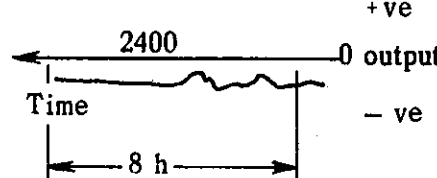
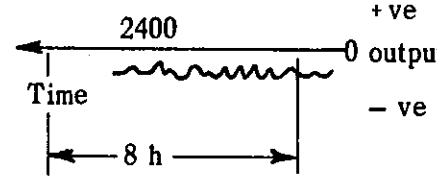
## A DESCRIPTION OF THE WIND DIRECTION TURBULENCE TRACE TYPES

Code	Characteristics
1	Fluctuations in the wind direction exceeding 90 degrees, period $\sim 4$ min – an open, widely fluctuating trace.
2	Fluctuations ranging from 15 to 45 degrees (period $< 1$ min) superimposed on a long period ( $\sim 30$ min) low amplitude ( $\sim 15$ degrees) wave – a dense trace with intermittent larger amplitude fluctuations.
3	Fluctuations ranging from 45 to 90 degrees with a more open trace (period 2–4 min) than traces 2 and 4 – again intermittent large amplitude fluctuations are superimposed.
4	Fluctuations $\geq 15$ degrees, period $< 0.5$ min, distinguished by an unbroken solid core of trace through which a straight line can be drawn without touching open space in a one hour interval.
5	Smooth trace with no high frequency oscillations present – associated with strong inversions and probably accompanied by very low levels of vertical turbulence.
6	Smooth trace (similar to type 5) punctuated by intervals of intermittent low amplitude ( $< 10$ degrees) high frequency fluctuations – associated with weaker inversions, low but measurable vertical turbulence indicative of the presence of intermittent mechanical turbulence.
7	Almost entirely turbulent flow with a high frequency and low amplitude ( $< 10$ degrees); only occasional smooth flow evident – measurable vertical turbulence indicated – indicative of mechanical turbulence.
8	Smooth trace punctuated by intervals of intermittent low amplitude ( $< 10$ degrees) high frequency fluctuations superimposed on a long period ( $\sim 30$ min) low amplitude ( $\sim 20$ degrees) wave – similar to a meandering trace 6 and therefore indicative of limited vertical and mechanical turbulence.
9	Turbulent trace with a high frequency, low amplitude ( $< 10$ degrees) trace, superimposed on a longer period ( $\sim 20$ min) low amplitude ( $\sim 20$ degrees) wave – similar to a meandering trace 7 and therefore indicative of the presence of both vertical and mechanical turbulence.
10	Stepping, square cornered or completely smooth trace caused by inability of the vane to follow all direction changes at low wind speeds – probably associated with little or no vertical turbulence.



TABLE 5

## A CLASSIFICATION SYSTEM FOR THE NET ALL WAVE RADIOMETER TRACES

Time of Day	Trace Characteristics	Code
Day	Smooth Trace 	1
	Disturbed (cloudy) Trace 	2
Night	Smooth Trace 	3
	Smooth Trace with occasional positive fluctuation 	4
	Disturbed Trace 	5

**TABLE 6**

**A FREQUENCY (%) TABLE OF SOUNDER PATTERN CATEGORIES VERSUS  
TEMPERATURE DIFFERENCE DATA**

Sounder Pattern	Temperature Difference (°C per 30 m)					
	-3 to -2	-2 to -1	-1 to 0	0 to +1	+1 to +2	+2 to +3
0	9.7	10.3	9.9	6.7	3.8	3.7
1	2.4	1.3	4.5	9.0	10.0	14.5
2	6.0	2.3	5.0	7.8	8.4	12.7
3	7.4	2.8	2.0	5.4	12.4	18.2
4	5.7	5.6	6.0	5.5	11.4	10.3
5	3.6	7.8	10.5	6.8	6.9	5.4
6	2.7	8.0	7.0	9.6	7.4	3.8
7	5.8	6.8	8.1	7.5	8.1	3.8
8	4.9	4.6	7.0	8.8	9.0	4.0
9	4.4	12.3	10.3	4.4	2.9	5.3
10	11.8	17.3	9.0	4.5	1.4	3.0
11	5.3	2.3	8.3	9.3	9.6	2.3
12	16.6	4.6	5.2	10.0	3.8	9.1
13	13.6	14.1	7.4	4.7	5.0	4.0

*The table was normalised with respect to the frequency of occurrence of the individual sounder patterns.*

*Columns total 100%*

TABLE 7

## THE DIURNAL VARIATION OF THE SOUNDER PATTERNS

Hours of Day Acous- tic Sounder Patterns	0000	0100	0200	0300	0400	0500	0600	0700	0800	0900	1000
0	4.4	4.8	5.4	4.9	5.2	5.4	5.5	6.3	8.0	11.4	14.1
1	9.0	6.9	3.1	3.6	5.7	5.0	5.4	4.3	6.0	4.1	0.0
2	8.2	8.2	7.2	7.8	10.8	7.2	7.8	8.2	4.8	3.8	0.7
3	10.7	11.8	11.2	8.5	7.9	9.5	8.5	10.9	12.4	6.6	2.6
4	11.9	11.2	8.3	11.9	10.3	12.4	10.9	9.4	11.8	9.7	8.9
5	8.5	8.3	7.6	5.4	4.5	7.0	6.6	1.9	3.3	2.5	6.9
6	7.7	3.8	3.8	7.7	9.1	8.6	5.9	3.3	0.5	2.5	4.4
7	6.2	9.1	10.1	7.1	7.2	7.7	6.2	6.8	5.5	6.9	9.2
8	8.7	9.9	8.4	8.7	9.5	9.5	5.7	4.8	5.6	7.0	7.1
9	4.5	1.6	9.5	4.5	3.2	4.7	9.0	15.4	15.0	4.2	7.3
10	6.0	5.3	7.4	12.0	5.3	0.0	1.0	5.1	7.7	20.8	16.2
11	5.4	8.9	8.9	9.2	12.2	9.7	5.4	5.5	4.3	1.1	0.0
12	3.0	4.8	4.8	4.6	4.8	9.5	16.7	12.5	6.7	4.2	2.5
13	5.7	5.4	4.1	4.1	4.4	3.9	5.3	5.6	8.5	15.2	20.1

**TABLE 7 (continued)**

Hours of Day Acous- tic Sounder Patterns	1100 1200	1200 1300	1300 1400	1400 1500	1500 1600	1600 1700	1700 1800	1800 1900	1900 2000	2000 2100	2100 2200	2200 2300	2300 2400
0	13.9	14.7	15.5	14.3	10.7	9.1	7.5	5.0	5.1	4.6	4.1	4.1	4.2
1	0.0	0.0	0.0	1.0	0.8	1.5	10.7	11.8	15.7	15.8	16.5	12.5	12.7
2	0.7	2.7	2.2	2.5	1.5	4.9	6.6	7.5	10.9	11.4	11.0	11.3	9.5
3	0.8	0.0	0.0	0.0	0.7	0.0	3.2	2.1	5.2	7.8	10.4	13.7	11.4
4	5.4	4.0	1.5	1.5	2.0	4.6	4.0	2.7	3.5	5.3	4.1	3.8	7.4
5	9.0	14.1	12.7	4.8	6.5	8.4	10.1	12.0	7.1	3.9	4.8	8.0	11.1
6	5.4	6.0	6.6	9.4	11.0	9.8	9.8	12.2	12.8	9.5	8.1	6.5	4.8
7	8.7	7.4	6.9	8.4	8.0	7.7	9.0	7.4	4.6	3.9	6.3	7.5	6.6
8	3.0	5.0	3.8	6.9	7.6	11.0	12.8	10.3	7.5	4.9	3.6	3.5	6.2
9	20.2	5.0	14.5	9.6	8.1	5.7	3.6	7.4	8.8	5.5	4.0	2.9	4.4
10	13.4	14.9	11.3	22.3	20.1	8.8	3.6	2.0	1.0	0.9	3.6	1.9	4.8
11	1.1	5.1	12.4	7.4	11.4	12.7	7.4	3.1	9.7	9.8	5.5	6.6	6.0
12	2.3	2.5	0.0	0.0	2.0	9.6	7.3	12.0	4.4	12.5	14.8	11.5	4.4
13	16.1	18.6	12.7	11.9	9.5	6.2	4.5	4.5	3.8	4.3	3.3	6.3	6.5

**TABLE 8****A DESCRIPTION OF THE WIND RECORDING STATION NETWORK, JERVIS BAY**

Station	Observation Period and Sampling Procedures	Comments
Murray's Beach Meteorological Compound – Manual Observations	27.9.1970 to 28.1.1972 0900 and 1500 EST observations/day	Wind speed measured from a 10 min wind run observation. Wind direction from a manually held vane or the Dines anemograph vane.
Murray's Beach Meteorological Compound – Dines Anemograph	18.2.1971 to 24.2.1972 24 hourly averaged observations/day	Installed on a 10 m high tower with a direct physical link to the recorder below.
Bowen Island	1.8.1970 to 31.12.1972 0900 and 1500 EST observations/day	Wind speed from a 10 min wind run on a Casella instrument. Wind direction from a manually held wind vane in a well exposed location.
Jindivik Airstrip – Dines Anemograph	31.3.1968 to 31.12.1969 24 hourly averaged observations/day	Wind measurements not accurate at low speeds.
Jervis Bay Settlement – Dines Anemograph	23.6.1972 to 4.1.1973 48 half-hourly averaged observations/day	Located on a 3 m high tower, 10 m above ground level.
HMAS Albatross – Nowra	1964 to 1968 inclusive	Manual observations.

TABLE 9

FREQUENCY OF OCCURRENCE (%) OF VARIOUS TEMPERATURE DIFFERENCES  
OR ATMOSPHERIC STABILITY CLASSES

Temperature Difference per 30 m									
-5 to -4	-4 to -3	-3 to -2	-2 to -1	-1 to 0	0 to +1	+1 to +2	+2 to +3	+3 to +4	> +4
0.4	1.9	5.3	14.4	24.4	29.4	15.7	6.6	1.9	0.2

TABLE 10

THE RELATIONSHIP OF THE WIND DIRECTION TURBULENCE TRACE  
TYPES TO TEMPERATURE DIFFERENCE OR ATMOSPHERIC STABILITY

(Frequency measured in %)

Turbulence Trace Type	Temperature Difference per 30 m					
	-3 to -2	-2 to -1	-1 to 0	0 to +1	+1 to +2	+2 to +3
1	20.2	22.6	14.2	7.2	5.8	3.2
2	12.9	16.0	17.3	12.9	5.5	0.6
3	25.9	25.5	14.2	7.0	3.5	1.9
4	11.5	16.2	15.2	18.1	2.7	0.1
5	2.8	2.3	4.6	6.7	9.2	20.9
6	5.7	2.4	3.8	8.0	14.5	18.4
7	7.8	3.0	6.7	9.0	14.9	16.1
8	2.2	3.5	7.3	11.8	13.4	13.3
9	5.8	6.6	12.3	9.1	12.9	9.1
10	5.1	1.9	4.5	10.2	17.6	16.3

TABLE 11

## THE FREQUENCY (%) OCCURRENCE OF THE WIND DIRECTION TURBULENCE TRACES VERSUS WIND SPEED

(a) Night (1900 to 0700)

Turbulence Trace Type	Wind Speed (m sec <sup>-1</sup> )											
	< 1		1 - 2		2 - 4		4 - 8		> 8		Total	
	J.B.	M.B.	J.B.	M.B.	J.B.	M.B.	J.B.	M.B.	J.B.	M.B.	J.B.	M.B.
1	0.2	0.6	0.4	0.4	0.4	-	-	-	-	-	1.0	1.0
2	0.1	4.3	1.5	13.7	13.2	14.5	9.2	0.2	0.9	-	24.9	32.7
3	0.2	1.1	1.5	1.6	3.1	0.8	0.8	-	-	-	5.5	3.5
4	-	-	0.7	5.0	5.3	15.8	12.1	0.7	2.1	-	20.2	21.5
5	0.7	3.4	0.7	0.2	0.3	-	-	-	-	-	1.7	3.6
6	1.1	3.6	2.8	0.2	1.5	-	-	-	-	-	5.4	3.8
7	0.7	7.0	4.0	5.1	8.3	0.2	1.2	-	-	-	14.2	12.3
8	2.3	4.6	4.5	0.7	2.8	-	0.1	-	-	-	9.7	5.3
9	0.6	3.2	2.5	2.0	1.9	0.2	0.2	-	-	-	5.2	5.4
10	8.3	10.2	3.3	0.2	0.5	0.1	-	-	-	-	12.1	10.5
(b) Day (0700 to 1900)												
1	0.2	1.4	0.9	0.5	1.1	-	0.3	-	-	-	2.5	1.9
2	0.2	3.3	1.6	14.6	15.2	22.0	16.5	0.3	0.9	-	34.4	40.2
3	0.9	1.1	3.3	2.6	10.8	2.9	5.2	0.1	-	-	20.2	6.7
4	0.1	0.2	0.3	3.4	6.2	23.5	21.1	2.1	3.2	-	30.9	29.2
5	0.2	1.0	0.2	-	-	-	-	-	-	-	0.4	1.0
6	0.1	1.6	0.4	0.2	0.2	-	-	-	-	-	0.7	1.8
7	0.2	3.7	1.1	2.8	1.8	0.4	0.3	-	-	-	3.4	6.9
8	0.8	1.6	1.7	0.6	0.7	0.1	-	-	-	-	3.2	2.3
9	0.1	3.3	0.6	2.2	0.9	0.4	0.1	-	-	-	1.7	5.9
10	1.9	4.2	0.6	0.1	0.1	-	-	-	-	-	2.6	4.3

J.B. - Jervis Bay settlement    M.B. - Murray's Beach

**TABLE 12**

**PASQUILL'S ATMOSPHERIC TURBULENCE CATEGORIES**  
(After Pasquill 1961)

Surface Wind Speed (m sec <sup>-1</sup> )	By Day Incoming (Solar Radiation)			By Night Outgoing (Terrestrial Radiation)		
	Strong	Moderate	Slight	Slight	Moderate	Strong
0 - 2	A	A - B	B	F - F <sub>1</sub>	F - F <sub>1</sub>	F <sub>1</sub>
2 - 3	A - B	B	C	E	F	F <sub>1</sub>
3 - 5	B	B - C	C	D	E	F <sub>1</sub>
5 - 6	C	C - D	D	D	D	D
> 6	C	D	D	D	D	D



TABLE 13

A TABLE RELATING THE WIND SPEED, DIRECTION TURBULENCE TRACE TYPES,  
AND THE PASQUILL-TYPE TURBULENCE CATEGORIES

(Frequency measured in %)

Turbulent Trace Type	Wind Speed (m sec <sup>-1</sup> )									
	0 < 1		1 < 2		2 < 4		4 < 8		> 8	
	Night	Day	Night	Day	Night	Day	Night	Day	Night	Day
1	75 D 25 E	100A	75 D 25 E	100A	80 D 20 E	90 A 10 B	5 C 85 D 10 E	80 A 20 B	10 C 90 D	70 A 30 B
2	60 B 30 C 10 D	50 B 40 C 10 D	45 B 35 C 20 D	40 B 45 C 15 D	25 B 40 C 35 D	30 B 35 C 35 D	15 B 40 C 45 D	20 B 30 C 50 D	15 B 30 C 55 D	5 B 30 C 65 D
3	30 B 60 C 10 D	100A 0 B 0 C	25 B 65 C 10 D	90 A 10 B 0 C	20 B 60 C 20 D	85 A 10 B 5 C	15 B 50 C 35 D	75 A 15 B 10 C	10 B 40 C 50 D	60 A 20 B 20 C
4	10 B 60 C 30 D	20 B 70 C 10 D	10 B 50 C 40 D	15 B 75 C 10 D	5 B 45 C 50 D	10 B 65 C 25 D	5 B 35 C 60 D	8 B 55 C 37 D	2 B 33 C 65 D	5 B 35 C 60 D
5	0 F 100F1	0 E 100F	5 F 95 F1	10 E 90 F	10 F 90 F1	20 E 80 F	20 F 80 F1	30 E 70 F	30 F 70 F1	40 E 60 F
6	5 D 5 E 90 F	20 C 40 D 40 E	10 D 10 E 80 F	15 C 50 D 35 E	10 D 20 E 70 F	15 C 55 D 30 E	20 D 30 E 50 F	10 C 65 D 25 E	35 D 40 E 25 F	10 C 75 D 15 E
7	10 C 10 D 80 E	20 B 60 C 20 D	10 C 20 D 70 E	20 B 55 C 25 D	10 C 35 D 55 E	15 B 50 C 35 D	5 C 50 D 45 E	15 B 45 C 40 D	5 C 55 D 40 E	10 B 40 C 50 D
8	10 C 20 D 70 E	20 B 50 C 30 D	10 C 25 D 65 E	20 B 50 C 30 D	10 C 35 D 55 E	15 B 55 C 30 D	5 C 50 D 45 E	10 B 50 C 40 D	5 C 60 D 35 E	10 B 40 C 50 D
9	10 C 20 D 70 E	20 B 50 C 30 D	10 C 25 D 65 E	20 B 50 C 30 D	10 C 35 D 55 E	15 B 55 C 30 D	5 C 50 D 45 E	10 B 50 C 40 D	5 C 60 D 35 E	10 B 40 C 50 D
10	0 F 100F1	0 D 10 E 90 F	0 F 100F1	0 D 15 E 85 F	5 F 95 F1	5 D 35 E 60 F	5 F 95 F1	15 D 50 E 35 F	20 F 80 F1	20 D 55 E 25 F

### FREQUENCY (%) DISTRIBUTION OF PASQUILL-TYPE TURBULENCE CATEGORIES

Pasquill Categories	Wind Speed (m sec <sup>-1</sup> )											
	< 1		1 - 2		2 - 4		4 - 8		> 8		All Speeds	
	%		%		%		%		%		%	
	Night	Day	Night	Day	Night	Day	Night	Day	Night	Day	Night	Day
A	-	1.1	-	3.9	-	10.2	-	4.1	-	-	-	19.3
B	0.1	0.3	1.1	1.8	4.3	6.9	2.2	5.9	0.2	7.9	15.1	
C	0.5	0.7	3.0	2.6	11.3	11.7	8.7	17.2	1.4	24.5	33.6	
D	1.0	0.4	4.0	1.5	13.2	8.1	12.9	16.2	2.6	33.0	28.8	
E	3.8	0.2	8.0	0.2	7.8	0.1	0.7	-	-	20.3	0.5	
F	0.7	2.0	2.3	0.7	1.1	0.1	-	-	-	4.1	2.8	
F <sub>1</sub>	8.5	-	1.0	-	-	-	-	-	-	10.2	-	
<p>Observation period 23rd June 1972 to 4th January 1973.</p> <p>Total night observations 3987. Total day observations 3924.</p>												
(b) MURRAY'S BEACH												
A	-	2.5	-	2.8	-	2.5	-	0.1	-	-	7.9	
B	3.0	3.4	7.2	7.8	4.7	9.4	0.1	0.3	-	15.0	20.9	
C	3.3	6.4	9.2	11.9	13.8	23.4	0.4	1.3	-	26.7	43.0	
D	3.3	3.2	7.0	4.4	13.7	13.8	0.6	1.0	-	24.6	22.4	
E	10.2	1.0	5.5	0.1	0.3	-	-	-	-	16.0	1.1	
F	3.3	4.8	0.2	0.1	-	-	-	-	-	3.5	4.9	
F <sub>1</sub>	13.8	-	0.4	-	0.1	-	-	-	-	14.2	-	
<p>Observation period 24th February 1971 to 18th February 1972.</p> <p>Total night observations 2416. Total day observations 2434.</p>												

Observation period 23rd June 1972 to 4th January 1973.  
Total night observations 3987. Total day observations 3924.

(b) MURRAY'S BEACH

Observation period 24th February 1971 to 18th February 1972.  
Total night observations 2416. Total day observations 2434.

TABLE 15

A FREQUENCY (%) TABLE OF WIND DIRECTION VERSUS TURBULENCE TRACE TYPES

Wind Direction	Site	Turbulence Trace Types									
		1	2	3	4	5	6	7	8	9	10
N	Murray's Beach	0.9	30.3	3.0	41.0	2.1	2.2	7.7	3.1	4.8	4.9
	Jervis Bay	2.0	32.1	11.6	37.1	0.3	1.4	3.5	4.6	1.7	5.7
NE	Murray's Beach	0.5	41.8	2.0	36.7	0.2	1.5	5.8	2.2	5.7	3.6
	Jervis Bay	1.8	36.6	20.7	8.8	0.3	2.6	5.9	7.8	3.2	12.2
E	Murray's Beach	1.2	45.0	2.8	17.5	2.6	2.1	12.4	3.7	5.6	7.2
	Jervis Bay	4.1	25.9	21.3	10.2	1.8	1.0	10.9	7.4	4.1	13.5
SE	Murray's Beach	1.1	42.4	6.1	18.2	0.8	2.8	14.0	3.3	5.0	6.3
	Jervis Bay	2.2	31.6	17.4	23.4	0.9	2.1	10.1	3.6	3.7	5.0
S	Murray's Beach	1.4	40.7	5.5	28.7	1.9	2.3	8.3	2.8	4.1	4.2
	Jervis Bay	1.0	31.5	6.7	19.2	1.6	3.8	18.4	7.0	4.1	6.6
SW	Murray's Beach	1.2	33.3	8.8	13.2	3.4	4.4	14.4	3.0	6.4	12.0
	Jervis Bay	1.3	18.5	9.1	38.0	1.5	4.7	9.9	8.5	3.4	5.1
W	Murray's Beach	1.8	30.2	5.0	24.0	3.4	3.5	11.0	5.3	4.4	11.2
	Jervis Bay	2.2	27.7	11.8	30.0	0.5	3.3	6.0	5.7	4.6	8.2
NW	Murray's Beach	2.8	38.8	7.2	14.5	2.9	3.4	6.5	6.5	9.7	7.7
	Jervis Bay	1.8	37.9	13.0	13.4	1.5	3.6	7.3	7.7	3.7	10.2

TABLE 16

## PERSISTENCE OF ALL WIND DIRECTIONS COMBINED

Location	Cumulative Probability (%)			Sector Width (°)	Averaging Time (hours)
	50	25	10		
Murray's Beach	3.2	5.1	10.4	45	1
Jervis Bay Settlement	1.5	3.2	5.9	45	0.5
Tarapur, India (Shirvaikar 1972)	2.0	3.6	6.2	22.5	1

TABLE 17

## THE DIURNAL VARIATION OF ATMOSPHERIC STABILITY MEASUREMENTS AT JERVIS BAY SETTLEMENT

23. 6.72 TO 4. 1.73

Time (h) Temp. (°C)/30 m	0000 0100	0100 0200	0200 0300	0300 0400	0400 0500	0500 0600	0600 0700	0700 0800	0800 0900	0900 1000	1000 1100	1100 1200	1200 1300	1300 1400	1400 1500	1500 1600	1600 1700	1700 1800	1800 1900	1900 2000	2000 2100	2100 2200	2200 2300	2300 2400
-5 to -4	0.0	0.0	0.0	0.0	0.0	0.0	0.0	0.0	1.7	4.4	3.6	0.3	0.0	0.0	0.2	0.0	0.0	0.0	0.0	0.0	0.0	0.0	0.5	0.0
-4 to -3	0.0	0.0	0.0	0.0	0.0	0.0	0.0	1.2	6.4	13.7	17.1	5.7	4.1	3.5	2.3	0.6	0.0	0.0	0.0	0.0	0.3	0.3	0.3	0.0
-3 to -2	0.0	0.0	0.0	0.0	0.0	0.0	0.4	7.0	13.4	18.6	26.2	29.1	13.1	8.6	6.2	5.4	3.6	0.7	0.0	0.0	0.0	0.3	0.3	0.8
-2 to -1	1.0	0.5	1.0	2.1	0.9	0.2	3.2	11.2	21.3	29.7	27.3	42.9	55.3	49.0	34.4	23.5	19.4	13.5	4.2	1.0	0.8	0.8	1.8	1.6
-1 to 0	10.4	7.5	6.7	6.2	6.9	7.2	13.7	23.0	30.2	24.5	20.5	19.0	24.4	34.3	43.0	37.6	49.4	54.6	40.7	24.1	12.4	10.9	15.2	15.4
0 to +1	37.3	40.1	34.1	33.8	31.5	25.9	25.0	24.9	17.1	7.2	4.2	2.1	2.3	2.0	3.0	4.8	4.8	18.5	44.9	53.3	59.1	54.7	53.0	48.4
+1 to +2	33.7	32.6	36.9	35.6	29.9	24.7	18.3	14.0	4.0	0.3	0.3	0.3	0.0	0.5	0.7	0.2	0.2	0.7	4.7	14.1	17.4	20.2	17.6	20.6
+2 to +3	14.5	16.0	16.2	15.1	14.9	8.8	4.9	7.0	1.5	0.5	0.5	0.3	0.3	0.0	0.0	0.0	0.2	0.0	1.5	4.5	9.1	7.5	7.1	7.8
+3 to +4	2.6	3.4	4.4	5.1	3.0	2.1	2.5	1.9	0.0	0.0	0.0	0.3	0.3	0.0	0.0	0.0	0.0	0.0	0.0	0.5	1.0	4.9	3.9	4.9
+4 to +5	0.5	0.0	0.3	0.8	0.7	0.5	0.0	0.0	0.0	0.5	0.3	0.3	0.0	0.0	0.0	0.0	0.0	0.0	0.0	0.0	0.0	0.3	0.3	0.5

**TABLE 18**  
**MURRAY'S BEACH AND BOWEN ISLAND TEMPERATURES**

Month	Time EST	MURRAY'S BEACH					BOWEN ISLAND		
		Dry Bulb Temp. °C	Ground Min. Temp. °C	Stev. Min. Temp. °C	Stev. Max. Temp. °C	Sea Water Temp. °C	Dry Bulb Temp. °C	Max. Temp. °C	Min. Temp. °C
<u>1970</u>									
Oct.	0900	18.3	5.0	10.8	21.1	—	18.8	23.6	14.2
Oct.	1500	19.4	—	—	—	—	21.6	—	—
Nov.	0900	18.6	10.0	10.7	19.6	—	20.0	24.0	15.3
Nov.	1500	19.7	—	—	—	—	22.5	—	—
Dec.	0900	21.3	14.8	14.9	—	20.0	22.7	26.7	17.1
Dec.	1500	22.0	—	—	—	20.7	24.9	—	—
<u>1971</u>									
Jan.	0900	22.0	15.4	16.0	24.3	21.5	22.9	28.3	20.4
Jan.	1500	22.6	—	—	—	22.0	23.9	—	—
Feb.	0900	22.4	16.8	17.2	24.7	22.4	23.7	27.4	19.5
Feb.	1500	22.9	—	—	—	23.1	25.9	—	—
March	0900	22.1	14.1	15.6	23.9	21.7	22.2	27.0	18.2
March	1500	22.5	—	—	—	21.9	24.4	—	—
Apr.	0900	18.0	11.2	13.0	21.5	19.7	18.7	23.8	16.0
Apr.	1500	20.0	—	—	—	20.2	21.8	—	—
May	0900	15.7	7.9	9.7	17.9	17.3	15.9	20.5	13.5
May	1500	17.4	—	—	—	17.8	18.1	—	—
June	0900	12.7	6.2	8.5	15.9	15.7	12.6	17.2	11.0
June	1500	14.8	—	—	—	16.4	16.1	—	—
July	0900	10.7	3.1	5.1	14.6	14.3	11.0	16.0	9.3
July	1500	13.4	—	—	—	14.9	14.7	—	—
Aug.	0900	12.4	3.5	5.3	16.8	14.0	12.5	17.3	10.2
Aug.	1500	15.8	—	—	—	14.8	16.2	—	—
Sept.	0900	15.8	2.5	4.6	20.3	15.1	15.2	20.1	11.5
Sept.	1500	16.9	—	—	—	15.9	18.5	—	—
Oct.	0900	17.7	7.5	13.6	22.0	16.0	17.8	23.2	13.0
Oct.	1500	18.9	—	—	—	16.3	20.6	—	—
Nov.	0900	16.9	—	10.7	19.6	16.0	17.0	23.3	13.7
Nov.	1500	18.4	—	—	—	17.4	20.5	—	—
Dec.	0900	19.7	—	12.8	22.6	18.9	19.5	25.3	16.9
Dec.	1500	21.7	—	—	—	20.5	24.3	—	—
<u>1972</u>									
Jan.	0900	19.4	—	11.0	23.2	19.8	19.8	25.8	17.5
Jan.	1500	21.2	—	—	—	20.7	24.2	—	—

TABLE 19

TABULATION OF RAINFALL AND WIND DATA FROM MURRAY'S BEACH, BOWEN ISLAND  
AND JERVIS BAY SETTLEMENT FOR THE DAYS OF HEAVY RAINFALL

Date	Rainfall (mm)			Wind Direction		Wind Speed (m sec <sup>-1</sup> )	
	M.B.	B.I.	J.B.	M.B.	B.I.	M.B.	B.I.
8.12.70	26.4	5.0	16.7	SE	S	5.6	—
9.12.70	106.9	116.3	119.1	SE	S	6.4	—
				SE	SW	5.1	—
10.12.70	28.1	45.2	61.7	S	S	3.3	—
				NE	NE	4.1	—
11.12.70	0	0	0	NE	NE	3.3	—
				NE	N	3.1	—
12.12.70	12.7	13.2	15.4	SW	NE	1.3	—
				NW	N	3.6	—
30. 1.71		4.5	25.1	NW	N	1.3	—
				—	S	—	—
31. 1.71	75.6	19.8	14.9	—	S	—	—
				—	SW	—	—
1. 2.71	75.6	46.9	71.8	—	E	—	—
				—	N	—	—
2. 2.71		—	0.3	—	NE	—	—
				NW	NE	2.8	—
3. 2.71	2.5	3.5	1.7	S	SE	5.3	—
				SE	E	3.1	—
4. 2.71	23.3	17.2	22.3	E	E	4.1	—
				E	NW	2.8	—
5. 2.71	37.3	33.0	66.0	SE	NE	5.3	—
				NE	E	5.3	—
6. 2.71	173.2	53.3	74.6	—	E	—	—
				—	E	—	—
7. 2.71	173.2	99.0	91.4	—	E	—	—
				NE	E	2.0	—
8. 2.71	2.9	2.5	2.0	—	E	—	—
				NE	E	4.6	—
9. 2.71	9.9	2.3	2.5	NE	E	3.1	—
				NE	E	2.3	—
10. 2.71	15.2	5.8	9.1	NE	E	3.6	—
				S	SW	6.4	—
11. 2.71	7.1	20.3	21.0	S	SW	5.6	—
				SW	S	3.8	—
13. 1.72	23.3	16.2	25.4	S	SW	5.6	—
				S	SW	7.6	—
14. 1.72	14.7	12.1	17.5	S	S	7.1	4.9
				SE	SE	7.4	—
15. 1.72		41.9	51.3	SE	SE	5.6	—
				—	SE	—	—
16. 1.72	61.7	20.5	36.3	—	S	—	—
				—	S	—	4.2
17. 1.72		9.6	13.9	—	S	—	2.6
				E	SE	5.8	—
				NE	SE	4.8	6.7

M.B. Murray's Beach

B.I. Bowen Island

J.B. Jervis Bay

Wind direction and speed taken at 0900 (upper value) and 1500 (lower value)

TABLE 20

A COMPARISON OF THE 1972 AND 11-YEAR AVERAGE RAINFALL  
FOR BOWEN ISLAND

July	August	September	October	November	December	Observation Period
2.9	62.7	3.8	50	73.1	7.1	1972
53.1	76.4	74.6	79.2	77.7	88.9	11-year average (mm)

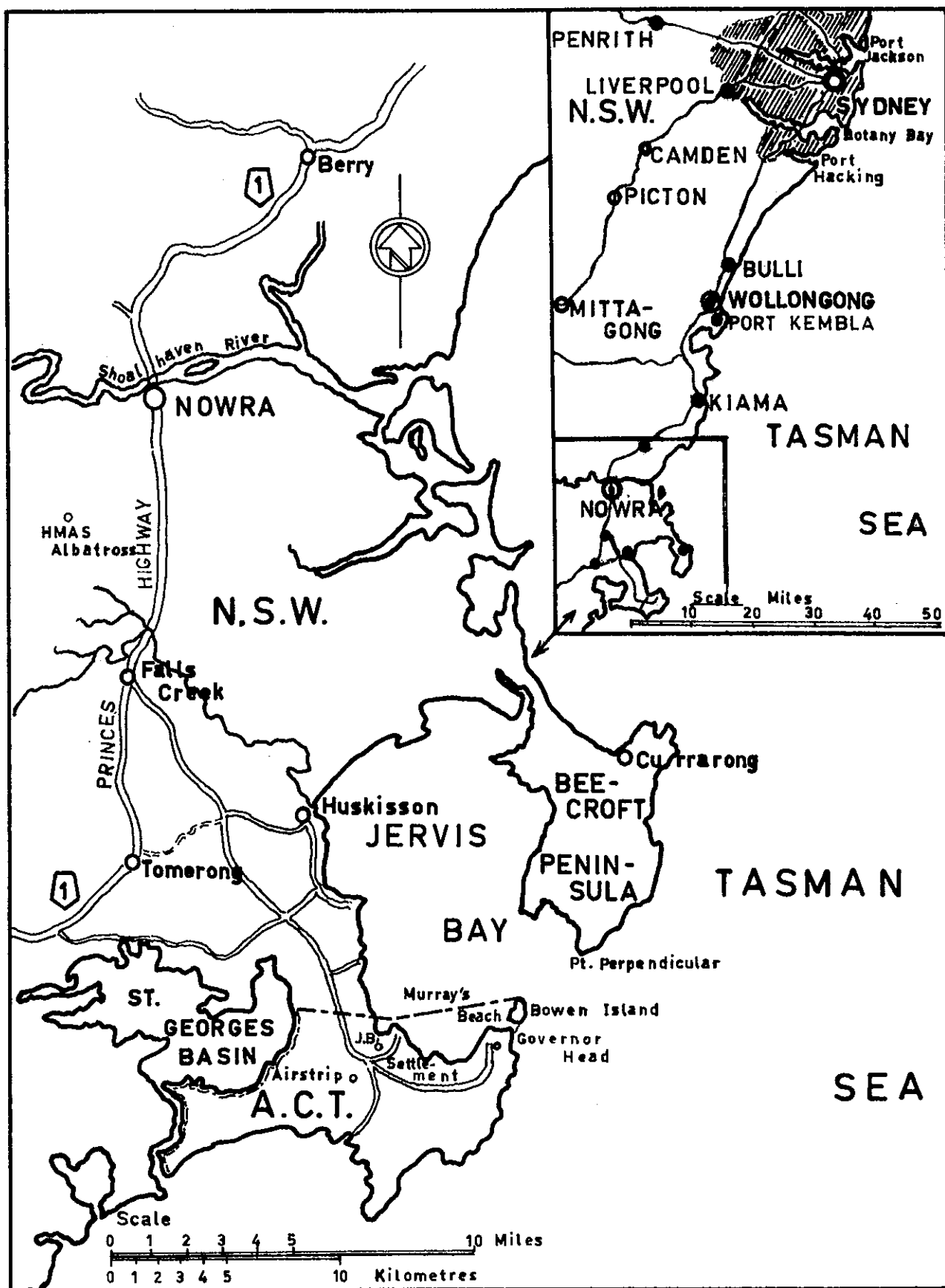


FIGURE 1. LOCATION, AREA OF JERVIS BAY



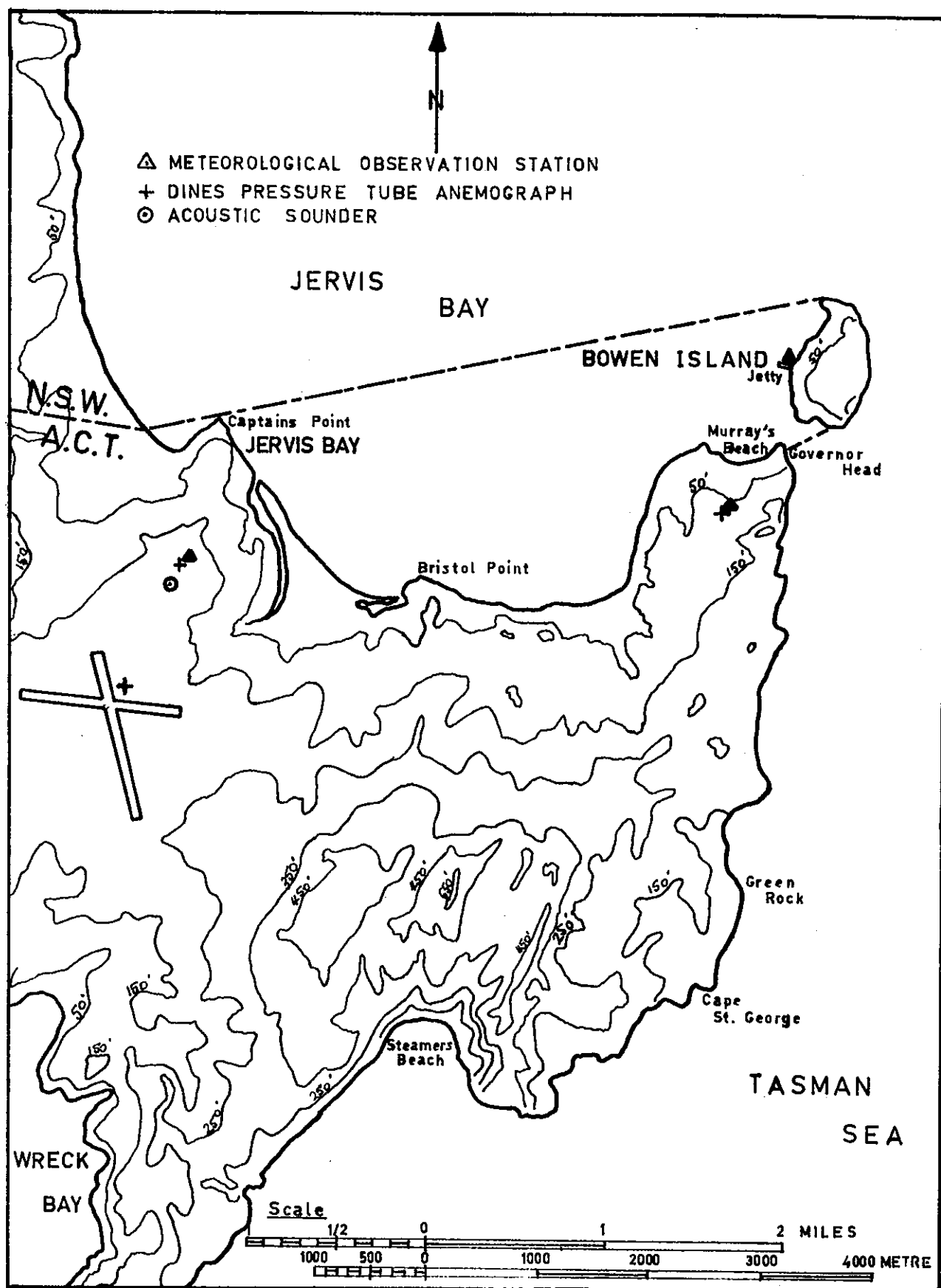


FIGURE 2. TOPOGRAPHICAL FEATURES OF THE JERVIS BAY AREA

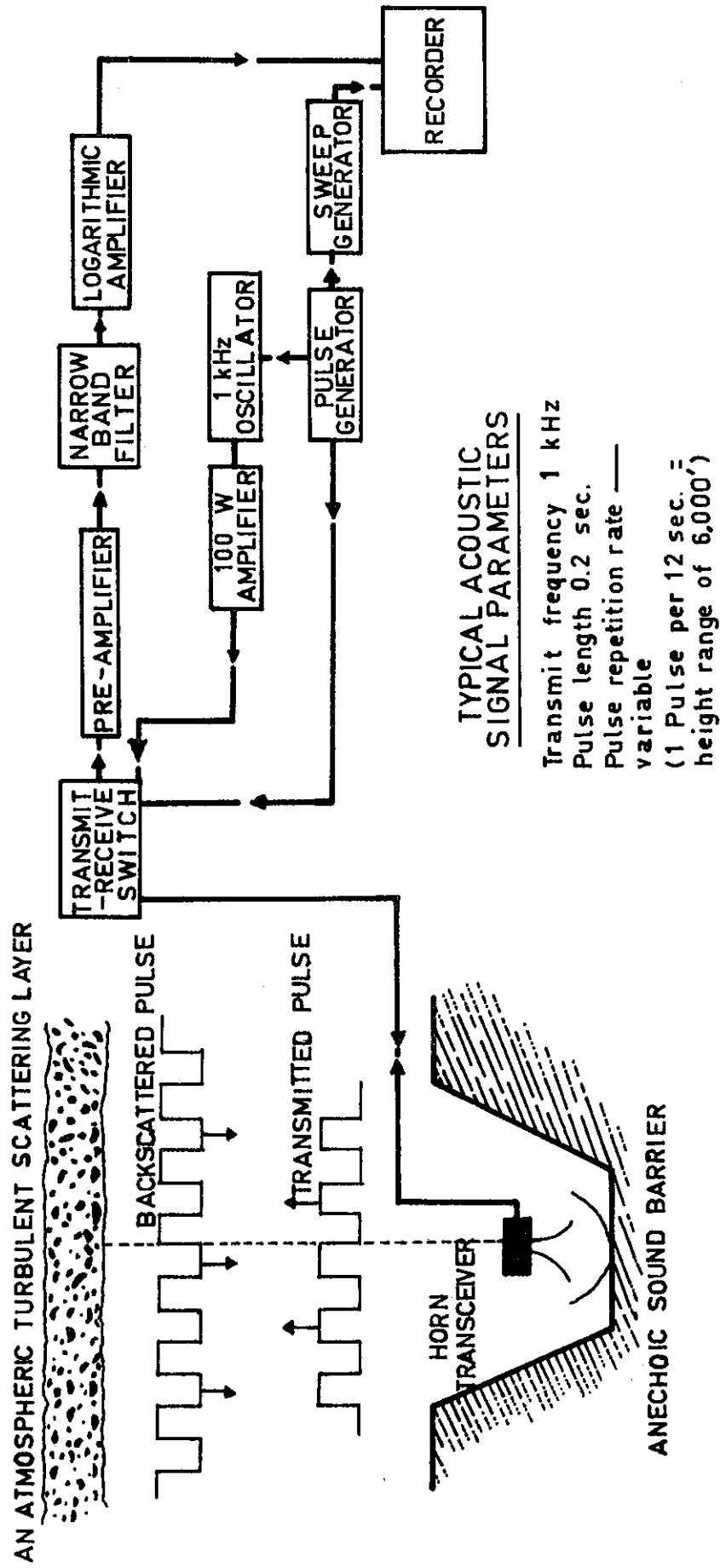


FIGURE 3. SCHEMATIC DIAGRAM OF AN ACOUSTIC SOUNDER

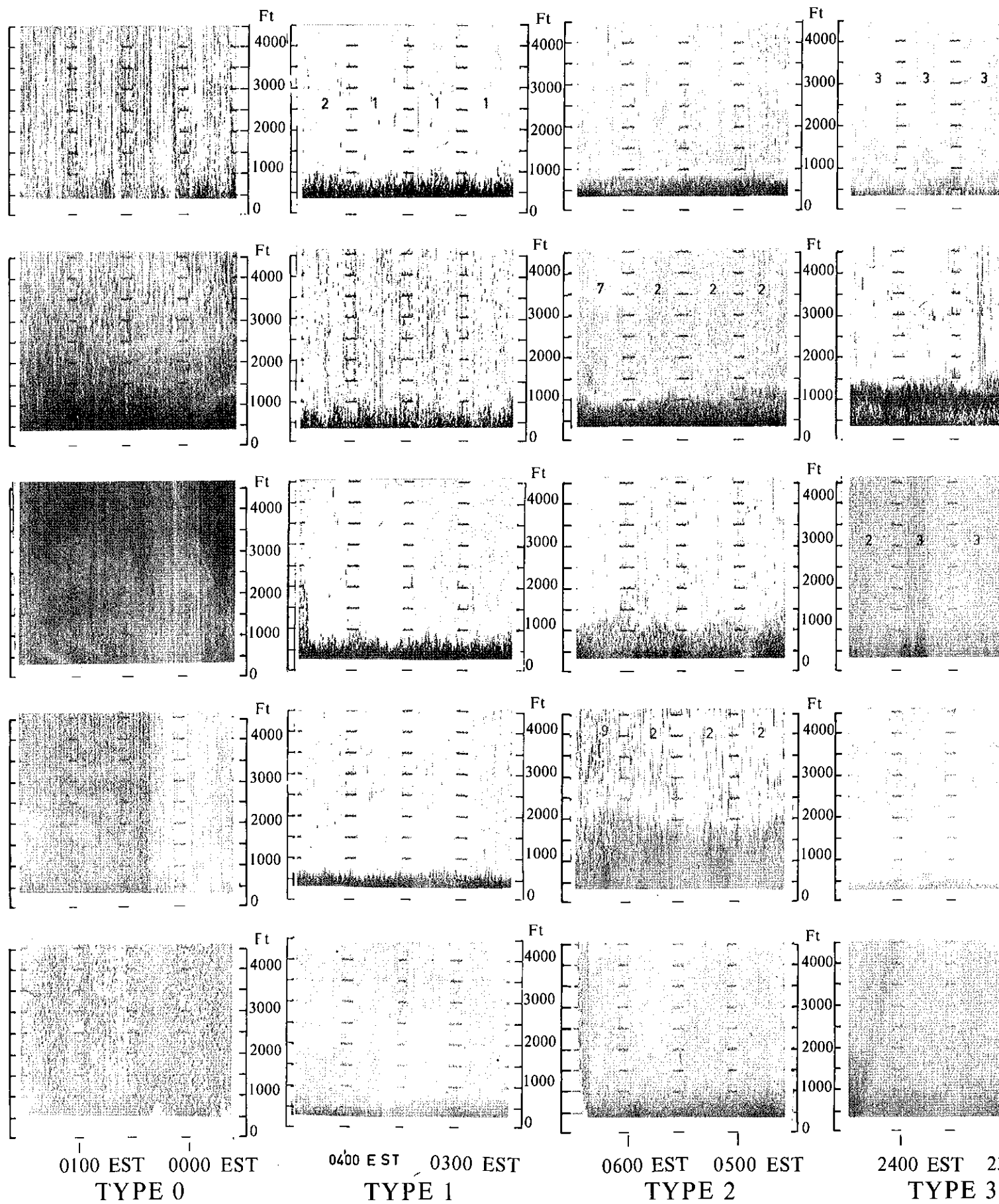


FIGURE 4. SOUNDER RECO



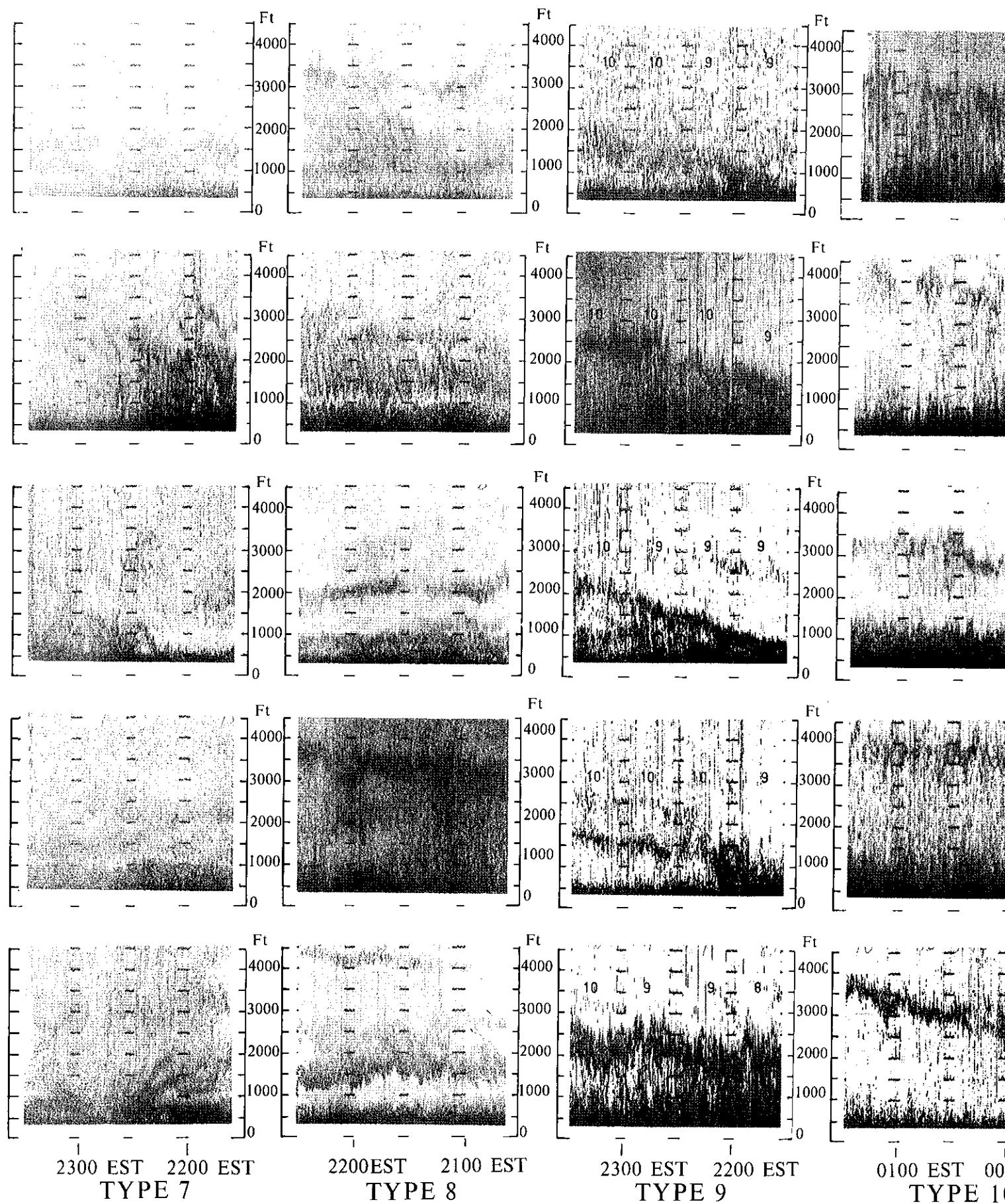


FIGURE 4. (C)



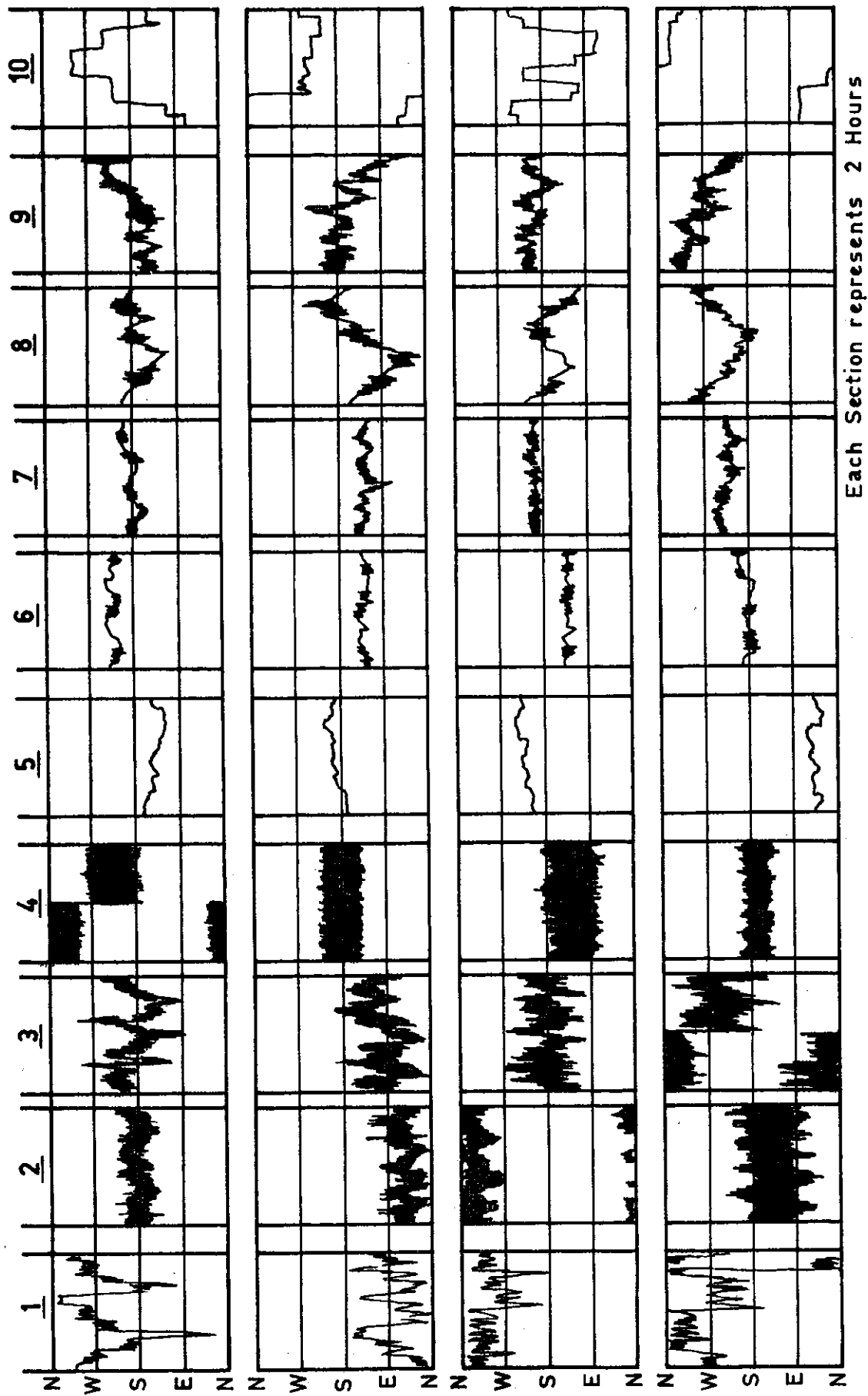


FIGURE 6. WIND DIRECTION TURBULENCE TRACE TYPES

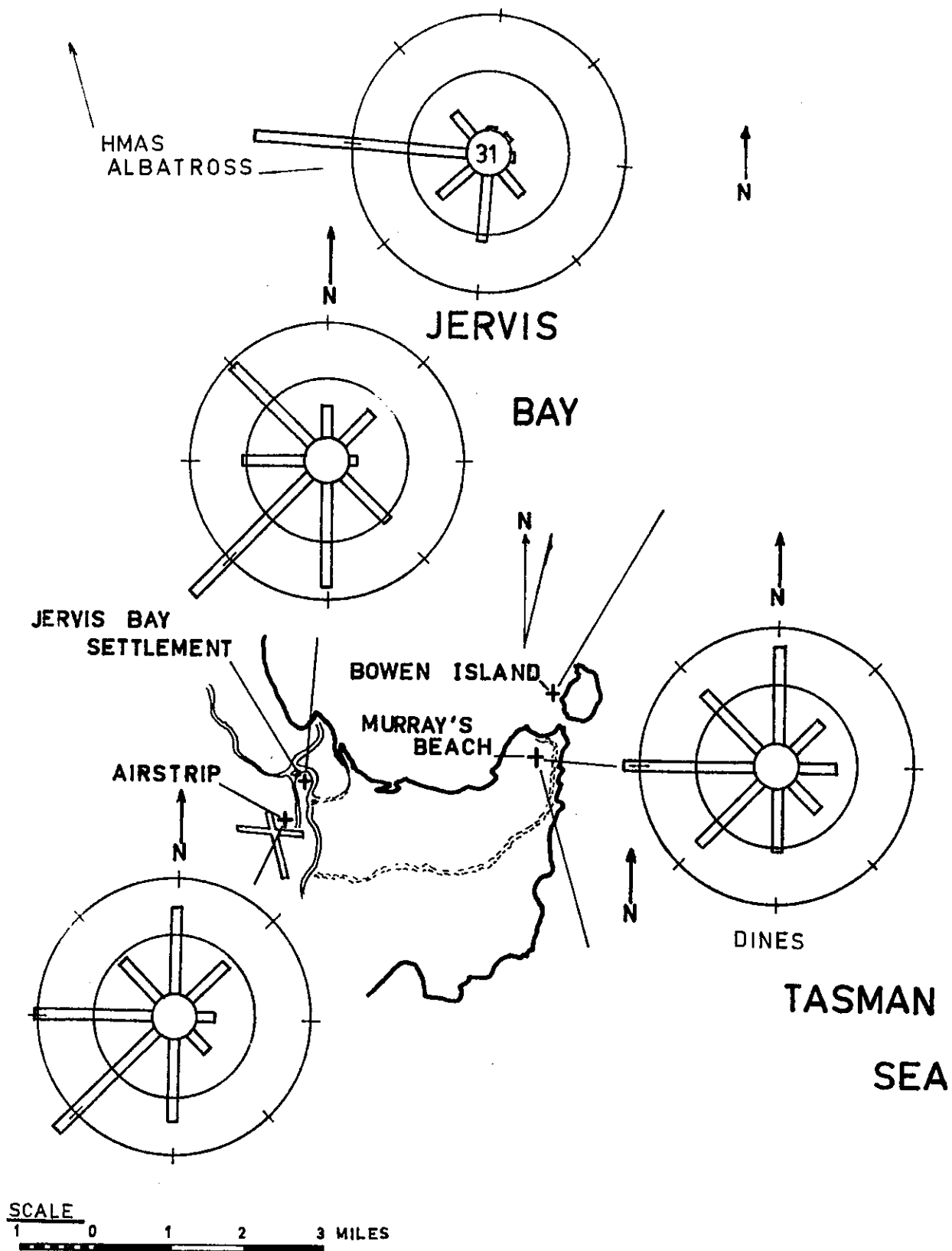


FIGURE 7(a) 0300 EST WIND DIRECTION ROSES  
ALL SEASONS COMBINED



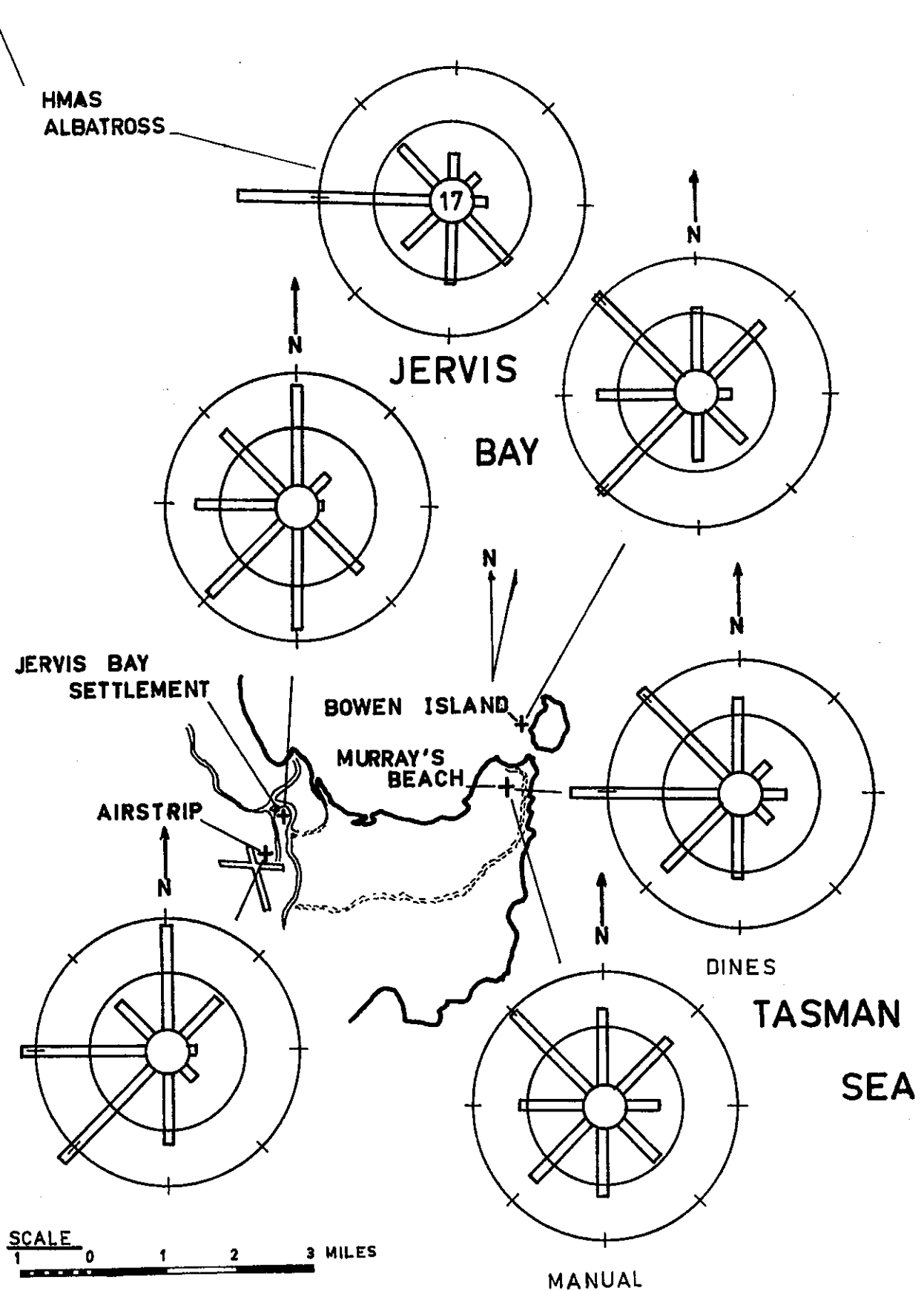


FIGURE 7(b) 0900 EST WIND DIRECTION ROSES  
ALL SEASONS COMBINED

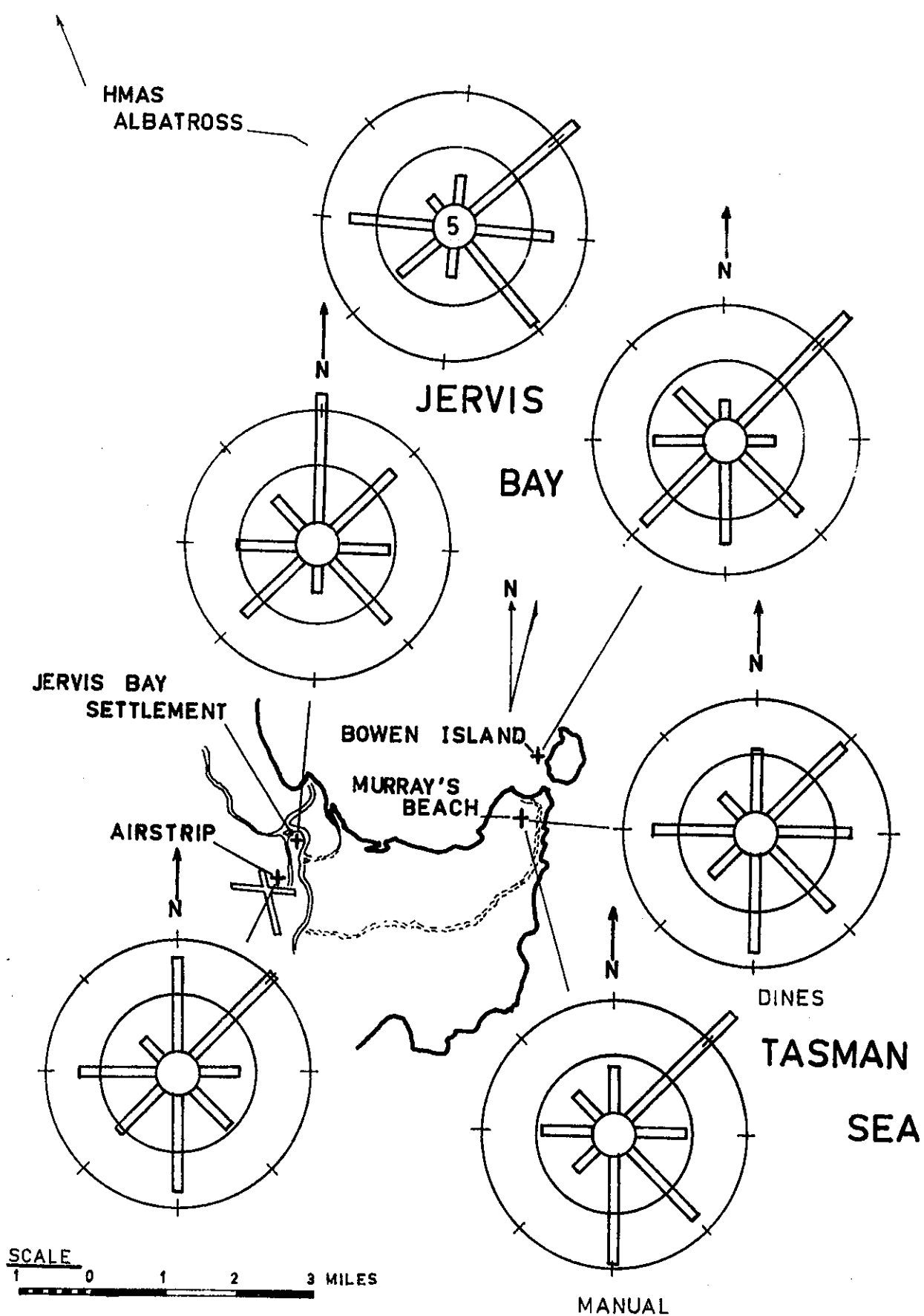


FIGURE 7(c) 1500 EST WIND DIRECTION ROSES  
ALL SEASONS COMBINED

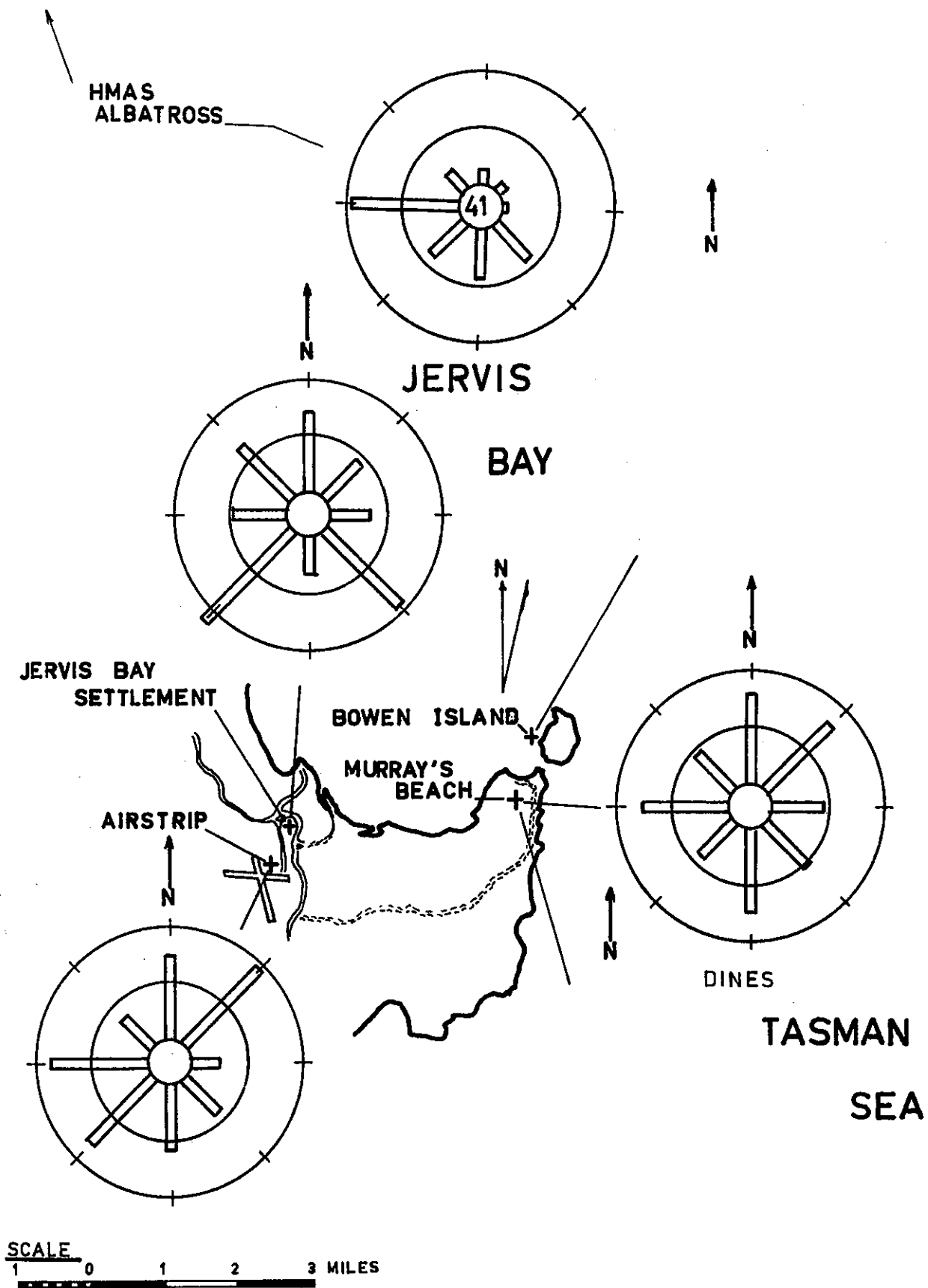


FIGURE 7(d) 2100 EST WIND DIRECTION ROSES  
ALL SEASONS COMBINED

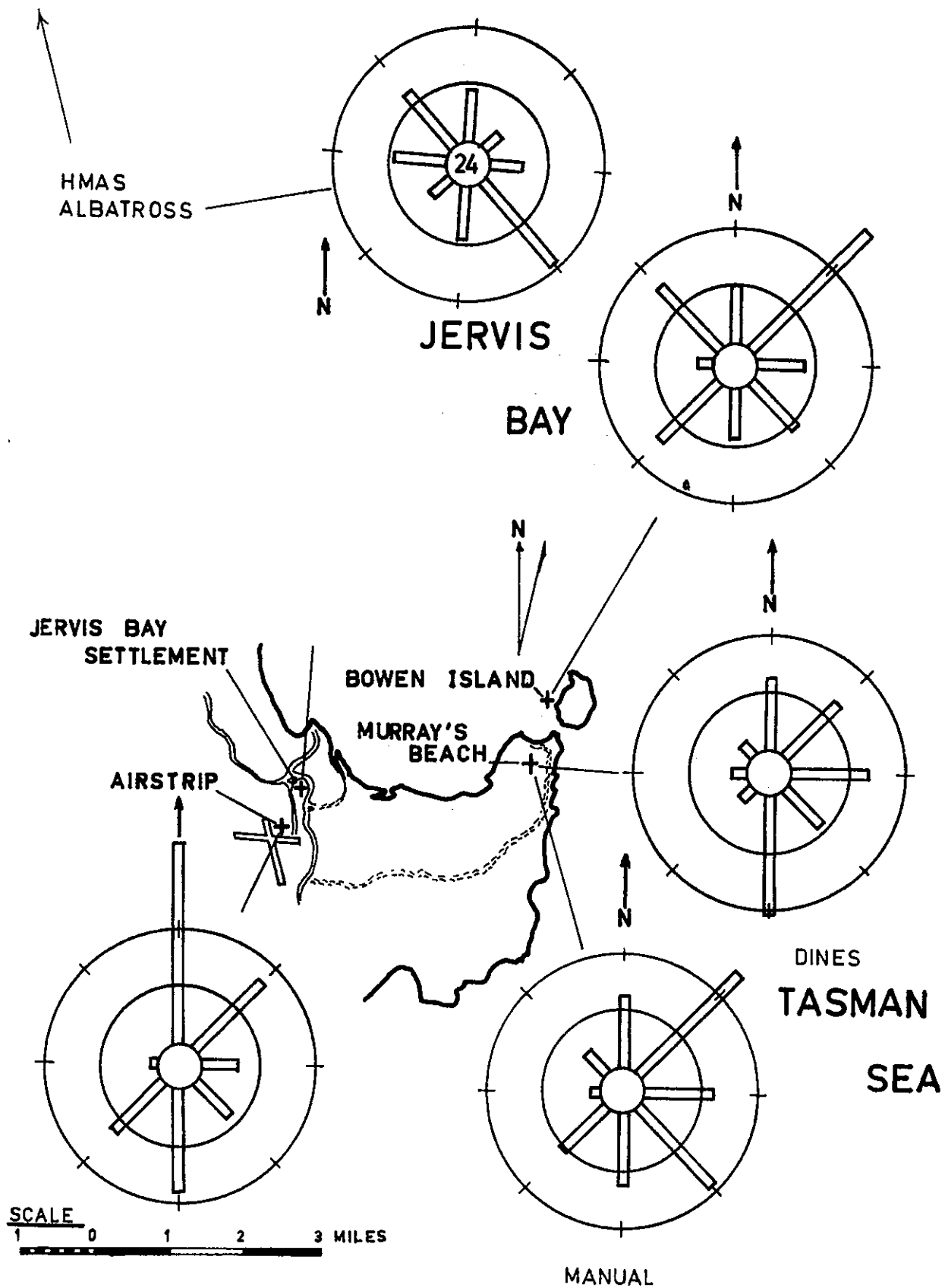


FIGURE 8(a) 0900 EST WIND DIRECTION ROSES  
SUMMER SEASON

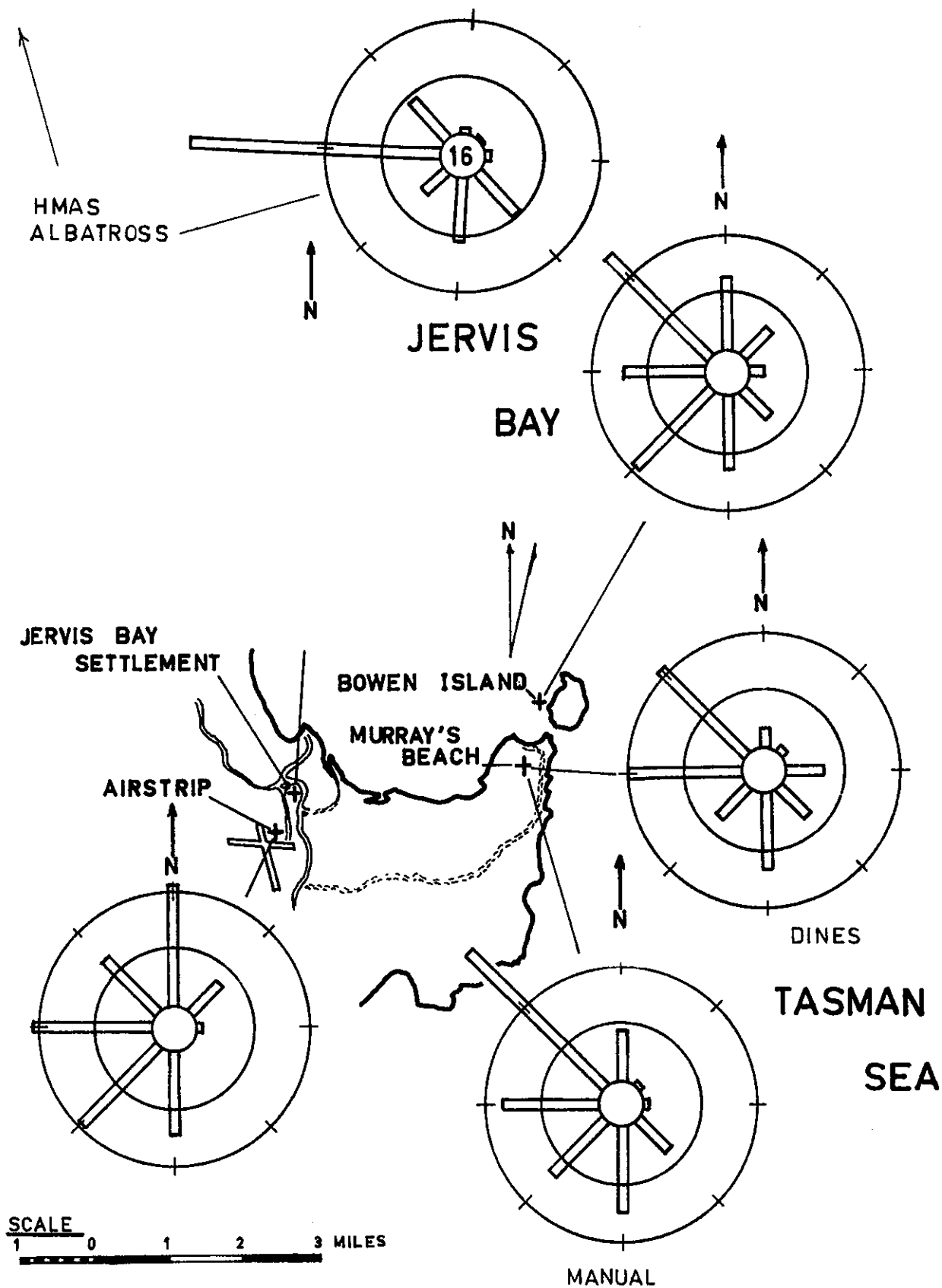


FIGURE 8(b) 0900 EST WIND DIRECTION ROSES  
AUTUMN SEASON

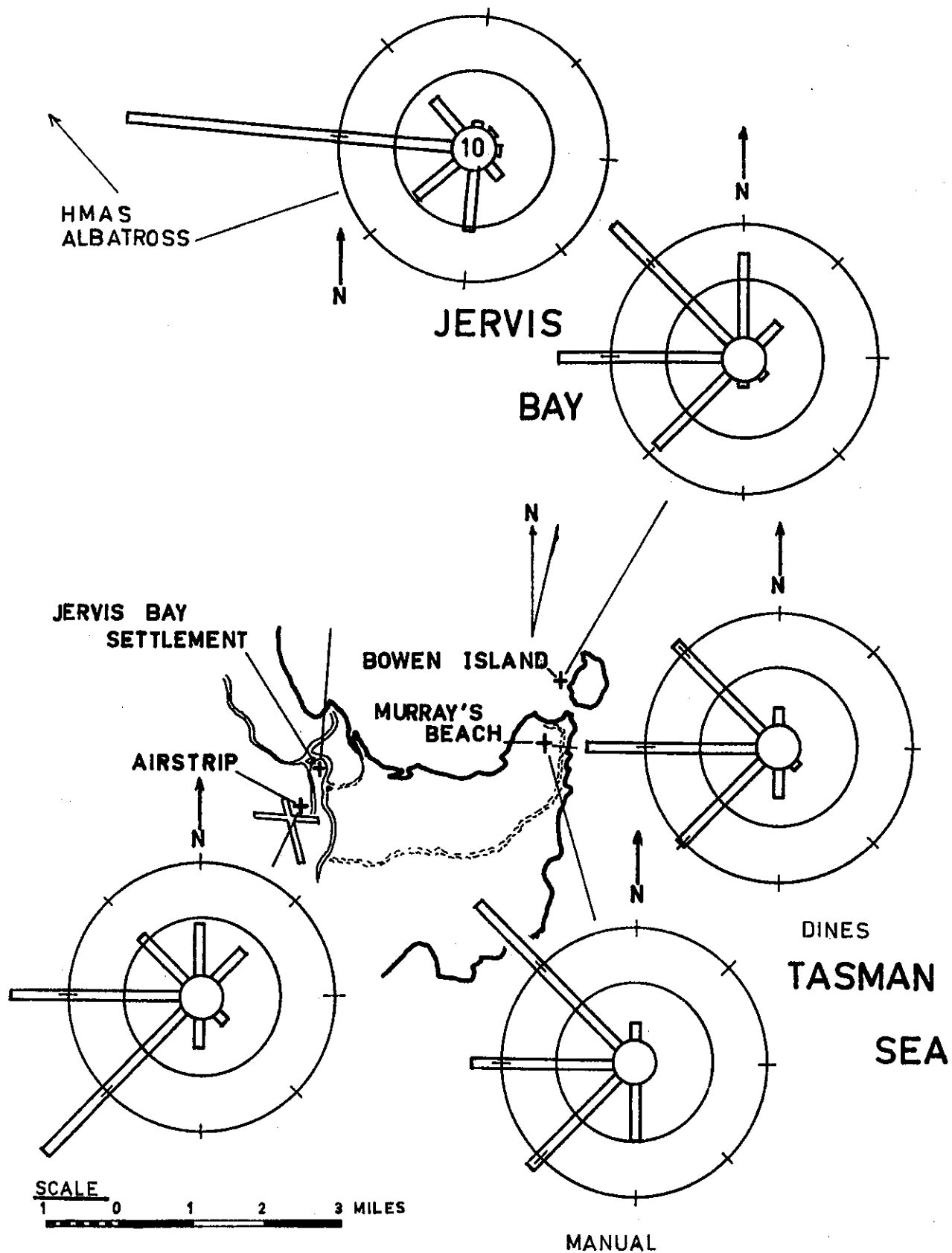


FIGURE 8(c) 0900 EST WIND DIRECTION ROSES  
WINTER SEASON

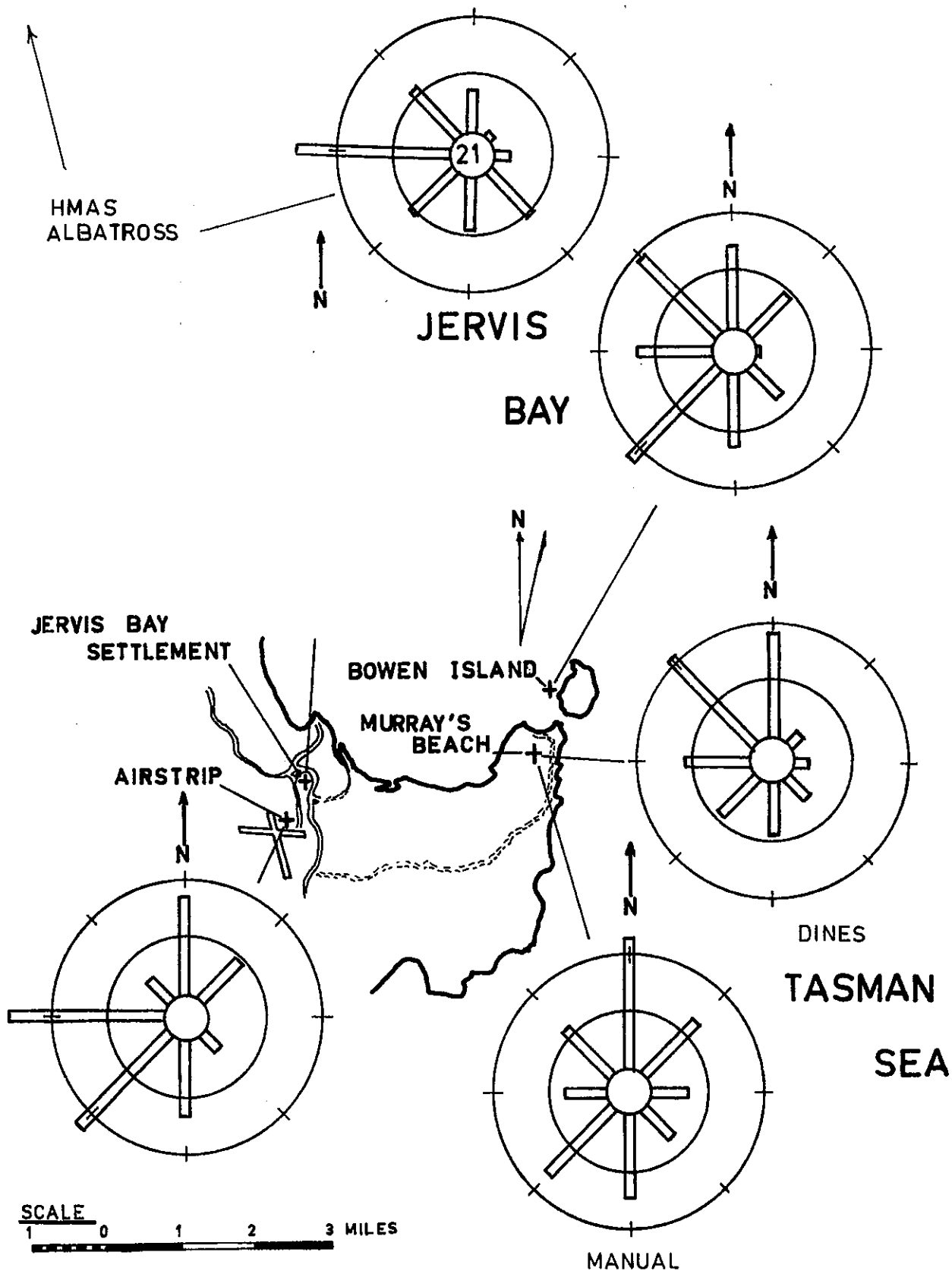


FIGURE 8(d) 0900 EST WIND DIRECTION ROSES  
SPRING SEASON

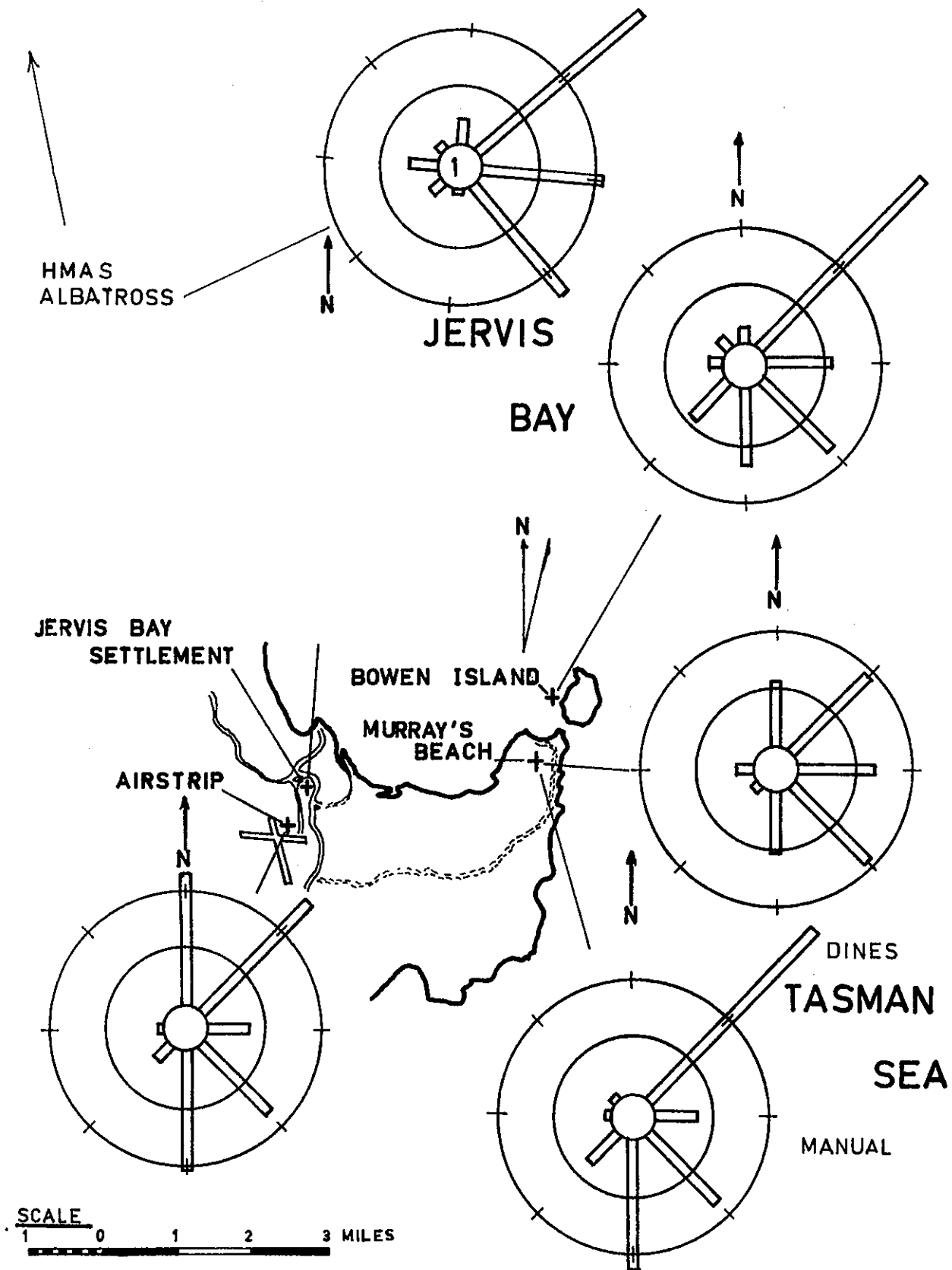


FIGURE 9(a) 1500 EST WIND DIRECTION ROSES  
SUMMER SEASON



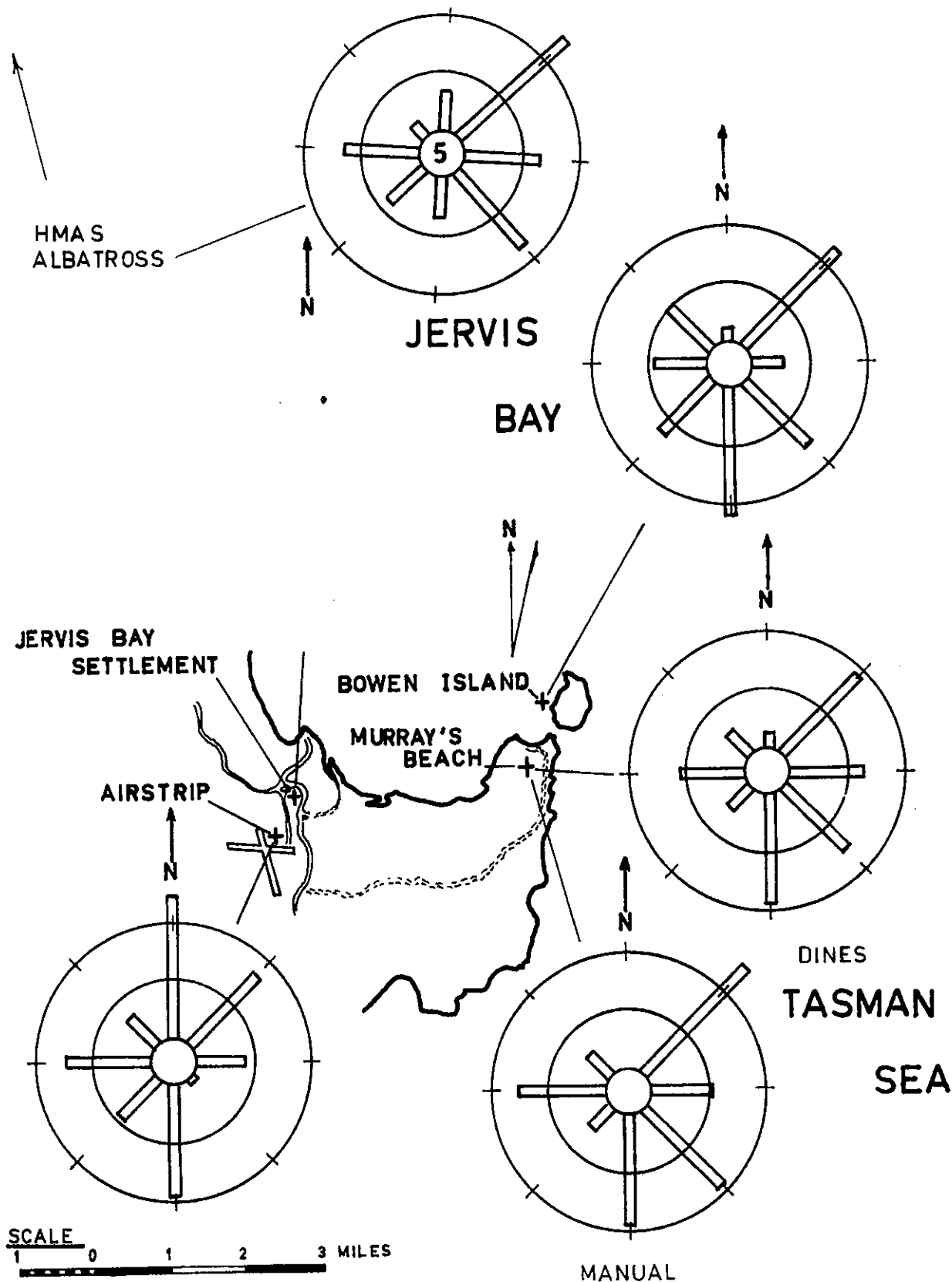


FIGURE 9(b) 1500 EST WIND DIRECTION ROSES  
AUTUMN SEASON

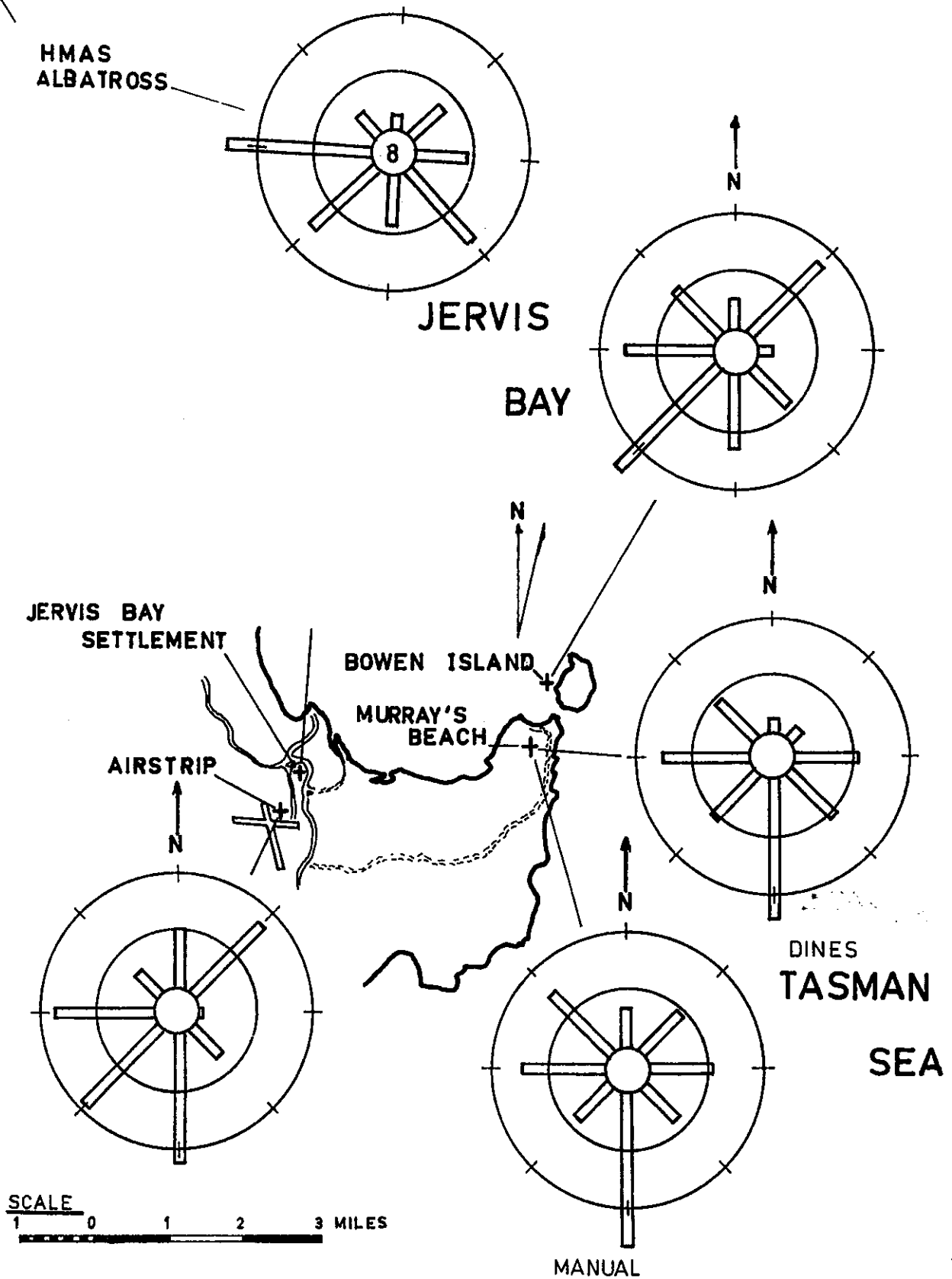


FIGURE 9(c) 1500 EST WIND DIRECTION ROSES  
WINTER SEASON

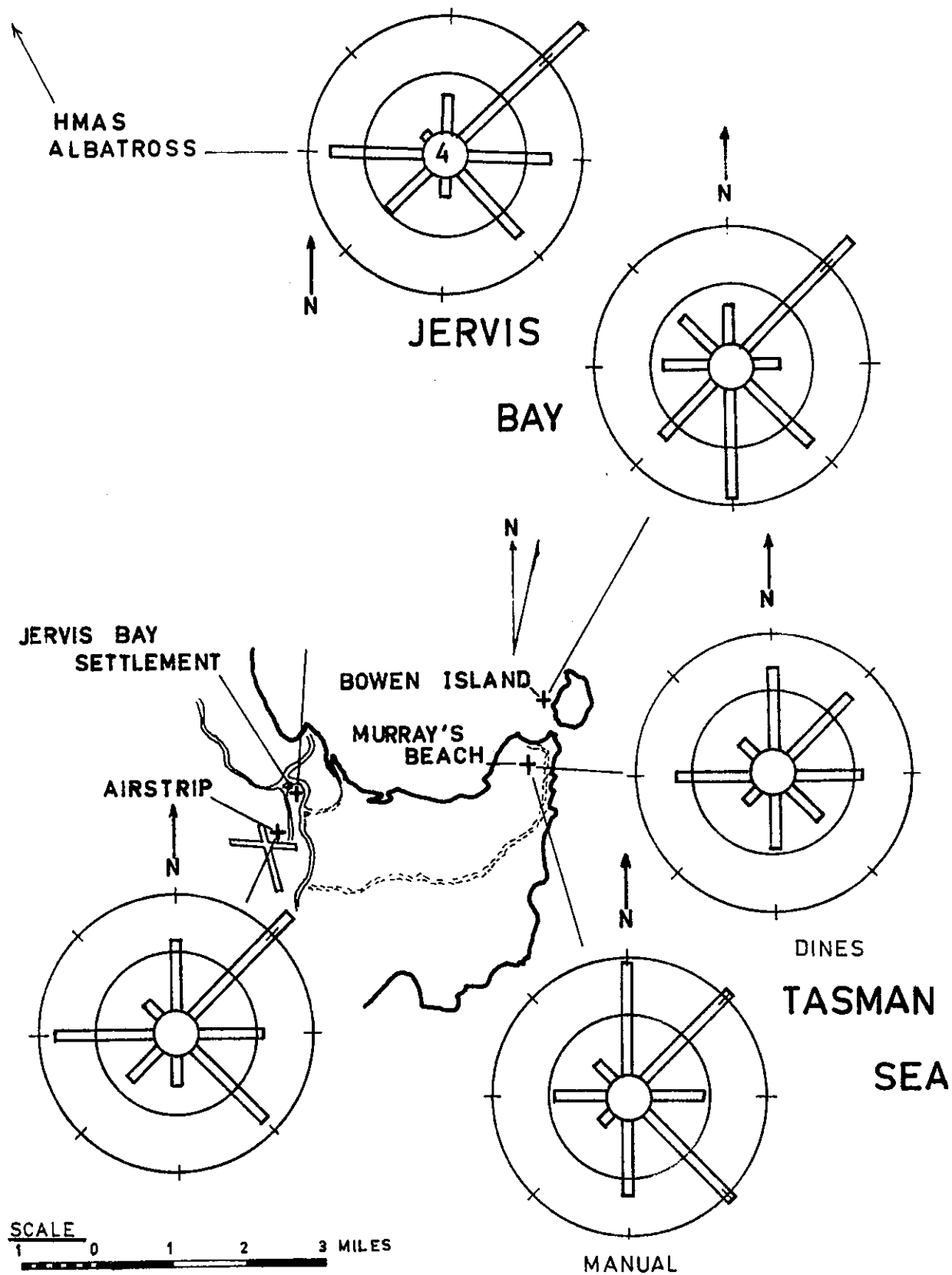


FIGURE 9(d) 1500 EST WIND DIRECTION ROSES  
SPRING SEASON

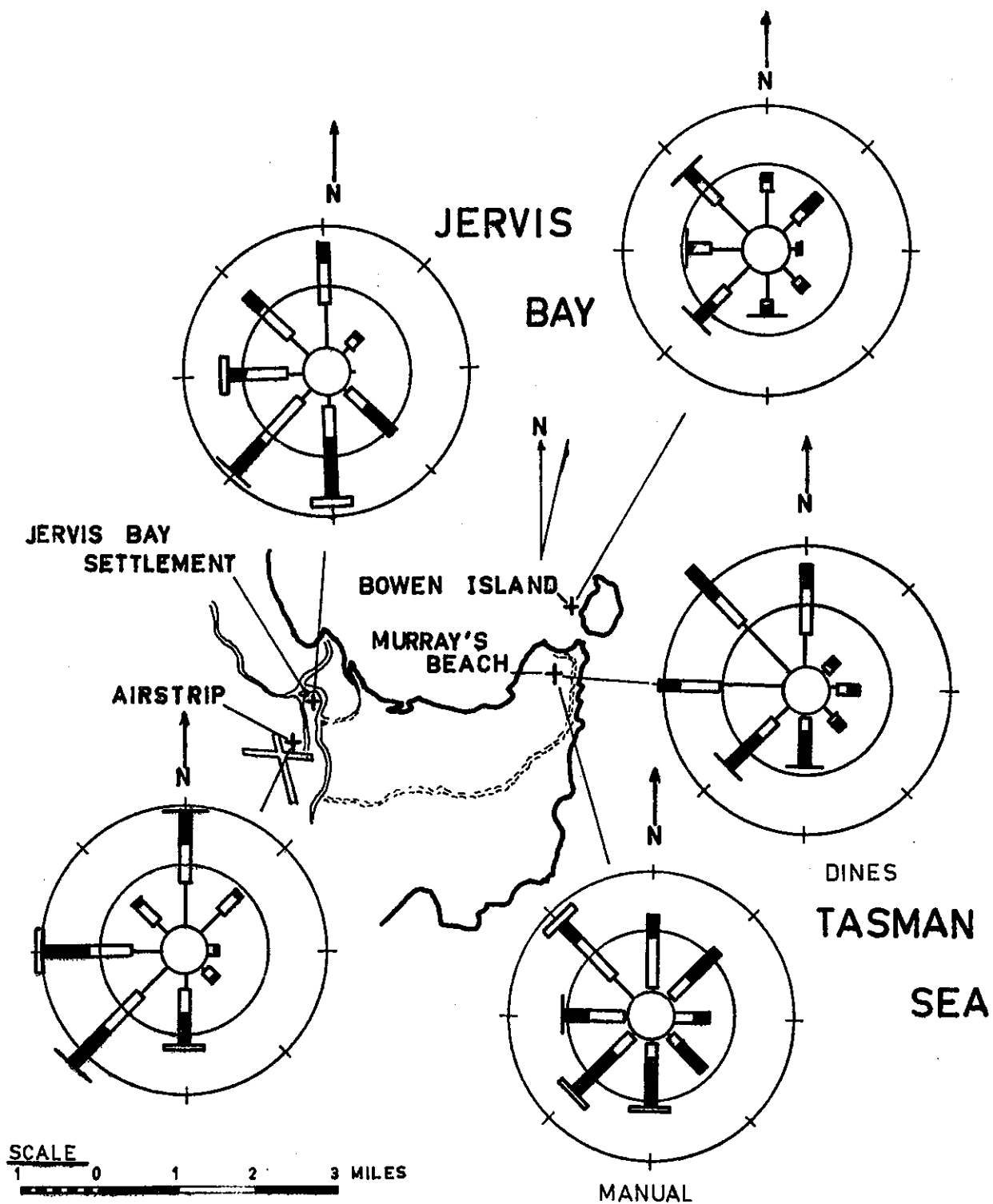


FIGURE 10(a) 0900 EST WIND SPEED AND DIRECTION ROSES  
ALL SEASONS COMBINED

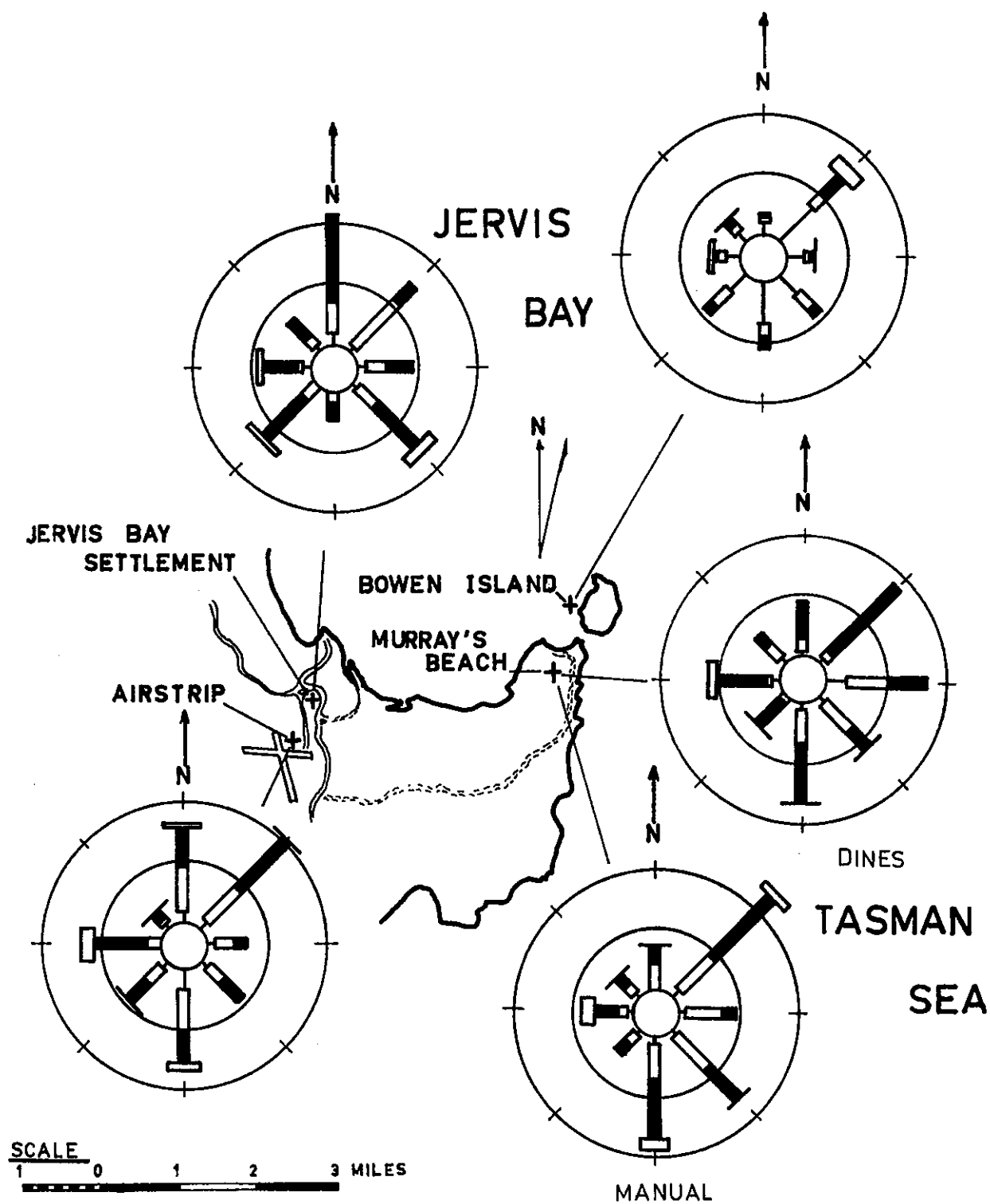


FIGURE 10(b) 1500 EST WIND SPEED AND DIRECTION ROSES  
ALL SEASONS COMBINED

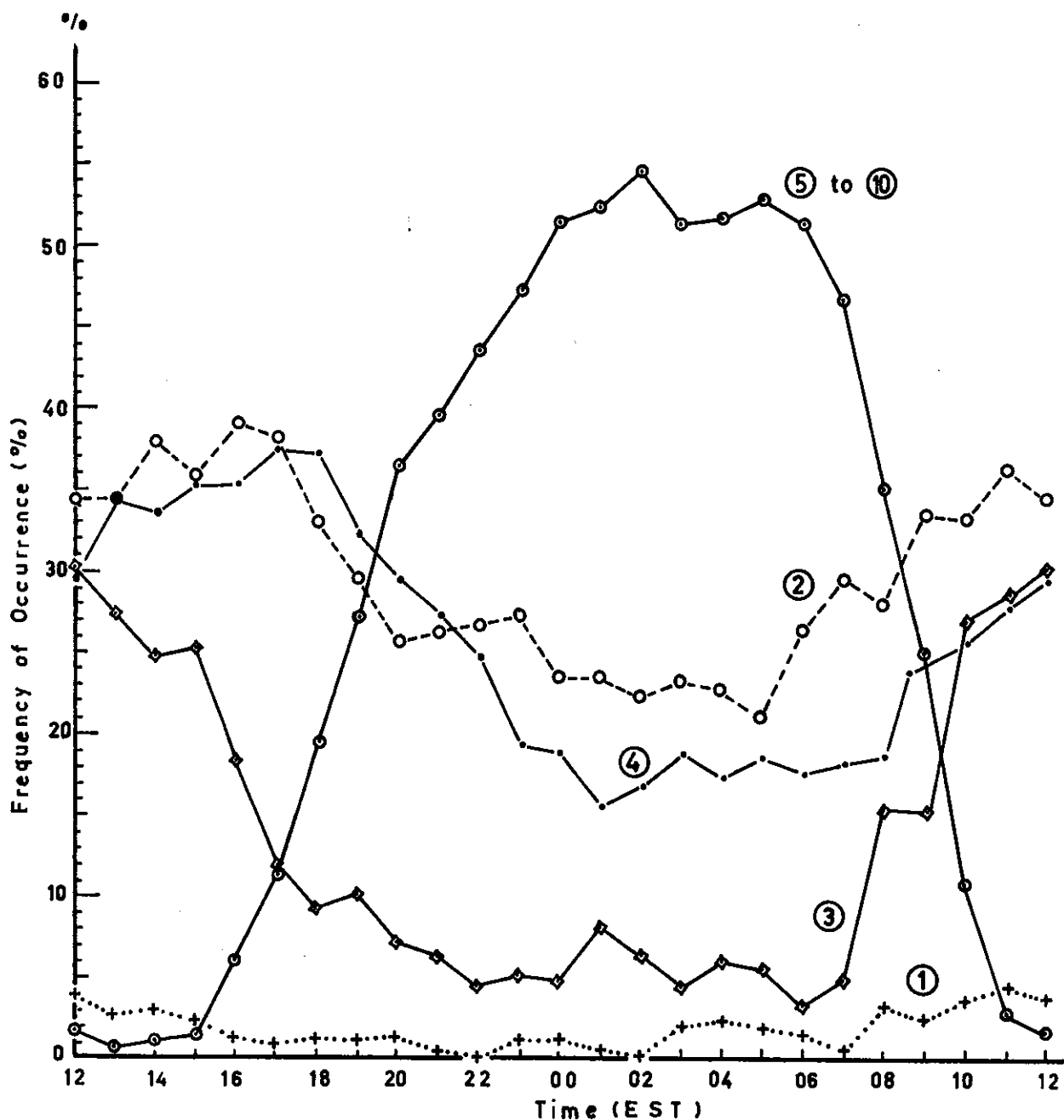


FIGURE 11(a) THE DIURNAL VARIATIONS IN THE OCCURRENCE OF THE WIND DIRECTION TURBULENCE CATEGORIES FROM THE DINES ANEMOGRAPH AT THE JERVIS BAY SETTLEMENT, 23.6.72 TO 4.1.73

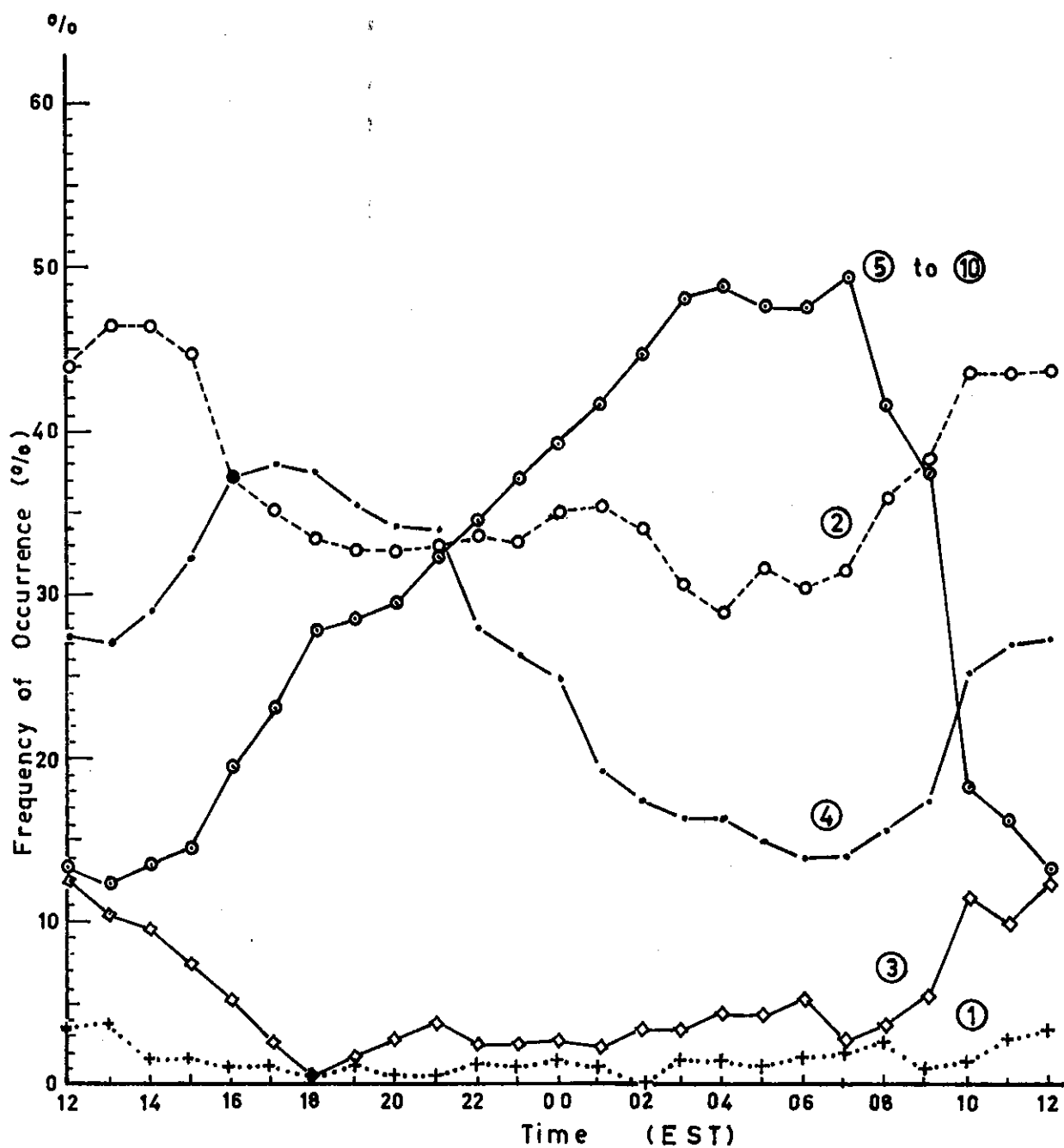


FIGURE 11(b) THE DIURNAL VARIATIONS IN THE OCCURRENCE OF  
THE WIND DIRECTION TURBULENCE CATEGORIES  
FROM THE DINES ANEMOGRAPH AT MURRAY'S  
BEACH, 24.2.71 TO 18.2.72

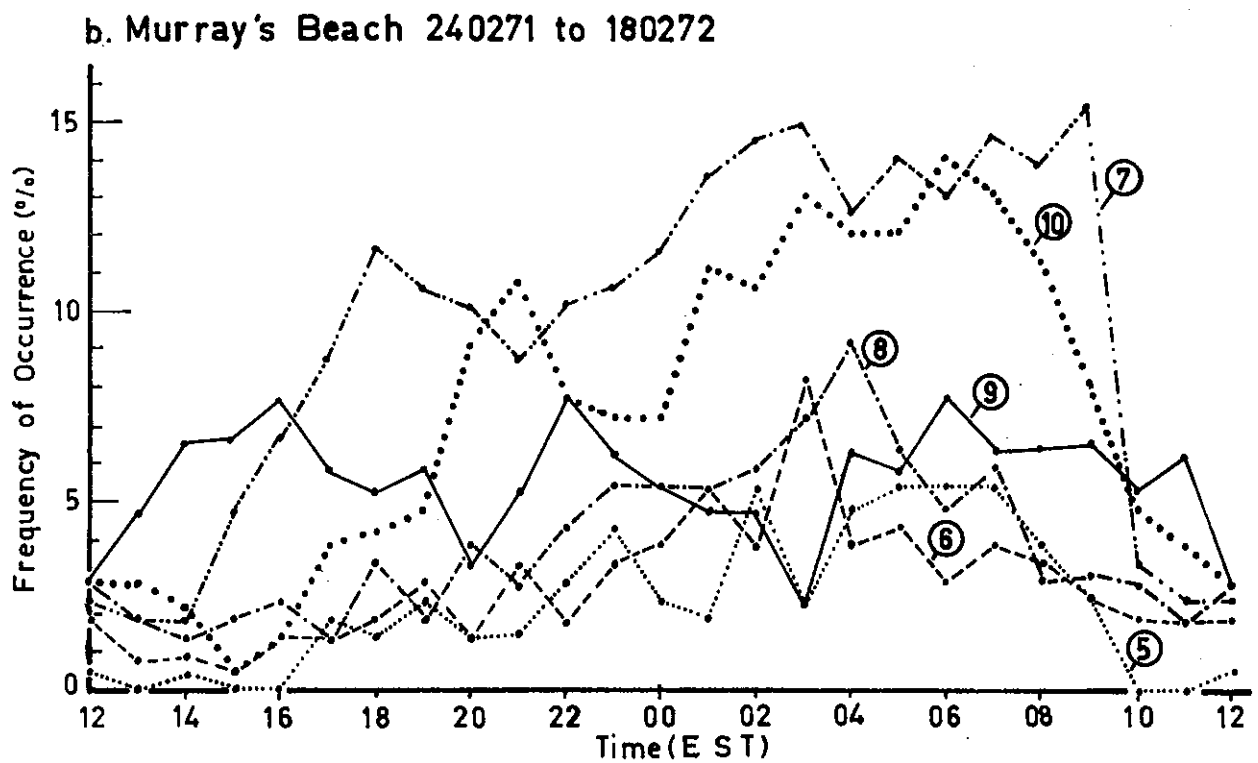
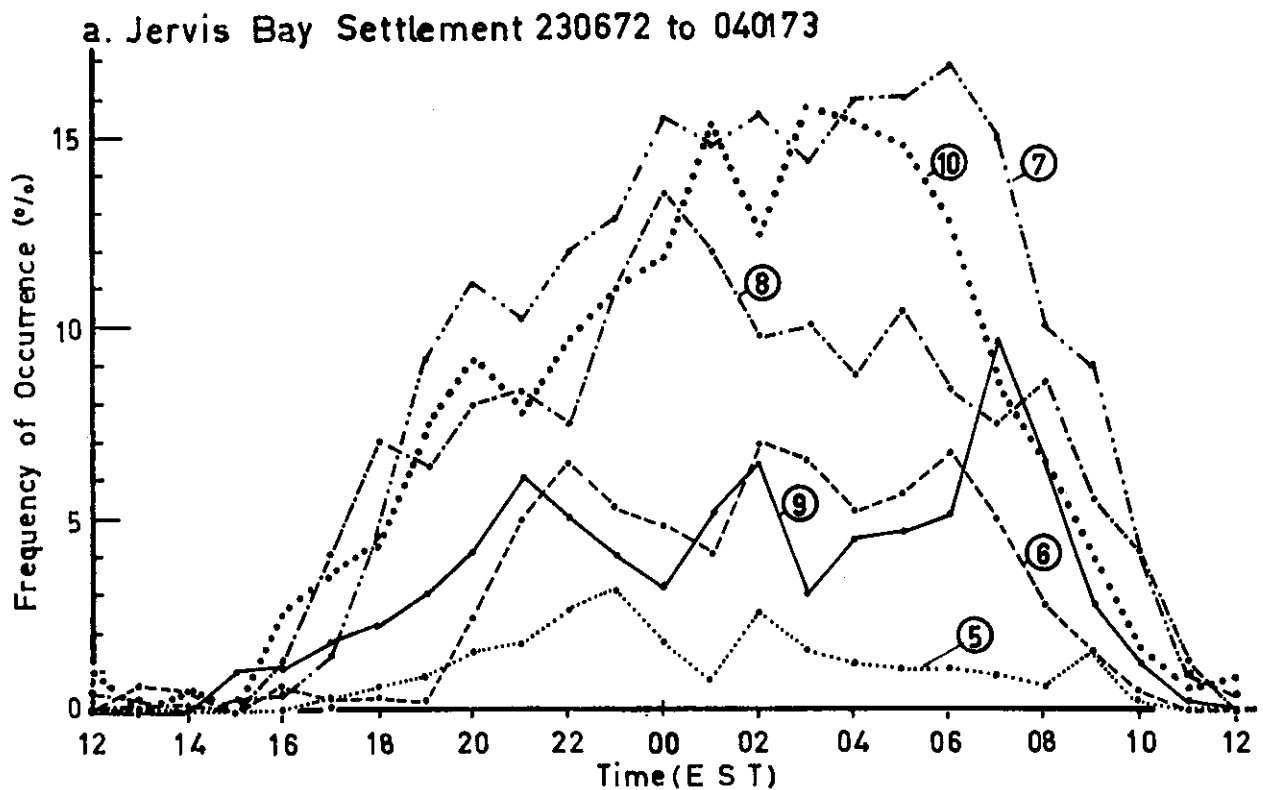


FIGURE 12. THE DIURNAL VARIATIONS OF THE DIRECTION  
TURBULENCE CATEGORIES 5 TO 10 FROM THE  
DINES ANEMOGRAPH



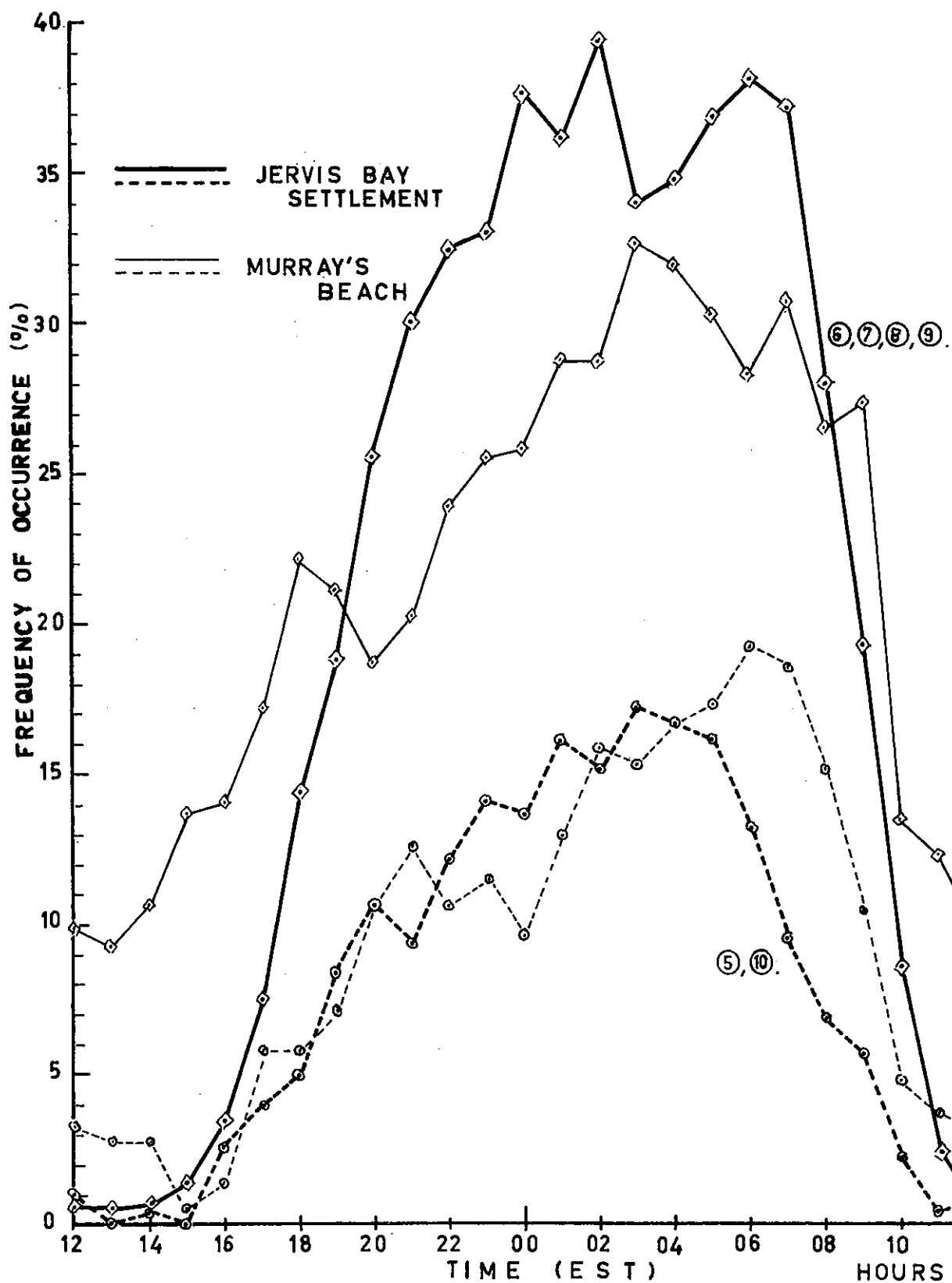
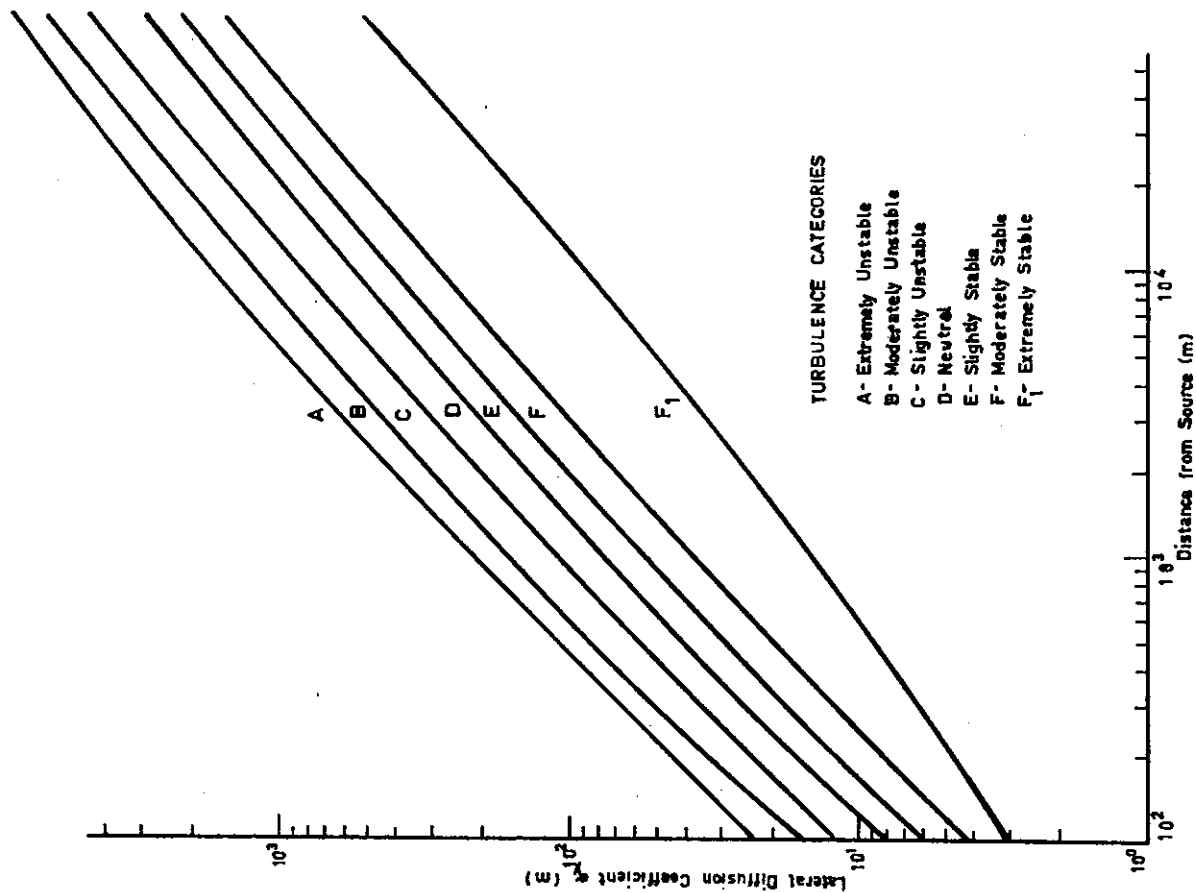


FIGURE 13. THE DIURNAL VARIATION OF 'STABLE' TURBULENCE CATEGORIES WITH RESTRICTED TURBULENCE (6, 7, 8 AND 9) AND SMOOTH FLOW (5, 10)



14(a) LATERAL DIFFUSION ( $\sigma_y$ ) AS A FUNCTION OF  
DOWNWIND DISTANCE FROM SOURCE

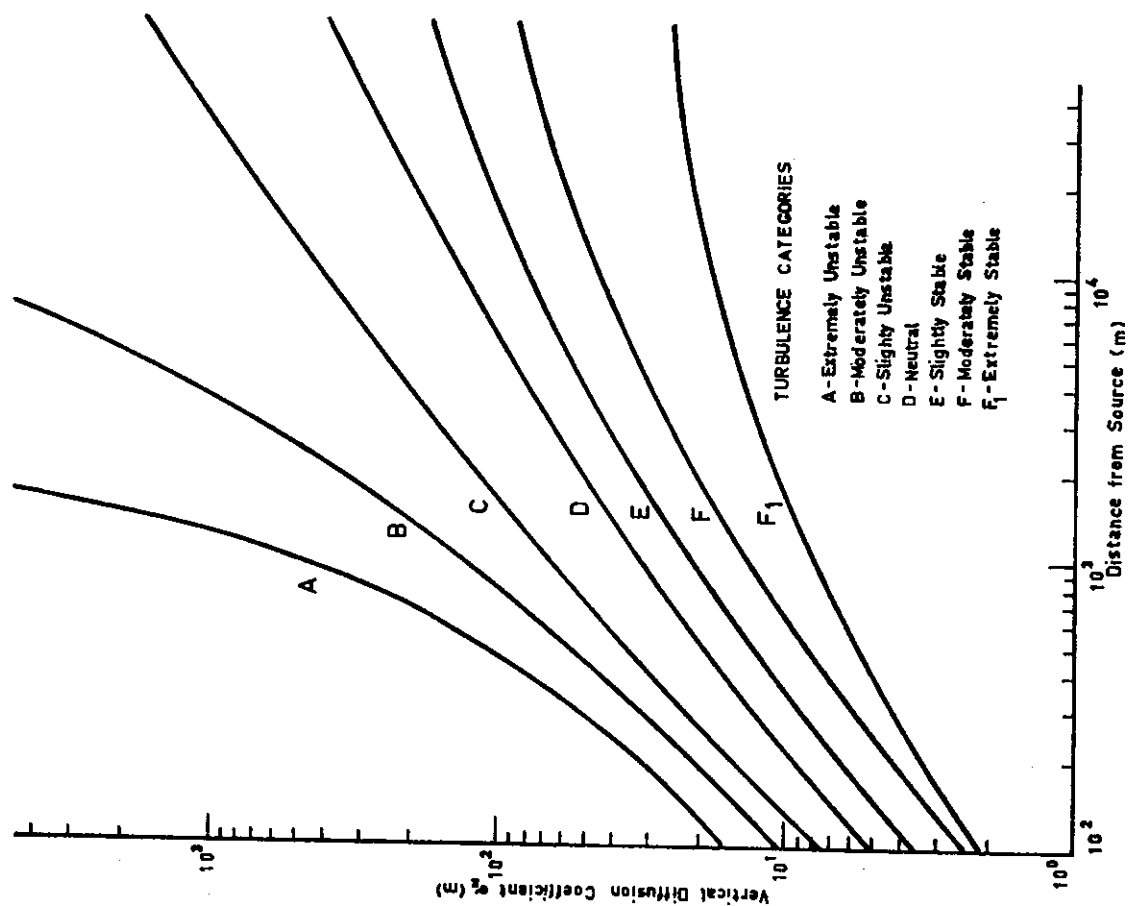
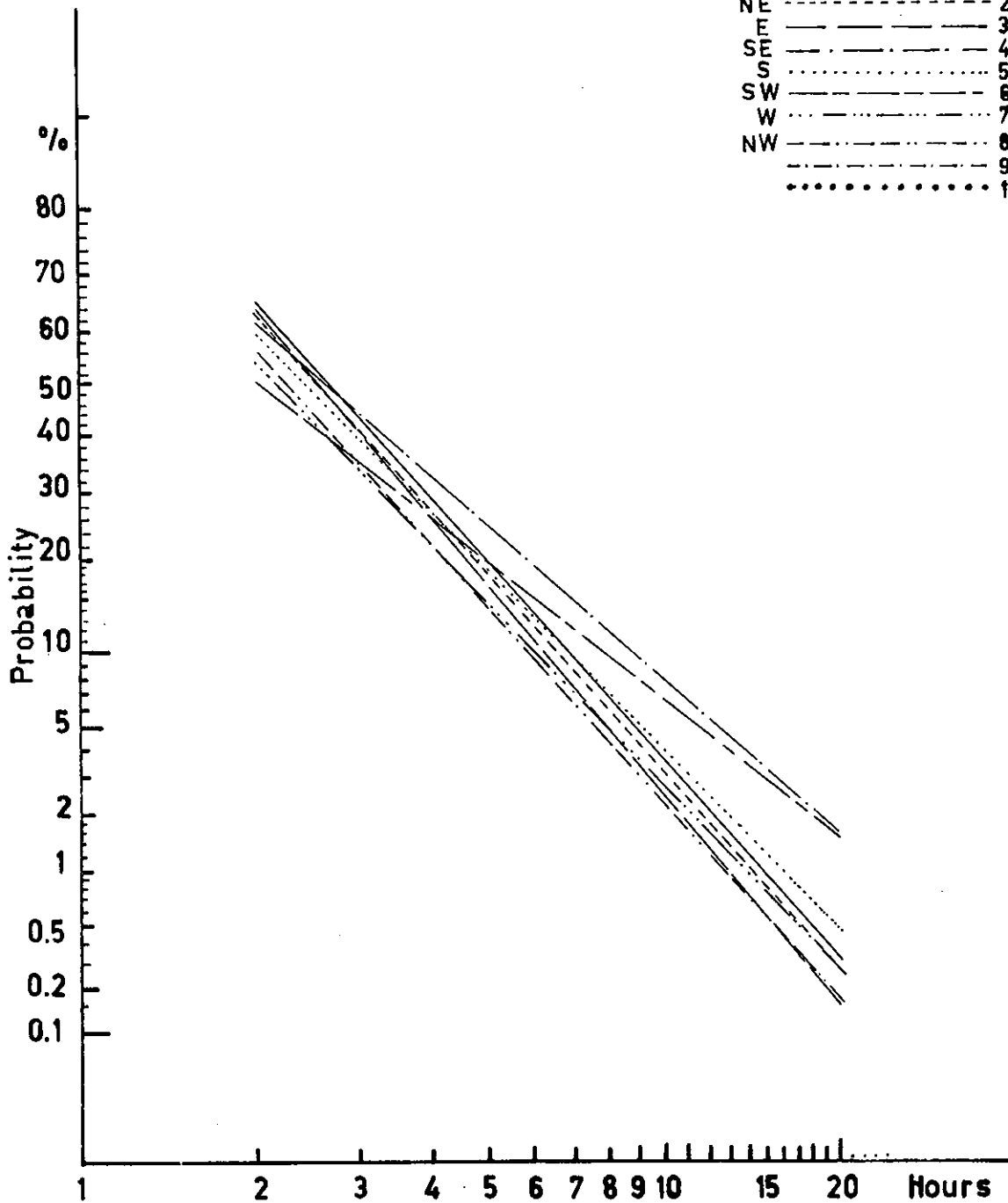


FIGURE 14(b) VERTICAL DIFFUSION ( $\sigma_z$ ) AS A FUNCTION OF  
DOWNWIND DISTANCE FROM SOURCE

# **LEGEND:**

WIND DIRECTION	TURBULENCE TRACE	TYPE
N	1	x
NE	2	o
E	3	◇
SE	4	•
S	5	○
SW	6	◇
W	7	+
NW	8	△
	9	□
	10	▣



**FIGURE 15(a) WIND DIRECTION PERSISTENCE  
JERVIS BAY, 23.6.72 TO 5.1.73**

# LEGEND:

WIND DIRECTION	TURBULENCE TRACE	TYPE
N	1	x
NE	2	⊙
E	3	◇
SE	4	•
S	5	⊖
SW	6	⊕
W	7	+
NW	8	△
	9	□
	10	⊠

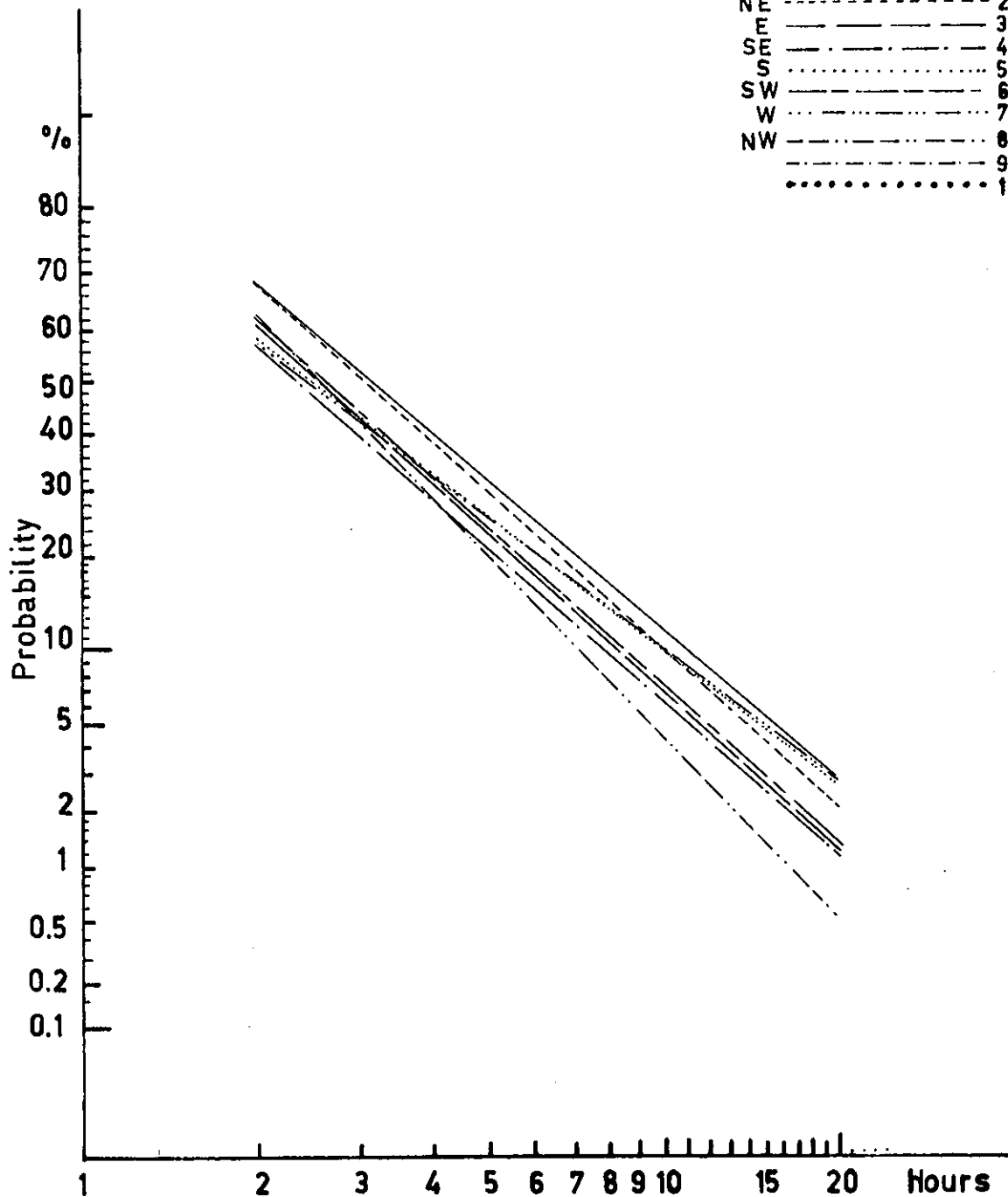


FIGURE 15(b) WIND DIRECTION PERSISTENCE MURRAY'S BEACH, 18.2.71 TO 24.2.72

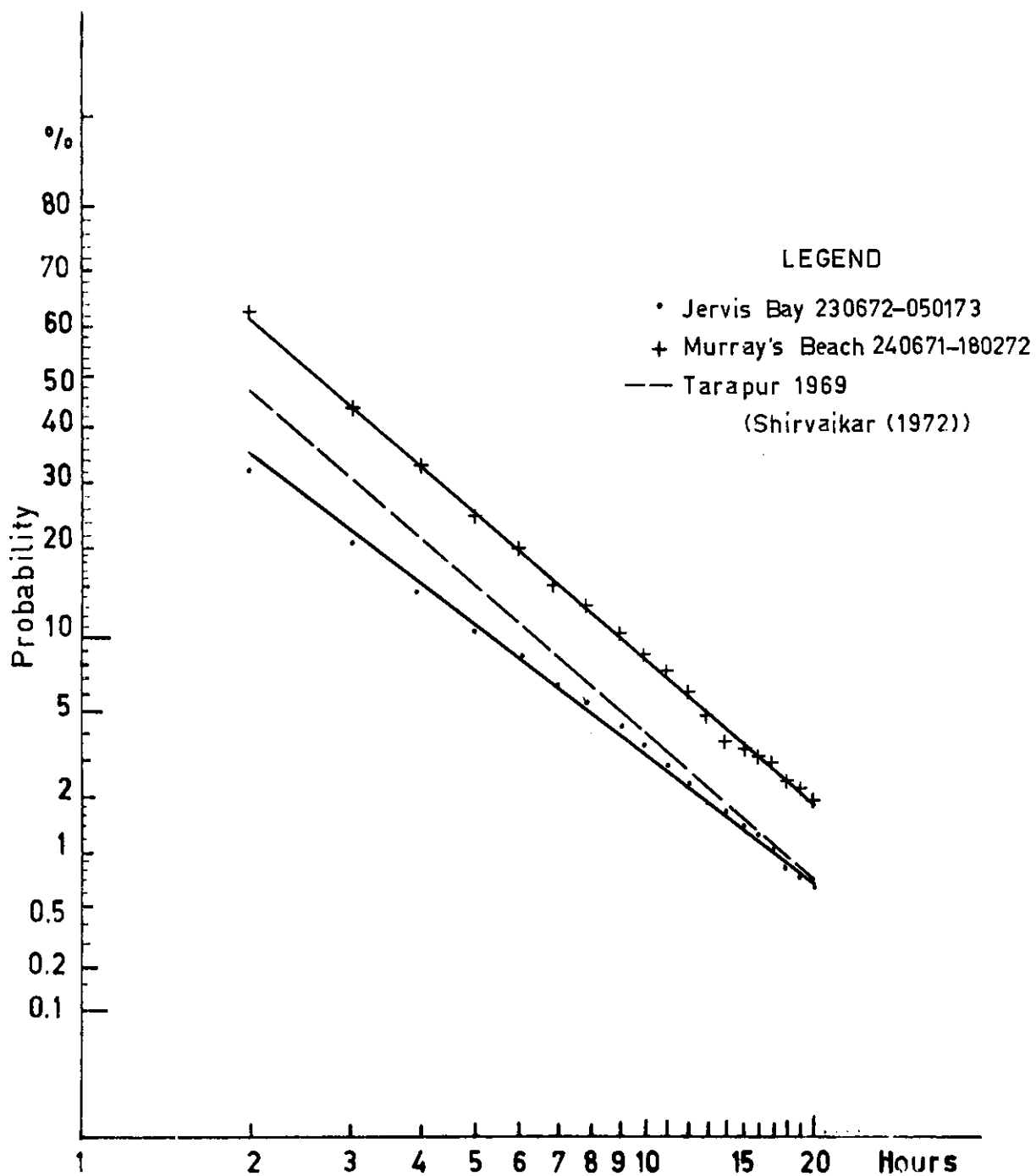


FIGURE 16. WIND DIRECTION PERSISTENCE ALL DIRECTIONS COMBINED

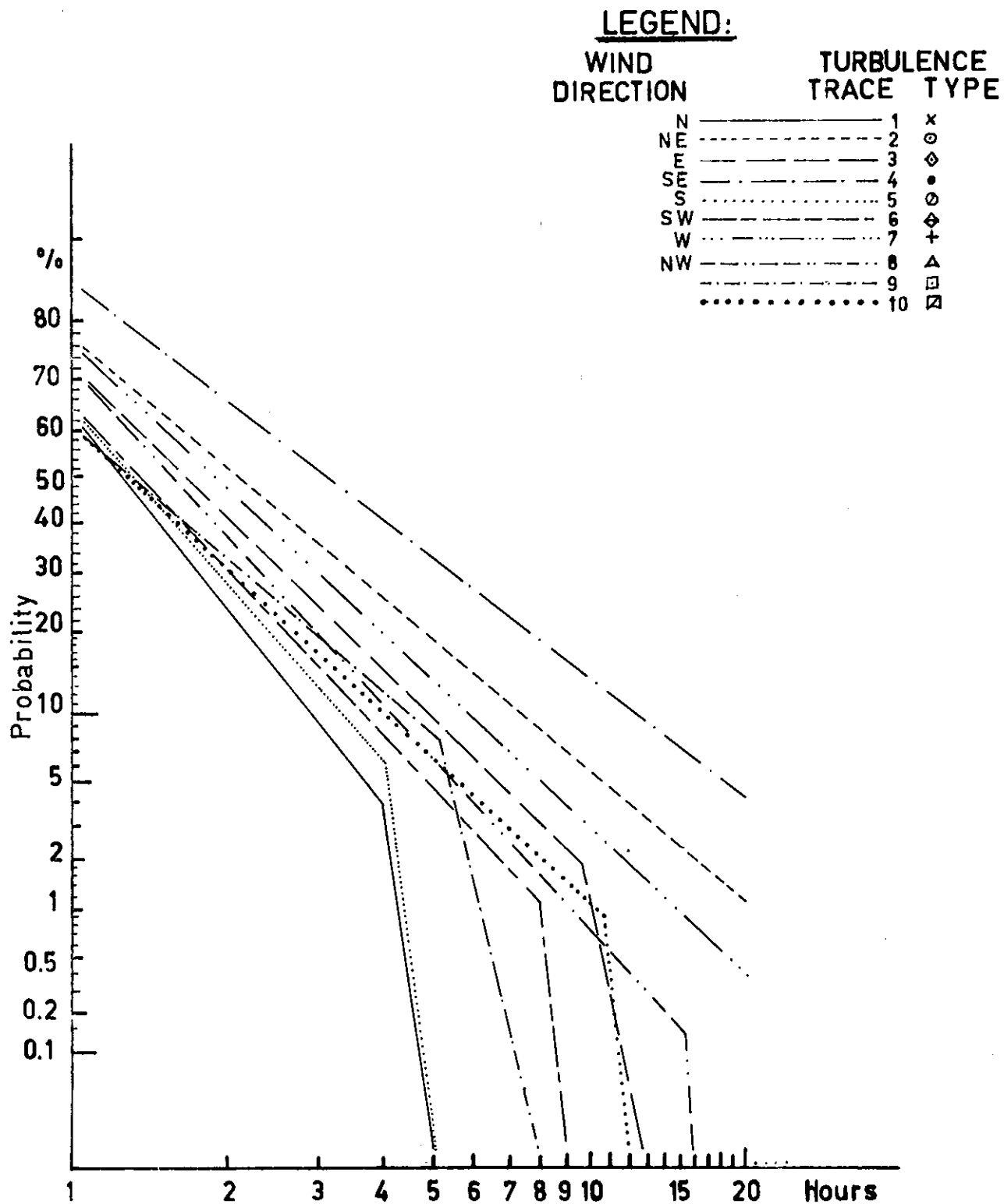


FIGURE 17(a) WIND DIRECTION TURBULENCE TRACE  
PERSISTENCE AT JERVIS BAY,  
23.6.72 TO 5.1.73

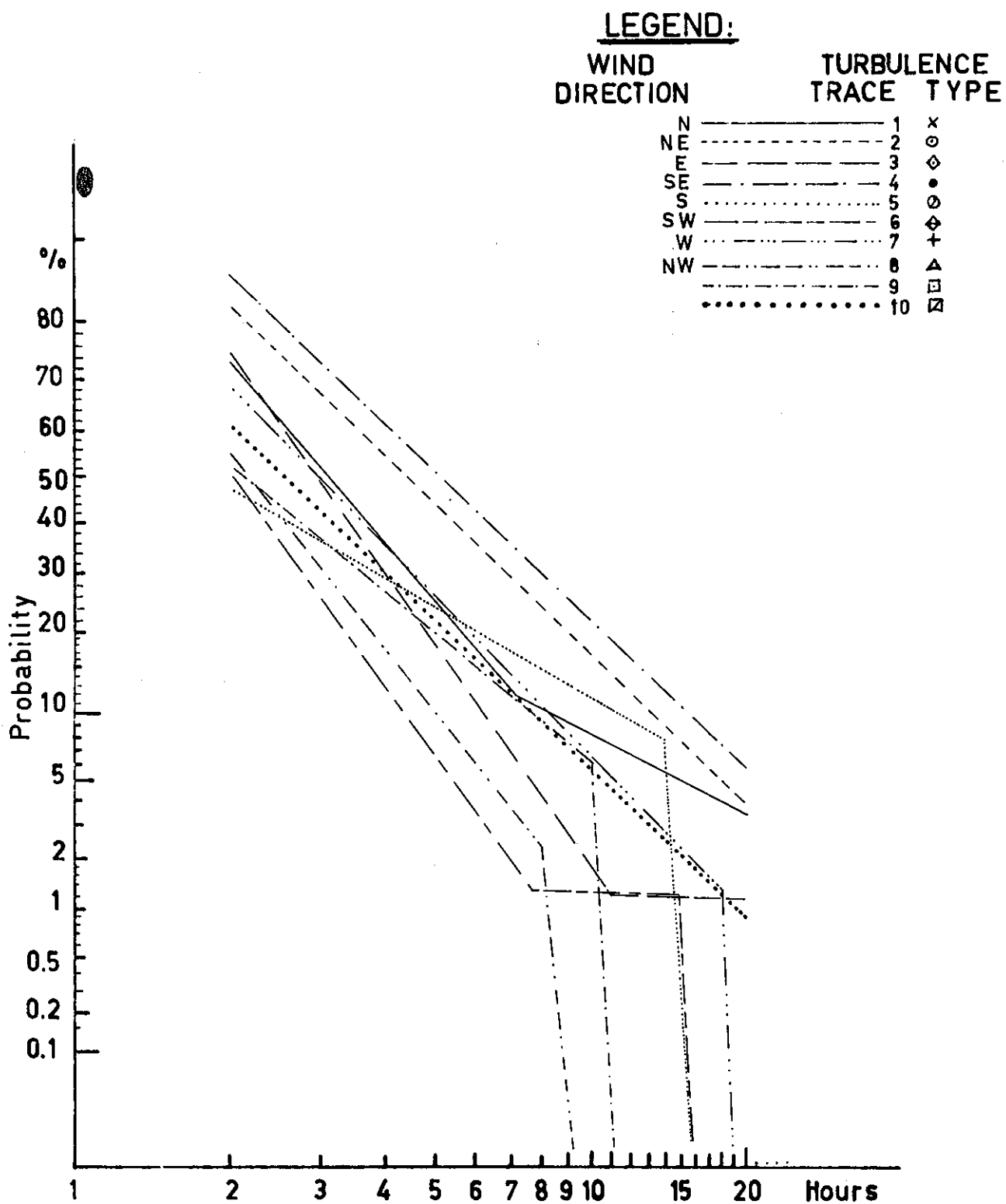


FIGURE 17(b) WIND DIRECTION TURBULENCE TRACE  
PERSISTENCE AT MURRAY'S BEACH

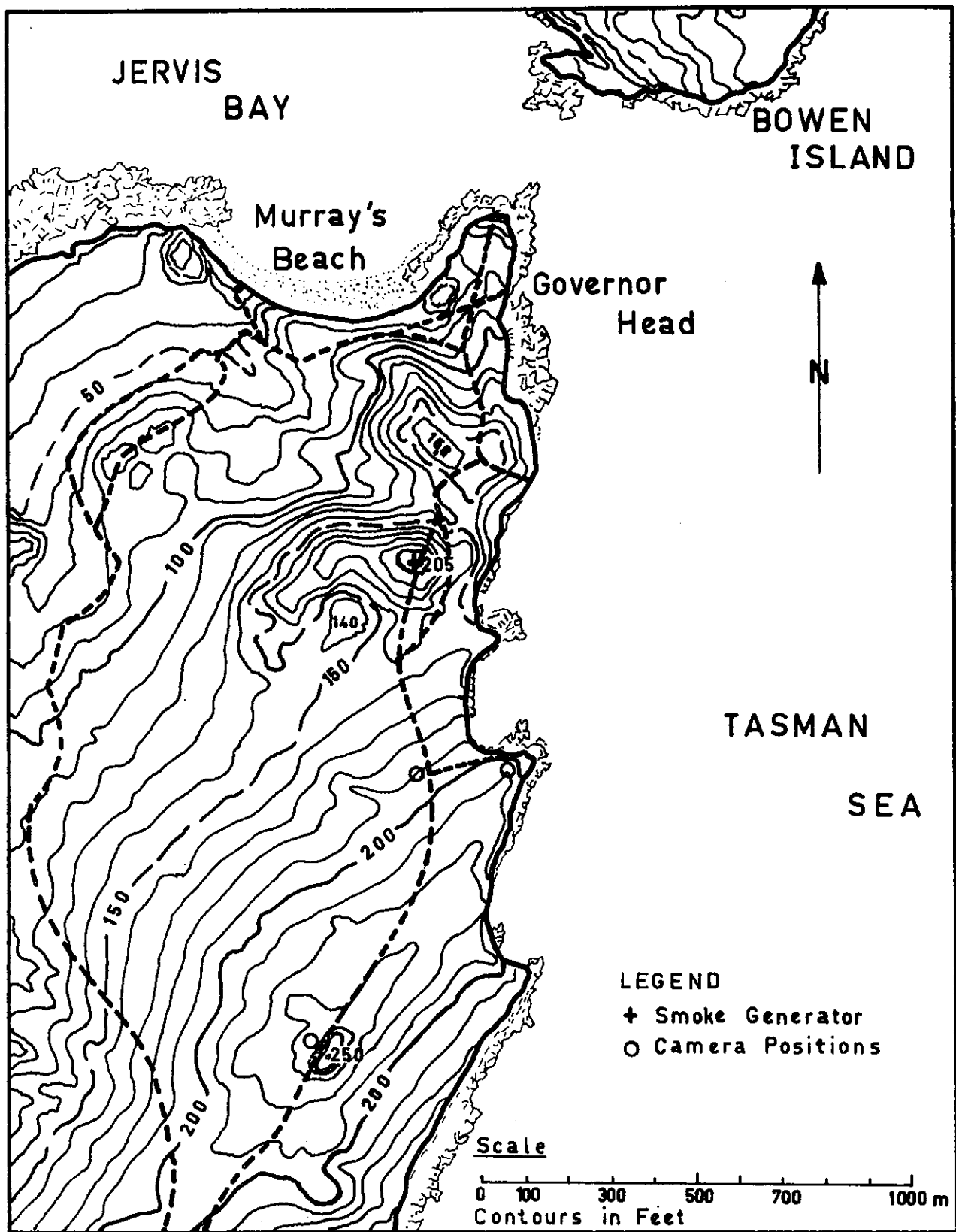
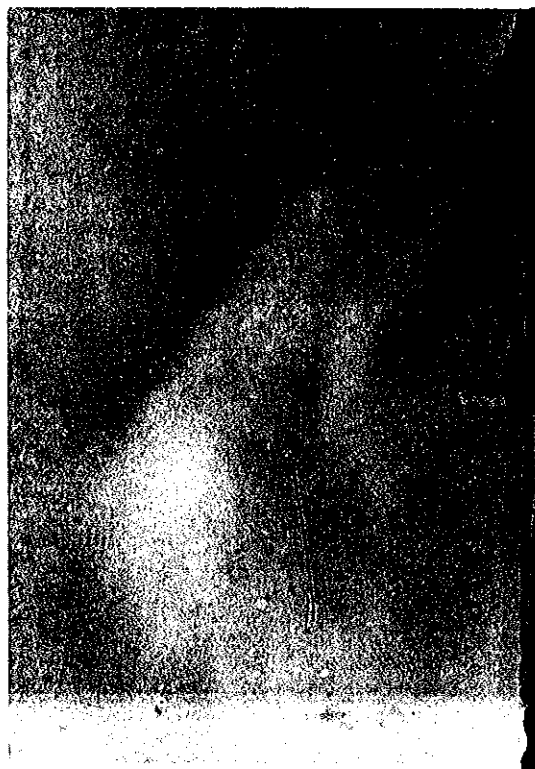


FIGURE 18 LOCATION OF CAMERA POSITIONS AND SMOKE GENERATOR AT MURRAY'S BEACH

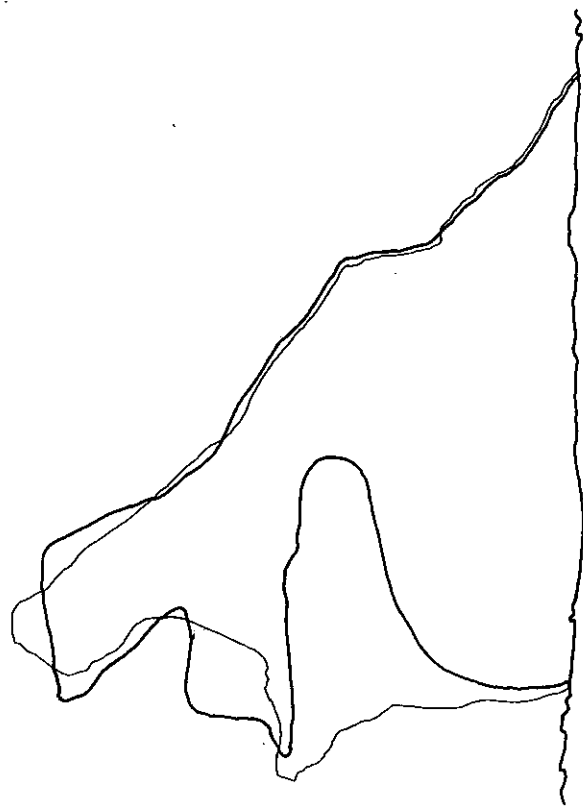




(a)



(b)



(c)

- (a) 1 min. Time Exposure. Photograph Aperture f11;  
Filter Factor 3,000.
- (b) Superimposition of 12 Instantaneous Photographs  
Taken at 5 s Intervals.
- (c) Tracings of Smoke Plume Envelopes  
—— Instantaneous ——— Time Exposure.

FIGURE 19. COMPARISON OF THE TIME EXPOSURE AND TIME SERIES OF INSTANTANEOUS  
PHOTOGRAPHIC TECHNIQUES AT 1224 EST ON 7.6.71

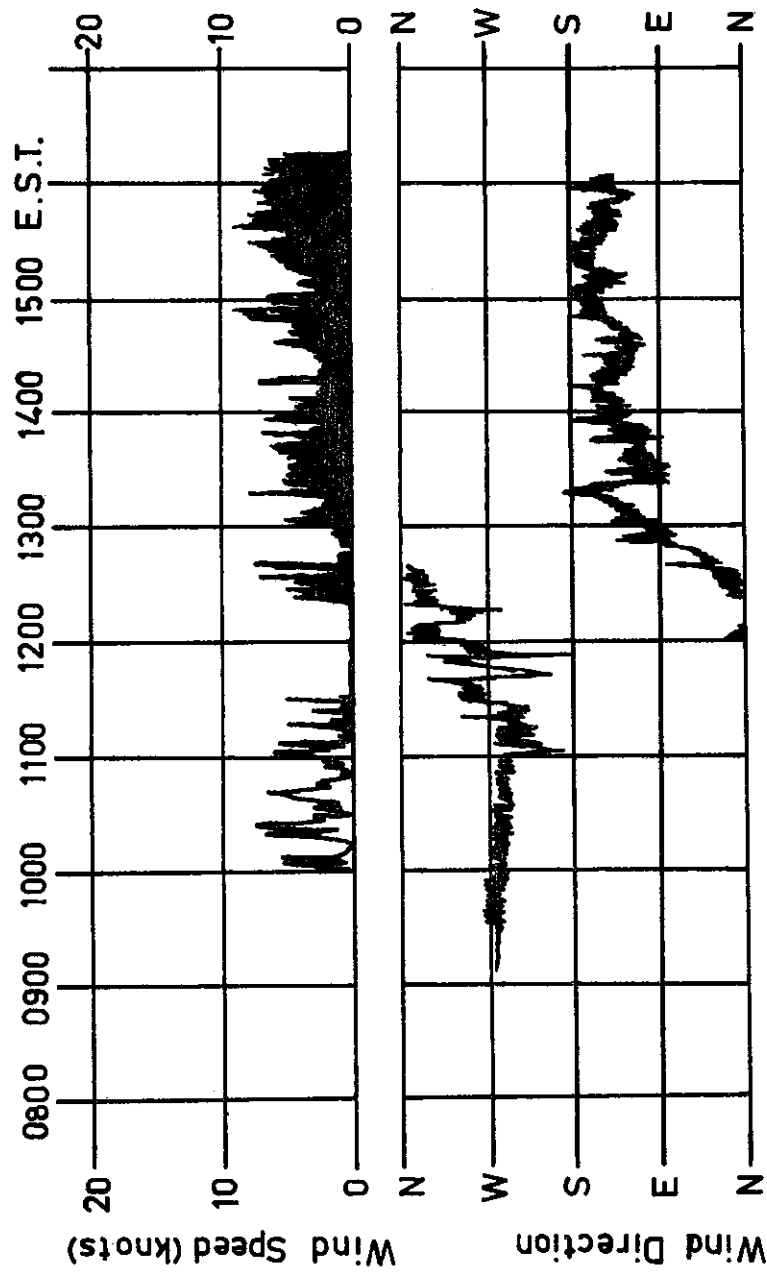


FIGURE 20. THE DINES ANEMOGRAPH WIND RECORD ON THE  
7.6.71 DURING THE SMOKE PLUME EXPERIMENT  
AT MURRAY'S BEACH

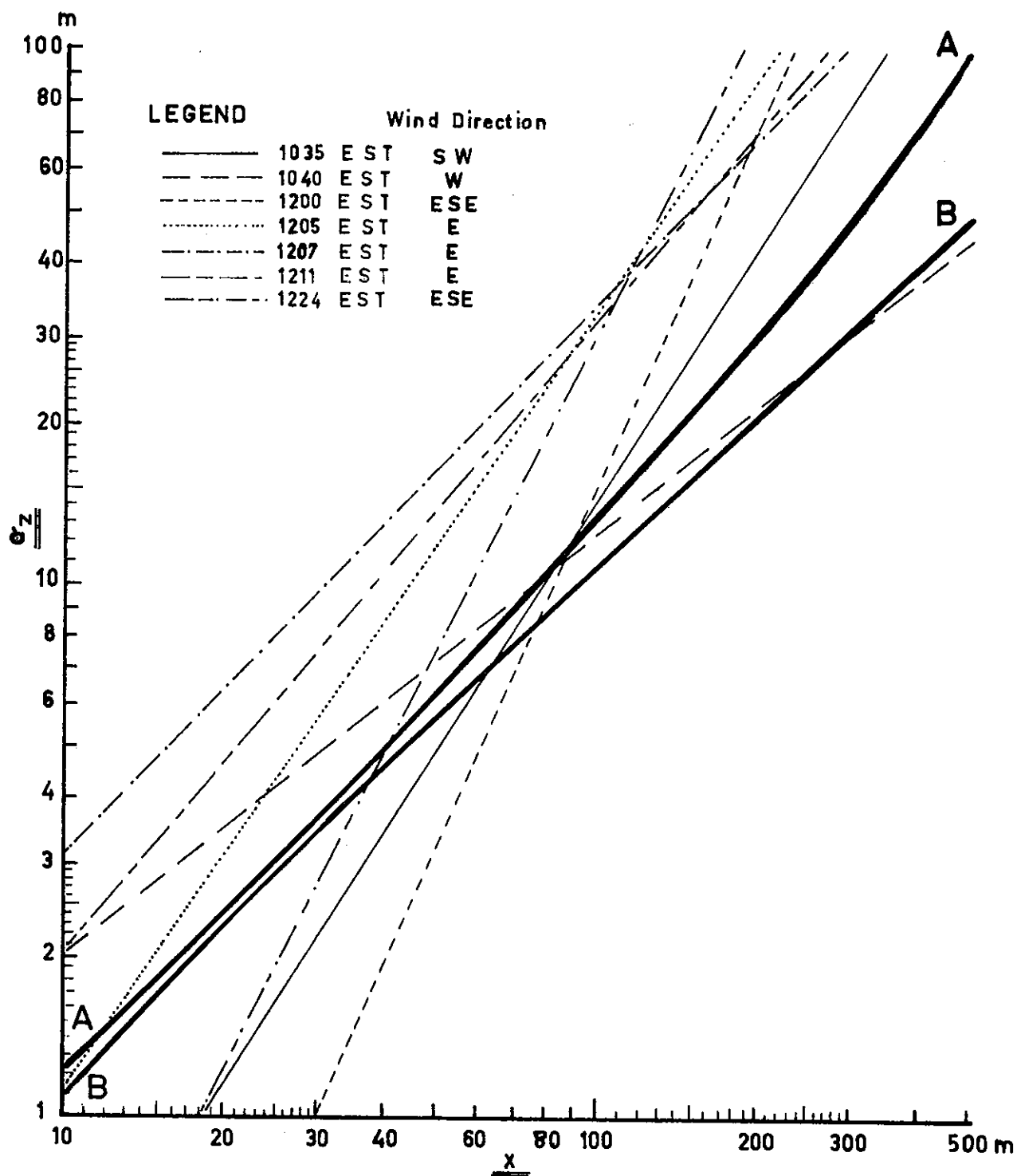
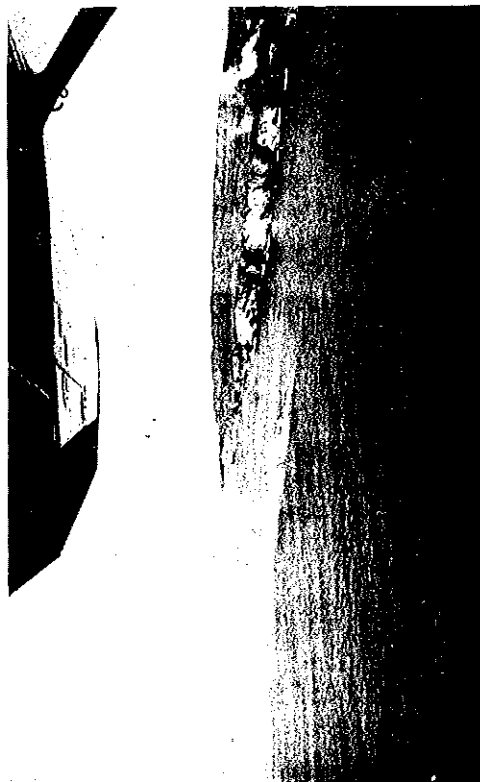


FIGURE 21. A PLOT OF THE VERTICAL STANDARD DEVIATION OF THE SMOKE PLUME ENVELOPE ( $\sigma_z(x)$ ) VERSUS DISTANCE DOWNWIND FROM THE SOURCE



(a)

- (a) 1050 EST. Vertical Photograph 3,500 ft. altitude
- (b) 1057 EST. Oblique Photograph
- (c) 1100 EST. Oblique Photograph



(b)



(c)

FIGURE 22. AERIAL PHOTOGRAPHS OF THE LAND AND SEA SMOKE PLUMES ON 10.6.71

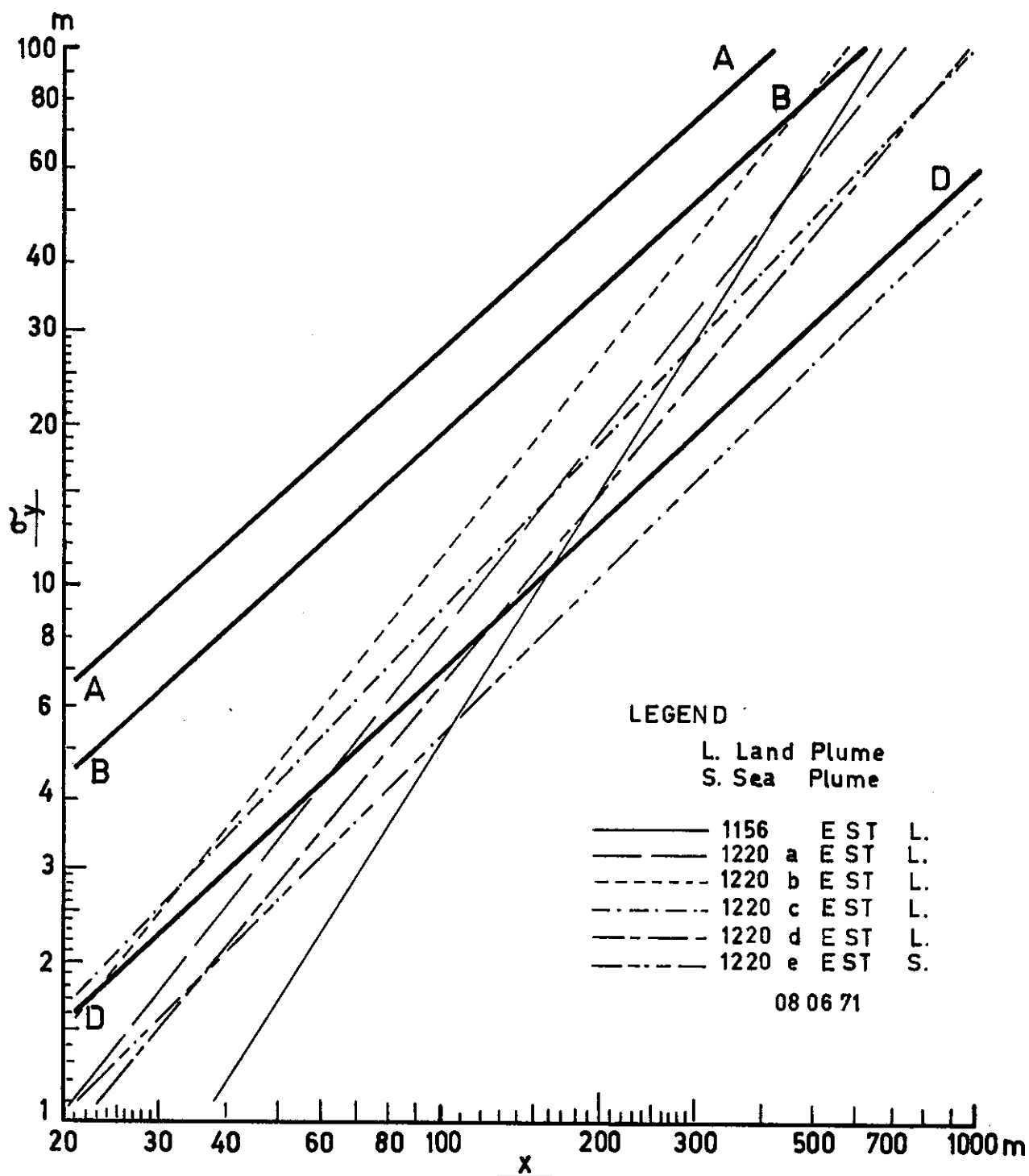


FIGURE 23(b) A PLOT OF THE HORIZONTAL STANDARD DEVIATION OF THE SMOKE PLUME ENVELOPE ( $\sigma_y(x)$ ) VERSUS DISTANCE DOWNWIND FROM THE SOURCE, 8.6.71

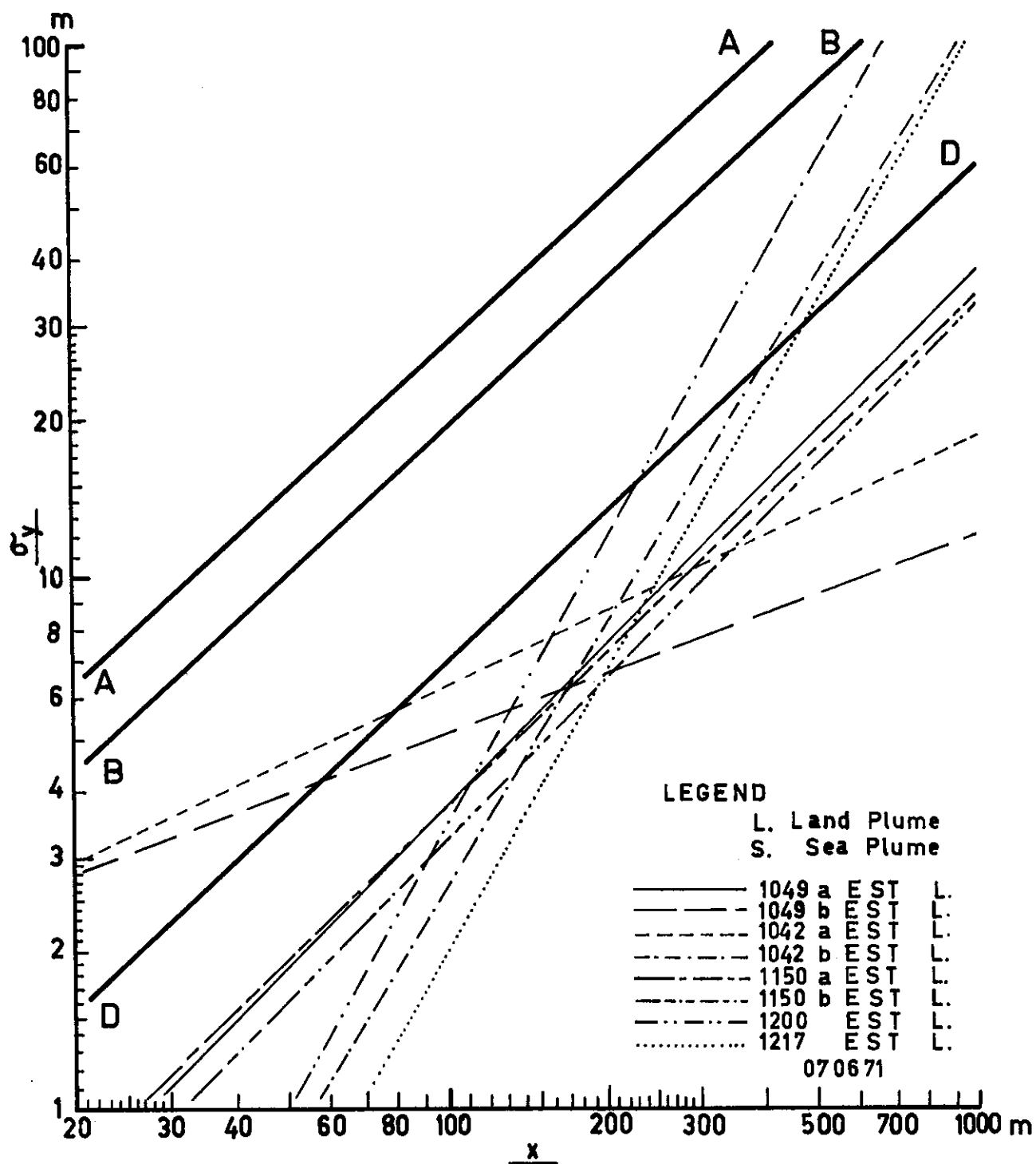


FIGURE 23(a) A PLOT OF THE HORIZONTAL STANDARD DEVIATION OF THE SMOKE PLUME ENVELOPE ( $\sigma_y(x)$ ) VERSUS DISTANCE DOWNWIND FROM THE SOURCE, 7.6.71

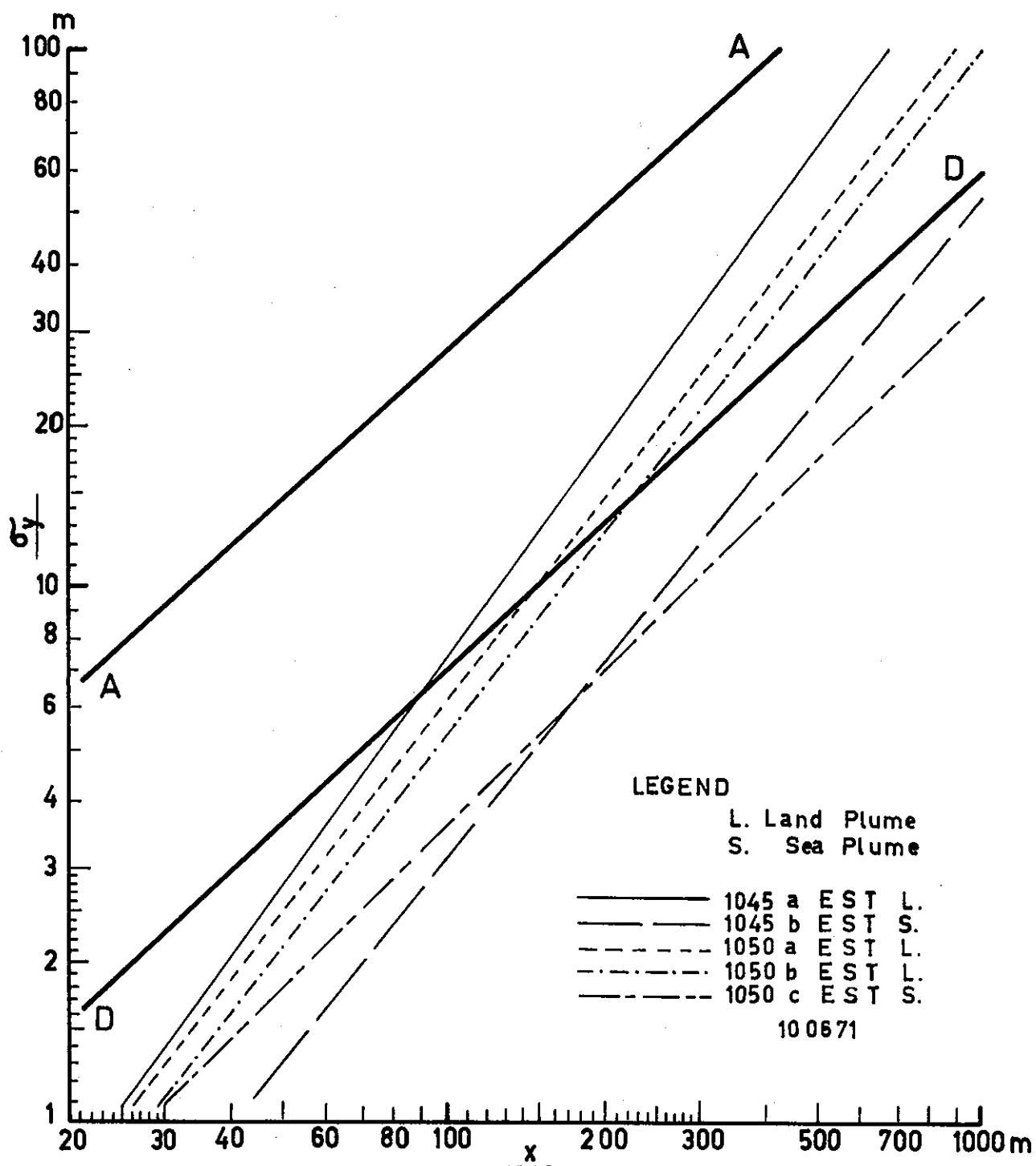


FIGURE 23(c) A PLOT OF THE HORIZONTAL STANDARD DEVIATION OF THE SMOKE PLUME ENVELOPE ( $\sigma_y(x)$ ) VERSUS DISTANCE DOWNWIND FROM THE SOURCE ,10.6.71

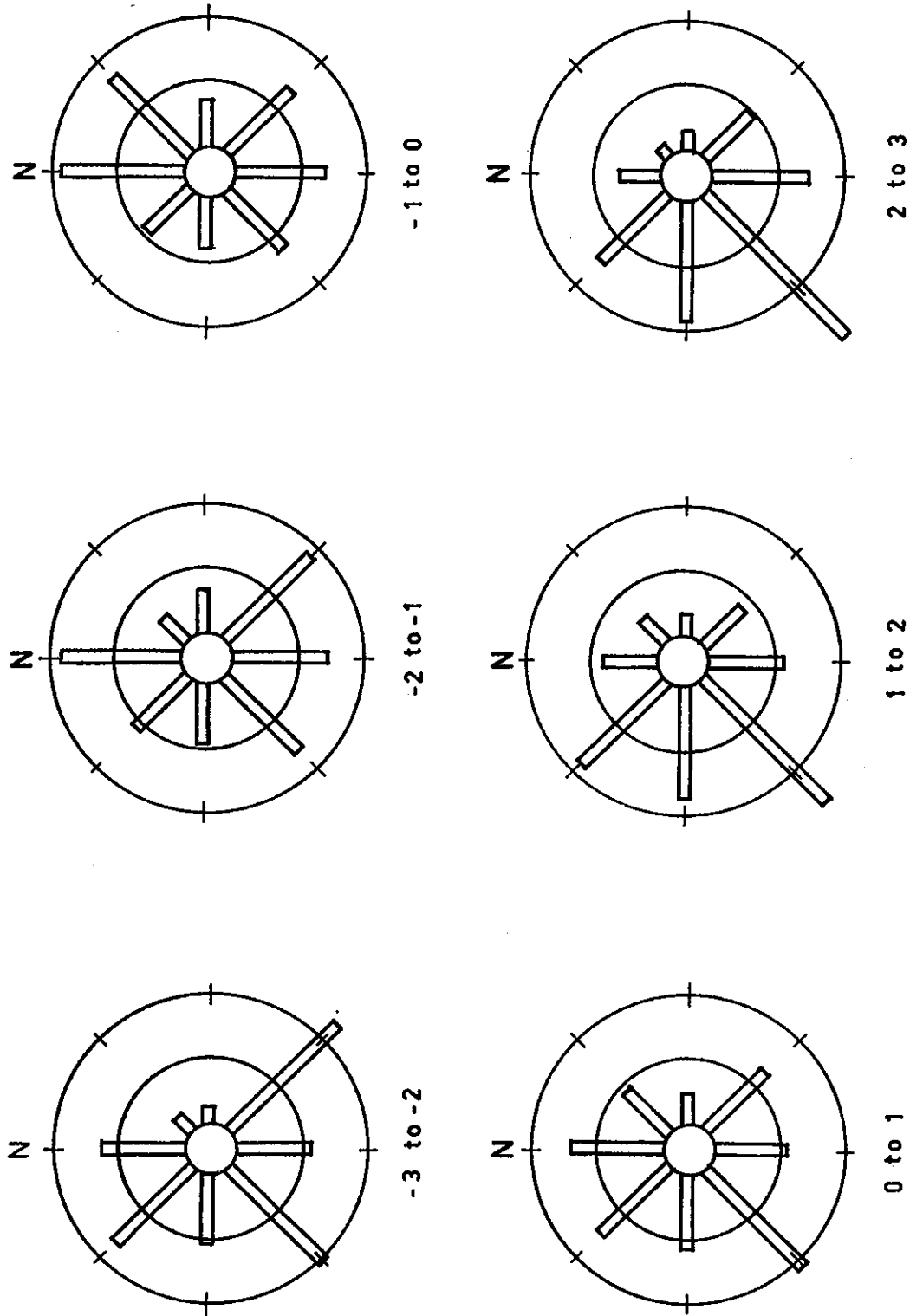


FIGURE 24. ATMOSPHERIC STABILITY WIND ROSES



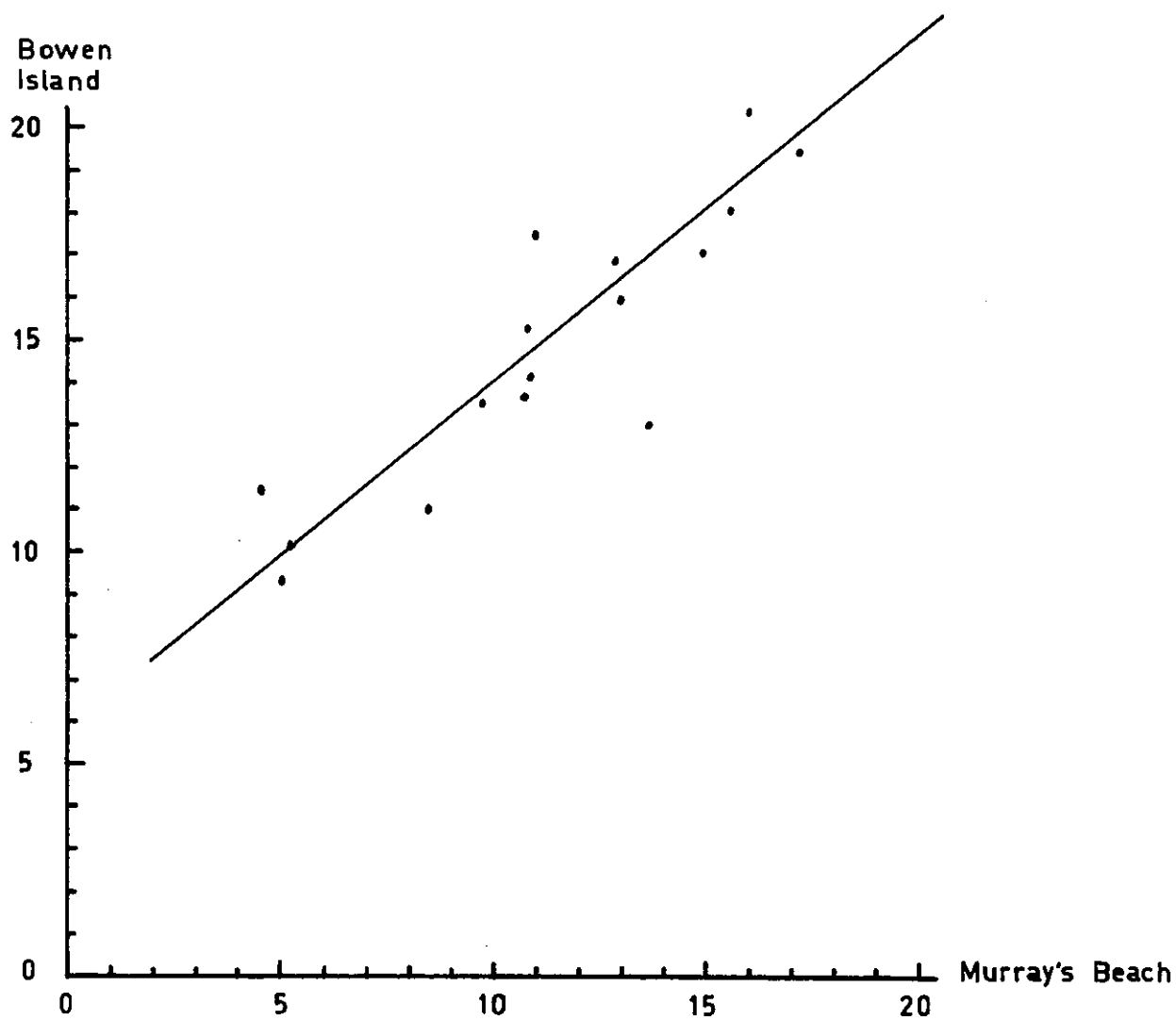


FIGURE 25. MINIMUM TEMPERATURES AT MURRAY'S BEACH  
(STEVENSON SCREEN LEVEL) AND  
BOWEN ISLAND

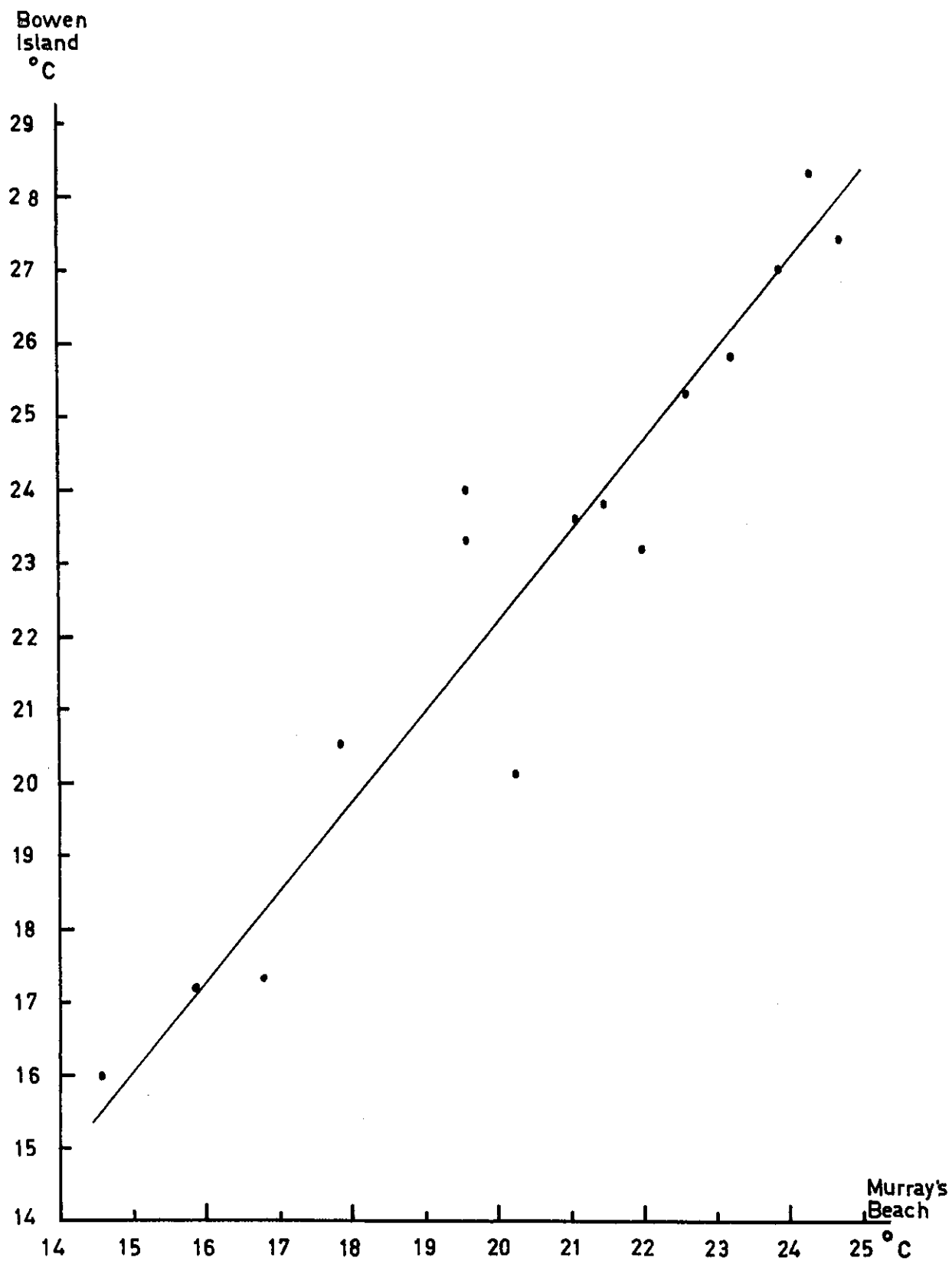


FIGURE 26. MAXIMUM TEMPERATURES AT MURRAY'S BEACH (STEVENSON SCREEN LEVEL) AND BOWEN ISLAND

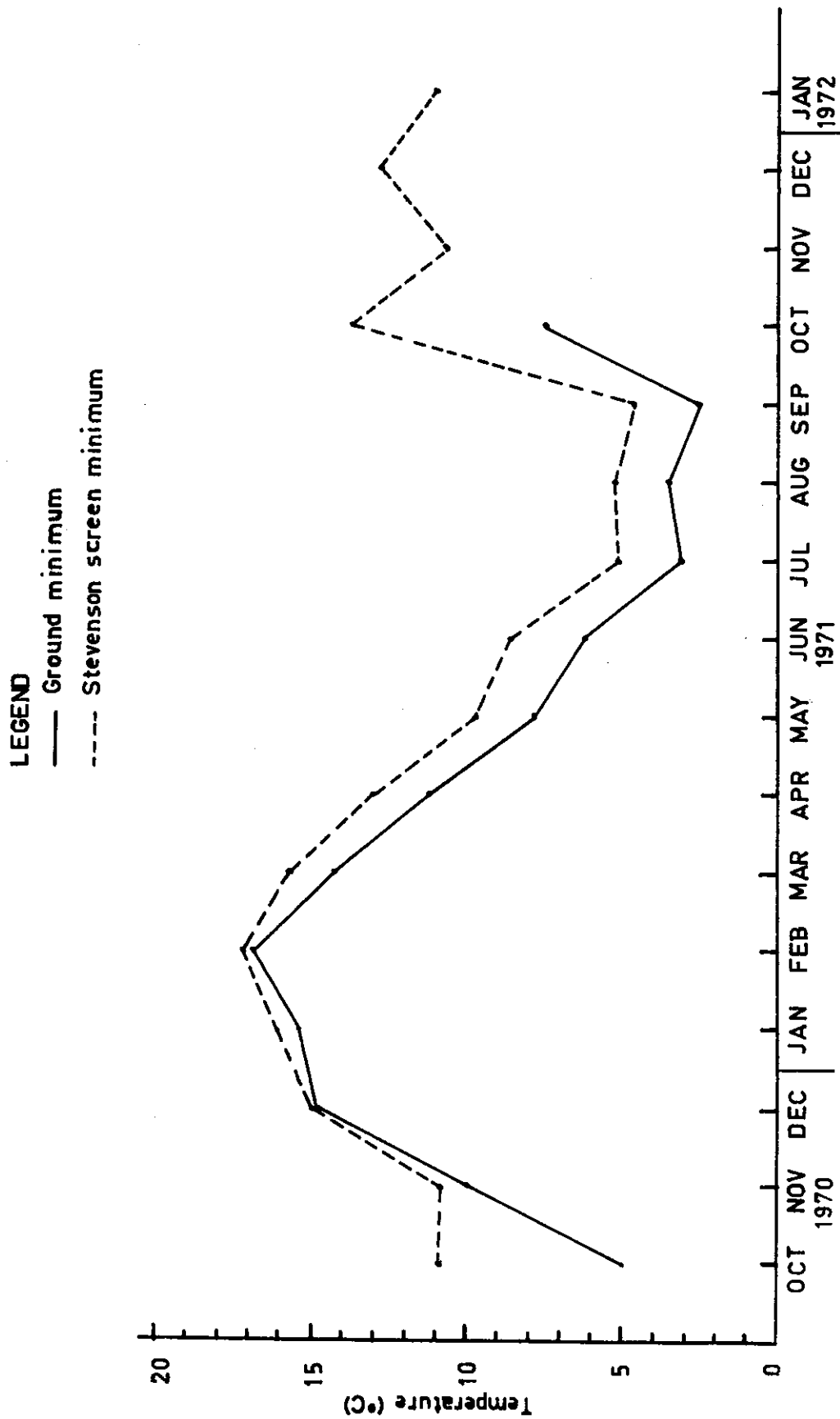


FIGURE 27. GROUND LEVEL AND STEVENSON SCREEN MINIMUM TEMPERATURES  
AT MURRAY'S BEACH

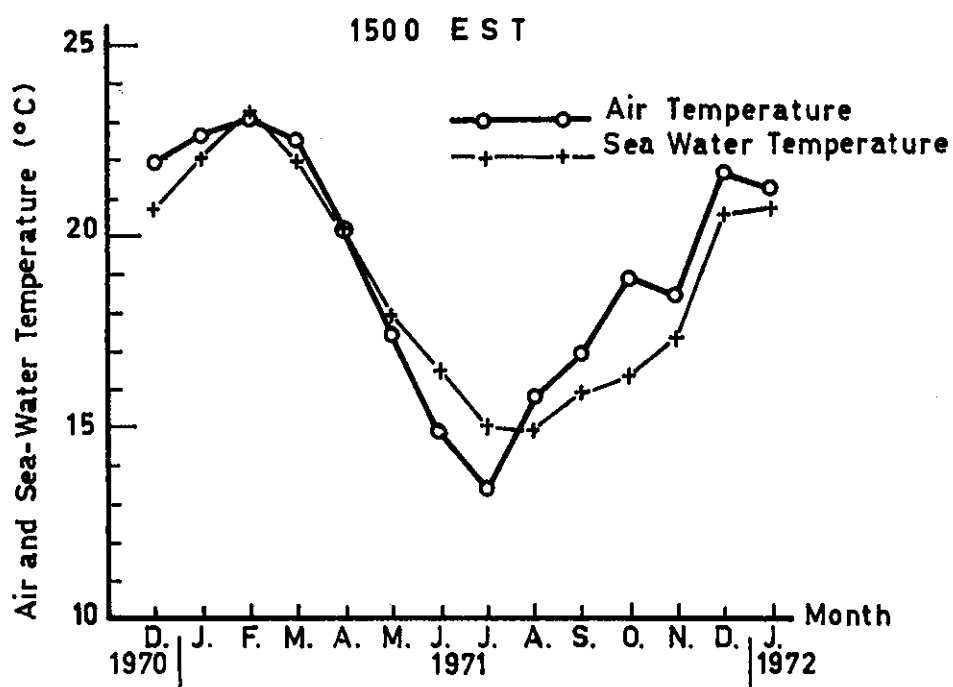
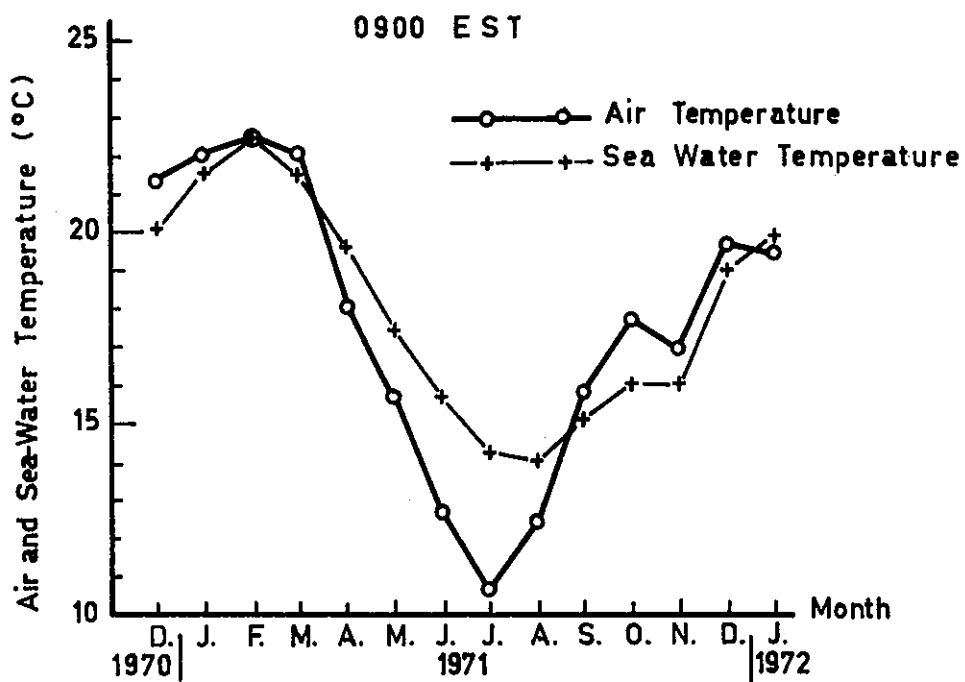


FIGURE 28. THE ANNUAL CYCLE OF AIR AND SEA WATER TEMPERATURES MEASURED AT MURRAY'S BEACH, JERVIS BAY

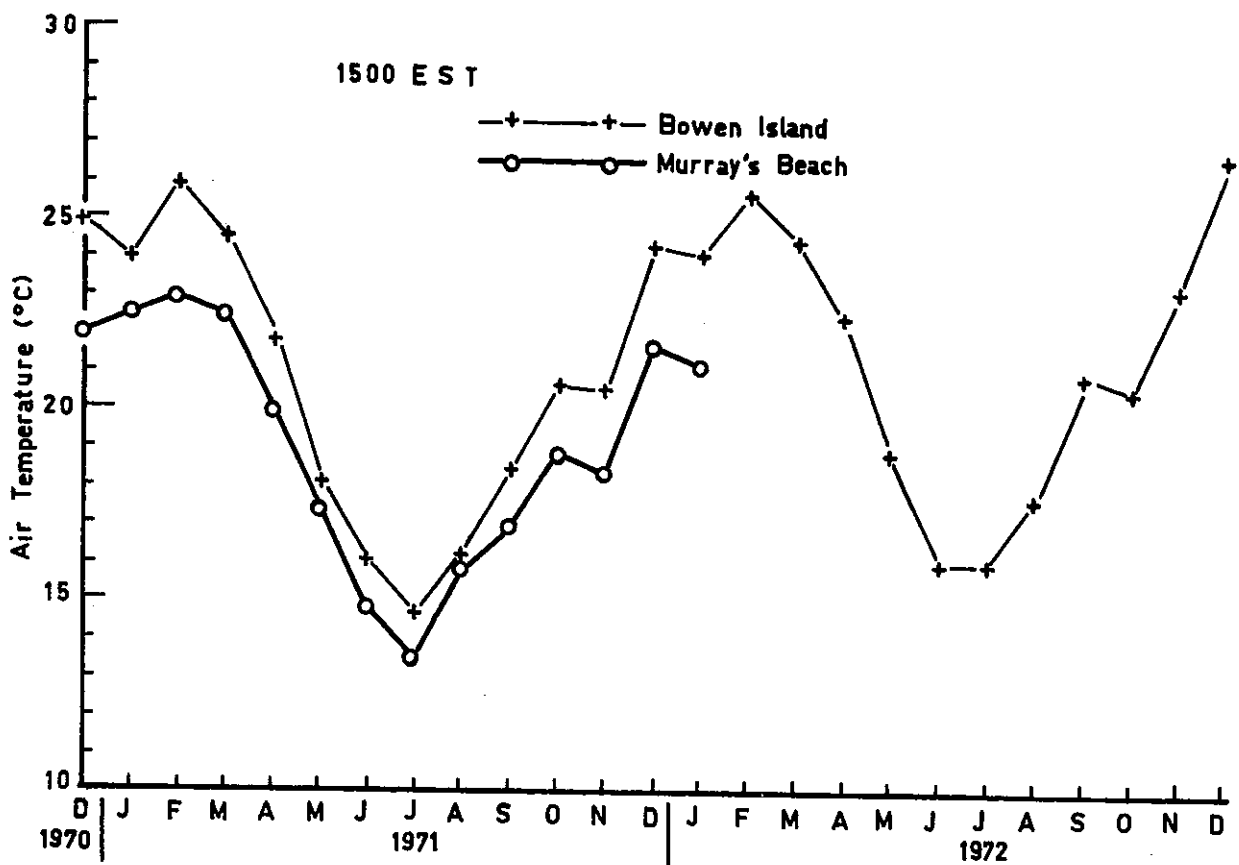
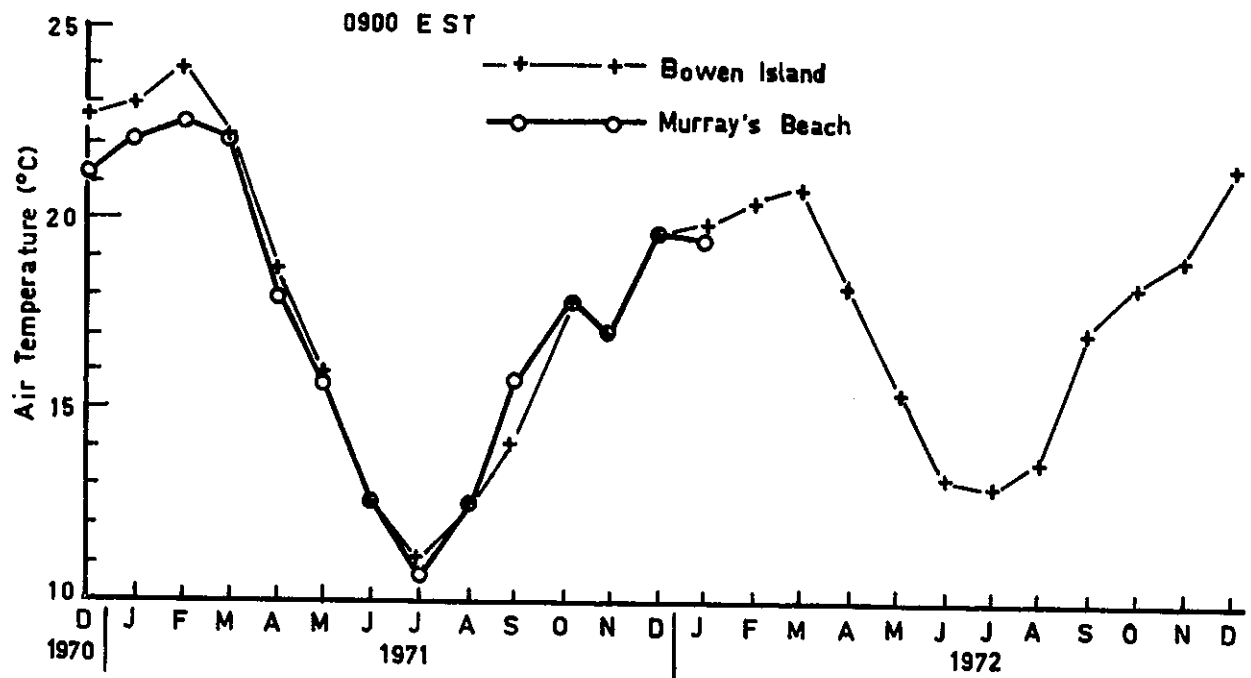


FIGURE 29. MONTHLY AVERAGED AIR TEMPERATURES FROM MURRAY'S BEACH AND BOWEN ISLAND AT JERVIS BAY

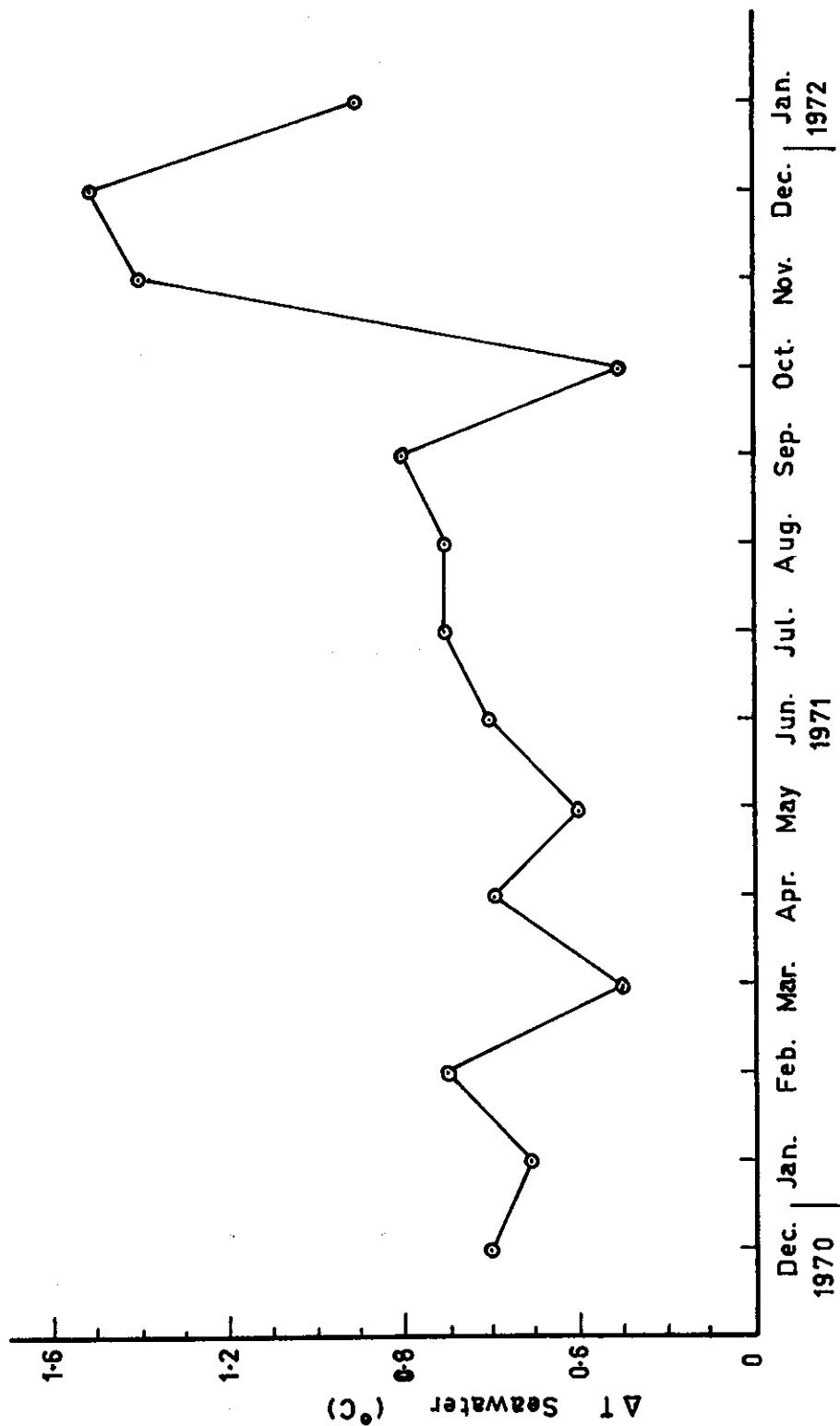


FIGURE 30. A GRAPH RELATING THE SEASONAL VARIATIONS IN THE SEA WATER TEMPERATURE DIFFERENCE BETWEEN 1500 AND 0900 E S T

Number of Days of Rain in each Month

11	16	13	13	19	13	10	6	8	6	5	7	9	13	15	14	14	10	5	11	12	5	8	4	16	16	5	9	21	J. B.
10	13	13	11	20	14	7	5	8	6	6	7	10	9	12	15	15	10	6	15	11	2	8	1	9	13	3	7	17	B. I.
6	8	12	12	16	10	8	5	8	4	5	4	8	7	9	11	M.B.													

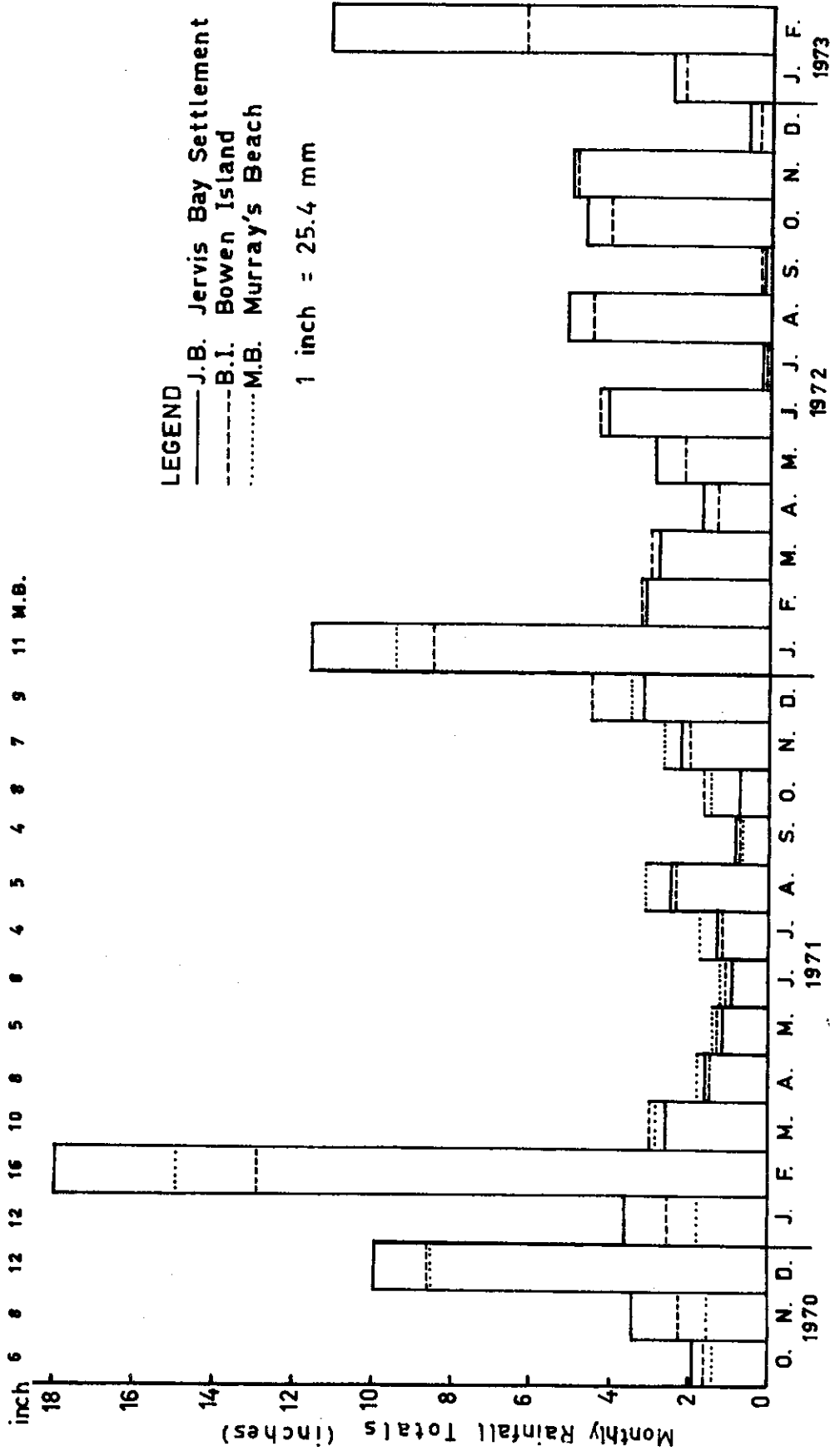


FIGURE 31. RAINFALL FOR JERVIS BAY AREA

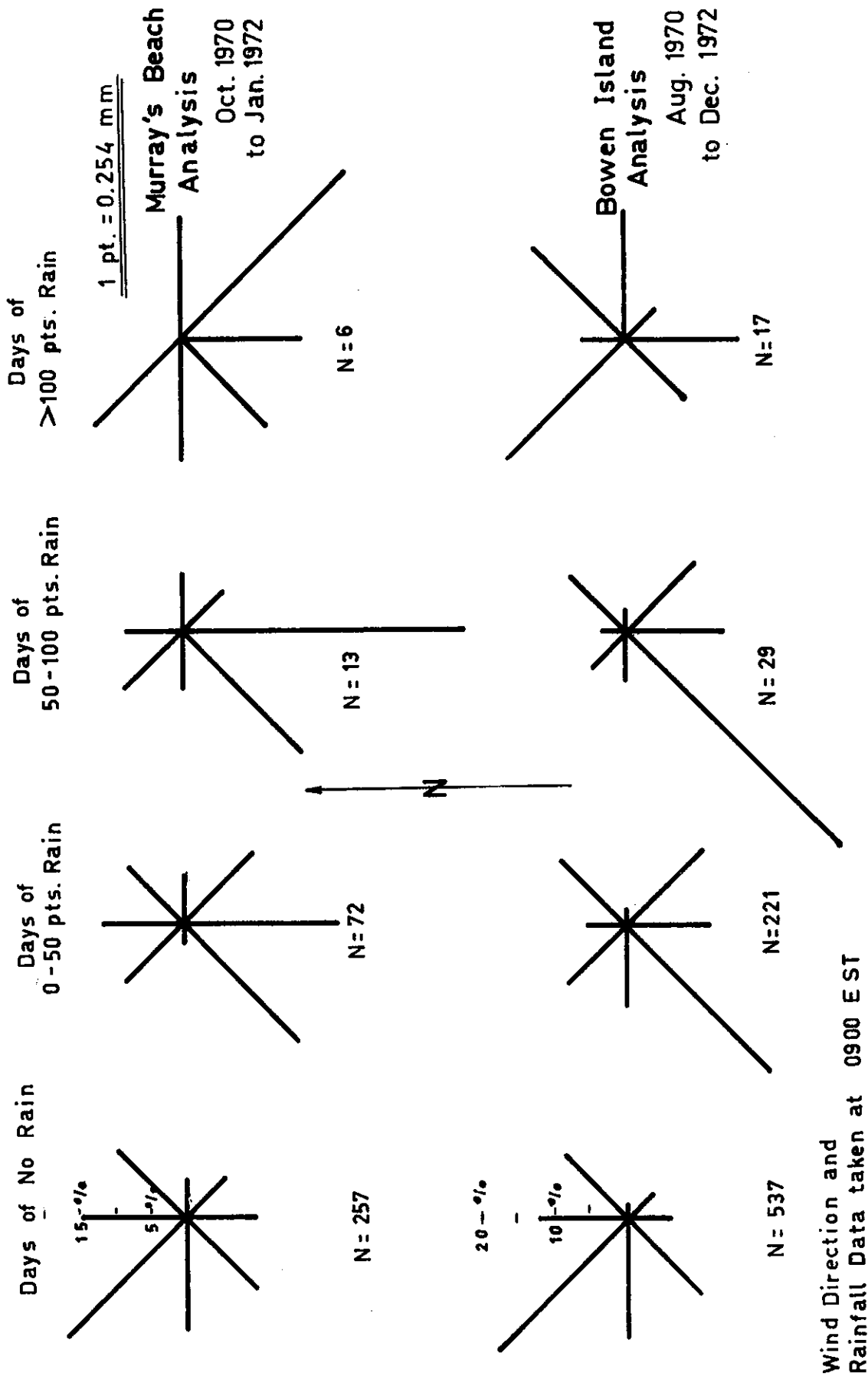


FIGURE 32. WIND ROSES FOR DAYS OF RAIN 0900 EST DATA



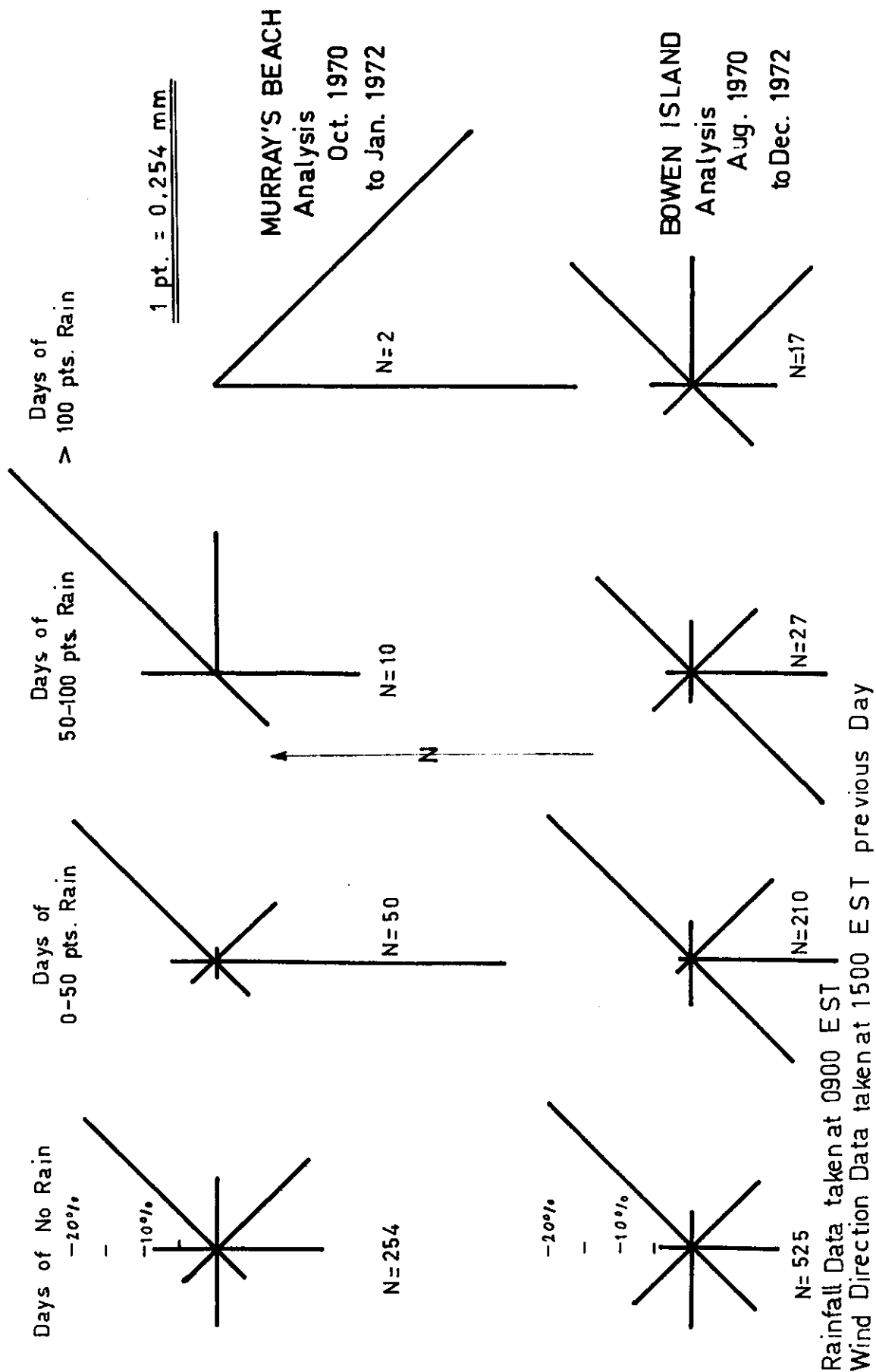


FIGURE 33. WIND ROSES FOR DAYS OF RAIN 0900 AND 1500 EST DATA



## APPENDIX A

### SAND DRIFT POLE DATA

In the initial environmental study at Jervis Bay, an oceanographic survey was conducted in the vicinity of Murray's Beach and Bowen Island to determine the most favourable locations for a cooling water inlet and outfall to the nuclear power station (E. Charash AAEC unpublished report). One of the proposed outfall locations was at the western end of Murray's Beach. In addition to the oceanographic and biological mapping programmes, another important aspect to be considered was the beach sand movement along Murray's Beach and its effect on the engineering design for the outfall channel.

To implement this study, eleven 25.4 mm diameter water pipes were painted, marked at decimetre intervals and driven into the sand at the following locations on the beach (Figure A1).

Poles 1 to 6 were located approximately two metres above the mean low water level and 7 to 11 near the mean high water mark. The poles were not referenced to any standard height which precluded any possibility of absolute measurements of sand volume movements along the beach. Instead it was decided to relate the relative changes of measured sand depths to the other observed physical variables. The 0900 and 1500 EST sea swell observations from Point Perpendicular were computerised for the period 1.8.1970 to 30.9.1971.

In addition to these sea observations, other meteorological variables considered of importance were the wind speed and direction and rainfall. Occasionally after heavy rain, rivulets were seen to erode sand from the centre of the beach.

Preliminary correlation analyses were inconclusive. Other research workers (P. Waterman private communication) have also found that the relationships between beach changes and tide, waves and other meteorological phenomena are extremely complex. It has been found that the synergistic effects of tide height, sea state and current deviations in the near shore zone are major contributing factors in the beach movement.

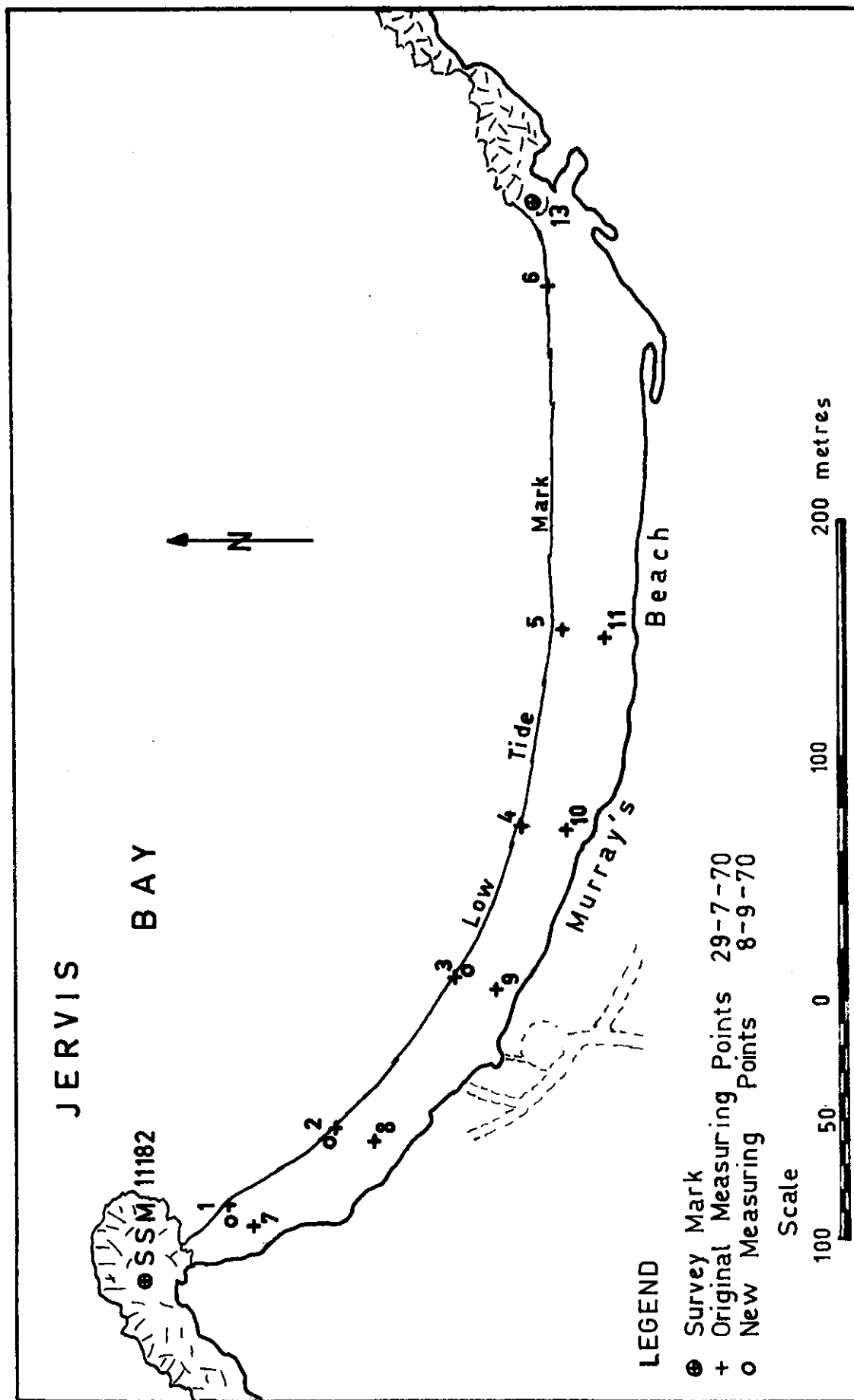


FIGURE A1. MURRAY'S BEACH SAND DRIFT MEASURING POINTS